RIBONUCLEASES AS CANCER AND VIRAL THERAPEUTICS: ROLE OF COULOMBIC INTERACTIONS

by

Rebecca Frances Turcotte

A dissertation submitted in partial fulfillment

of the requirements for the degree of

Doctor of Philosophy

(Biophysics)

at the

UNIVERSITY OF WISCONSIN–MADISON

2008

Committee's Page. This page is not to be hand-written except for the signatures

A dissertation entitled

Ribonucleases as Cancer and Viral Therapeutics:
Role of Coulombic Interactions

submitted to the Graduate School of the
University of Wisconsin-Madison
in partial fulfillment of the requirements for the
degree of Doctor of Philosophy

by

Rebecca F. Turcotte

Date of Final Oral Examination: September 16, 2008

Month & Year Degree to be awarded: **December** 2008 **May** **August**

****

Approval Signatures of Dissertation Committee

Signature, Dean of Graduate School

Committee's Page. This page is not to be hand-written except for the signatures

RIBONUCLEASES AS CANCER AND VIRAL THERAPEUTICS: ROLE OF COULOMBIC INTERACTIONS

Rebecca Frances Turcotte

Under the supervision of Professor Ronald T. Raines

at the University of Wisconsin–Madison

Ribonuclease A (RNase A) is one of the most studied proteins. It has served as a favorite model for protein chemists for decades, used for studies on synthesis, structure, folding, and enzymology. More recently, it was discovered that several members of the RNase A superfamily have interesting biological properties, including angiogenic, antimicrobial, antiviral, and cytotoxic effects. Indeed, one homologue, Onconase (ONC), is in late-stage clinical trials for the treatment of malignant mesothelioma.

Several requirements must be met for a ribonuclease to be cytotoxic. First, the ribonuclease must retain conformational stability at physiological temperatures. It also must have intact catalytic activity. It must not interact with the cytosolic ribonuclease inhibitor protein (RI), which binds to members of the RNase A superfamily with extremely high affinity. Finally, a cytotoxic ribonuclease must be able to bind to the cell surface and enter the cytosol of cancer cells. Three of these requirements—catalytic activity, RI interaction, and cellular entry—are strongly dependent on Coulombic interactions. A cationic ribonuclease must interact with its anionic RNA substrate and the cell surface, which largely consists of lipids, proteins, and carbohydrates displaying many

negatively charged groups; yet a cytotoxic ribonuclease must not interact with the anionic RI.

This thesis focuses on the role of Coulombic interactions in two of these processes—cellular internalization and RI binding. ONC, the prototypical cytotoxic ribonuclease, is the model ribonuclease in this work. In CHAPTER 2, a systematic analysis of the role of positively charged surface residues in the cytotoxicity of ONC is described. This study supports a model in which positively charged residues on the surface of ONC influence the translocation of the protein from endosomes to the cytosol. In CHAPTER 3, a productive interaction between RI and ONC in a solution of low salt concentration is detected, providing the first direct measurement of the affinity of these proteins.

The potential use of cytotoxic ribonucleases for their antiviral properties is described in CHAPTER 4. A zymogen that has the potential to specifically kill HIV-infected cells was created from RNase A. Cleavage of this zymogen by HIV protease results in a 50-fold increase in ribonucleolytic activity. This activation is dependent on the interaction between two positively charged proteins, the zymogen and HIV protease. In this case, Coulombic interactions do not favor this activation, but potentially limit it.

Finally, in CHAPTER 5, several potential future directions of this work are proposed. A project aimed at understanding the role of ONC and its putative inhibitor protein in *Rana pipiens* is put forward. A number of ideas for furthering our understanding of the mechanism of action of cytotoxic ribonucleases are proposed, as well as suggestions for the design of more desirable therapeutics based on this remarkable family of proteins.

Acknowledgements

First and foremost, I thank God, the giver of all gifts, who indeed is faithful and has never let me be tried beyond my strength (1 Cor 10:13). This manuscript is dedicated to Mary, Mother of God and Seat of Wisdom.

My parents, Pauline and Jim Rogers, have been a source of unwavering support to me. They have always encouraged my education, both in school and out, via newspapers, books, and living life. While they were always rooting for me in my time in graduate school, I always knew that they would love me no matter what degrees I had, and for that I am grateful. My extended family, which lives entirely on the east coast, has been a source of encouragement through these years, also. My friend, John Dias, is the closest I've ever come to having a sibling—thank you for that. I am also grateful to Julia Drees, Karie Dahlgren, and Keith Bersch for their support during my time in Madison.

Many thanks to those connected to the Medical Scientist Training Program, for their guidance throughout my time in Madison. Especially, I want to thank Deane Mosher, our co-director who is also on my thesis committee, and Paul Cook, our administrator. In addition, I am grateful to my classmates—Elizabeth Felton, Stephanie Markovina, and Emily Stevens—for our frequent dinners and discussions of science, the program, and life. I have been blessed to have such wonderful colleagues and friends.

Special thanks to the members of my thesis committee—Deane Mosher, George Phillips, Rob Striker, and Tom Record, as well as Ruth Saecker—for their helpful guidance and advice.

Thanks to all members of the Raines Laboratory, past and present, who have been an invaluable source of advice, support, and friendship to me during these four years. When I first began my research here, Jeremy Johnson and Kim Dickson were extremely helpful and welcoming. My initial projects stemmed from work by Jeremy, Steve Fuchs, and Eugene Lee, and the three of them were ready to lend a hand when I needed it. My bay-mates and office-mates, Kelly Gorres, Mike Palte, Margie Borra, and Kim, have all offered cheerful encouragement and advice when I needed it. Thank you to the MSTP members of our laboratory—Mike Levine, Nadia Sundlass, and Mike P.—for bringing their excitement and ideas over the last couple of years. I am grateful to my collaborator, Luke Lavis, for his great ideas and helpful discussions. Thank you to many past and present laboratory members—Joe Binder, Ben Caes, Cindy Chao, Sayani Chattopadhyay, Amit Choudhary, Greg Ellis, Daniel Gottlieb, Greg Jakubczak, Jeet Kalia, Frank Kotch, Langdon Martin, Nicky McElfresh, Eddie Myers, Kelsey Rudd, Tom Rutkoski, Matt Shoulders, Bryan Smith, Annie Tam, and Rex Watkins—for helpful discussions and contributing to a positive work environment.

Lastly, I would like to thank my advisor, Ron Raines. Ron has cultivated a collaborative environment, where we are encouraged to pursue interesting questions from a number of different angles. He has taught me much, especially regarding communicating about my research with others. I am grateful for the opportunity he has given me to pursue my Ph.D. thesis work in his research group.

Table of Contents

List of Figures

List of Tables

List of Abbreviations

ε	extinction coefficient
5-IAF	5-iodoacetamidofluorescein
6-FAM	6-carboxyfluorescein
6-TAMRA	6-carboxytetramethylrhodamine
AIDS	acquired immunodeficiency syndrome
ANG	angiogenin
BCA	bicinchoninic acid
BisTris	2-bis(2-hydroxyethyl)amino-2-(hydroxymethyl)-1,3-propanediol
BSA	bovine serum albumin
BS-RNase	bovine seminal ribonuclease
CD	circular dichroism
Da	dalton
DEF	2′,7′-diethylfluorescein
DEFIA	2′,7′-diethylfluorescein-5-iodoacetamide
DMF	dimethylformamide
DMSO	dimethylsulfoxide
DNA	deoxyribonucleic acid
DTNB	5,5′-dithiobis(2-nitrobenzoic acid)
DTT	dithiothreitol
ECP	eosinophilic cationic protein; RNase 3

EDTA	ethylenediaminetetraacetic acid
FPLC	fast performance liquid chromatography
FRET	Förster resonance energy transfer
GSH	reduced glutathione
GSSG	oxidized glutathione
h	hour
HAART	highly active antiretroviral therapy
HCl	hydrochloric acid
HIV	human immunodeficiency virus
HIV PR	HIV-1 protease
hRI	human ribonuclease inhibitor
HS	heparan sulfate
HSPG	heparin sulfate proteoglycan
IPTG	isopropyl-1-thio-β-D-galactopyranoside
k_{cat}	first-order enzymatic rate constant
K_d	equilibrium dissociation constant
kDa	kilodalton
K_i	inhibitor dissociation constant
K_M	Michaelis constant
λ_{em}	emission wavelength
λ_{ex}	excitation wavelength

LB	Luria–Bertani medium
MALDI–TOF	matrix-assisted laser desorption/ionization time-of-flight
MES	2-(*N*-morpholino)-ethanesulfonic acid
min	minute
NaCl	sodium chloride
NaOH	sodium hydroxide
NBS	non-binding surface
ONC	Onconase®; ranpirnase; P-30; Pannon
OVS	oligo(vinylsulfonic acid)
PBS	phosphate-buffered saline
PDB	protein data bank
PEG	poly(ethylene glycol)
p*I*	isoelectric point
pK_a	log of the acid dissociation constant
poly(C)	poly(cytidylic acid)
pRI	porcine ribonuclease inhibitor
PTD	protein transductions domain; cell penetrating peptide
RI	ribonuclease inhibitor
RNA	ribonucleic acid
RNase A	bovine pancreatic ribonuclease
RNase 1	human pancreatic ribonuclease

RNase 7	human ribonuclease 7
s	second
SDS	sodium dodecyl sulfate
SDS–PAGE	sodium dodecyl sulfate poly(acrylamide) gel electrophoresis
TAT	transactivating transcriptional activator protein
TB	terrific broth
T_m	temperature at the midpoint of the denaturation curve
TML	trimethyl lock
TNB	2-nitro-5-thiobenzoate
Tris	2-amino-2-(hydroxymethyl)-1,3-propanediol
UV	ultraviolet
Z	net molecular charge (Arg + Lys – Asp – Glu)

CHAPTER 1

Introduction:

Coulombic Forces in the Actions

of Cytotoxic Ribonucleases

1.1 Overview

Studies of macromolecular interactions are essential for the advancement of human health. The understanding of such interactions is applicable to the fields of physiology, pathology, and pharmacology. For example, one of the best-characterized protein–protein interactions, that between antibodies and antigens, is active in a healthy immune system, as the individual fights off many pathogens on a daily basis (Parham, 2005). Antigen–antibody interactions can be inappropriate, as in pathological states such as autoimmune disease (Plotz, 2003) or allergies (Kawakami and Galli, 2002). Finally, knowledge of these interactions has improved human health, as evidenced by the increasing numbers of antibody therapies in use and in development for diverse diseases (Brekke and Sandlie, 2003; Rastetter *et al.*, 2004; Steinman, 2005; Pastan *et al.*, 2007).

In the case of antibodies and antigens, the two molecules make contact in the extracellular environment. Many other contacts take place in the cytosol of the cell. In either case, the macromolecules are bathed in water, ions, small molecules, and other macromolecules, which greatly modify the affinity and the rates of association of these complexes (Jarvis *et al.*, 1990; Record *et al.*, 1998; Kozer and Schreiber, 2004; Zhou *et al.*, 2006).

1.2 Coulombic forces in biology

In a vacuum, the interaction between two ions of opposite charge is driven by enthalpy. The energy of this interaction is stated with Coulomb's law:

$$E_0(r) = \frac{z_1 z_2}{4\pi\varepsilon_0 r} \tag{1.1}$$

which expresses the potential energy E_0 between two charges of magnitude z_1 and z_2 at a distance r. ε_0 is the permittivity constant (Daune, 1999; Gitlin *et al.*, 2006).

Interactions between macromolecules, however, including proteins, lipids, nucleic acids, and carbohydrates, do not take place in a vacuum. In water, the free energy of interaction ΔG between two ions is decreased due to the high dielectric constant ε of the medium:

$$\Delta G_{H_2O} = \Delta E_0 \frac{1}{\varepsilon_{H_2O}} \tag{1.2}$$

The dielectric constant describes a continuous medium, but is actually a result of the molecular properties of water. The water molecules that hydrate the ions are more ordered than those that make up the "bulk water" outside of the hydration shell. As two ions of opposite charge approach each other, some of the water molecules in the hydration shell are released, increasing the entropy of the system. Indeed, it is entropy, rather than enthalpy, that drives the interactions between charges in water (Daune, 1999; Gitlin *et al.*, 2006). This entropic effect is compounded for macromolecules, which bury a larger, more heterogenous surface area (Record *et al.*, 1998).

Solutes, including electrolytes, can also affect the strength of the interactions between macromolecules. These effects are a result of the preferential interactions that many solutes have with the surfaces of macromolecules, which lead to a local accumulation of solutes. The release of these molecules upon the binding of the macromolecules increases the entropy of the system, driving the interaction. The mathematical expressions for the dependence upon solute concentrations differs significantly depending on both the nature (size and charge density) of the macromolecules and the nature (charged or uncharged) of the solutes, as well as the concentration range of the solutes (Record *et al.*, 1998).

Coulombic interactions are but one example of a host of noncovalent forces that govern the interactions between macromolecules. Other examples include hydrogen-bonding, dipole–dipole interactions, and van der Waals interactions. It is interesting to note that Coulombic interactions are dominant at a significant distance. Whereas the energy of dipole–dipole interactions varies in proportion to $1/r^3$, where r is the distance between the interacting molecules, and the attraction component of the energy of van der Waals interactions varies in proportion to $1/r^6$, the energy of Coulombic interactions varies as $1/r$ as shown above. This results in the persistence of these forces in the long-range (Tinoco *et al.*, 2002), and the special role that they play in the formation of macromolecular complexes (Schreiber and Fersht, 1996; Sheinerman and Honig, 2002). Specifically, Coulombic forces play a major role in determining association rates of complexes, while other interactions have more of an effect on dissociation rates (Johnson *et al.*, 2007c).

Although Coulombic forces are essential for many interactions, this work will focus on their part in the macromolecular interactions that are relevant to the mechanism of action of cytotoxic ribonucleases.

1.3 Cytotoxic ribonucleases

Bovine pancreatic ribonuclease (RNase A; Figure 1.1a) (Raines, 1998; Marshall *et al.*, 2008) is arguably the most studied protein of the 20th century. It has been an attractive model protein for several reasons: (1) its ready availability from the cow pancreas; (2) its extraordinary stability; (3) its ability to refold without the aid of chaperones (Anfinsen, 1973); and (4) its near-perfect catalytic efficiency (Park and Raines, 2003). Indeed, work on RNase A has led to four Nobel prizes (Anfinsen 1972, Moore and Stein 1972, and Merrifield 1984) (Raines, 1998).

In the late 20th century, interest in RNase A experienced a resurgence. Previously, it had been noted that RNase A caused the regression of tumors if the protein was injected in vast amounts (Ledoux, 1955a; Ledoux, 1955b; Alexsandrowicz, 1958). Subsequently, two homologues of RNase A were found to be much more effective cytotoxins, bovine seminal ribonuclease (BS-RNase; Figure 1.1d) (D'Alessio *et al.*, 1991; Lee and Raines, 2005) and Onconase® (ONC; Figure 1.1c) (Ardelt *et al.*, 2008; Lee and Raines, 2008). In addition, several members of the RNase A superfamily were found to have other interesting biological properties, including roles in immune function (Snyder and Gleich, 1997; Zhang *et al.*, 2003) and angiogenesis (Riordan, 1997; Snyder and Gleich, 1997).

The cytotoxic activity of embryonic extracts of the Northern leopard frog *Rana pipiens* was first reported in 1973. Eighteen years later, the active component, ONC, was found to be a member of the RNase A superfamily (Figure 1.2) (Ardelt *et al.*, 1991). It was found to be cytostatic and cytotoxic to many tumor cell lines *in vitro* (Darzynkiewicz *et al.*, 1988). *In vivo*, ONC caused dose-dependent tumor growth inhibition and increased survival in mice that had been transplanted with murine and human tumors (Mikulski *et al.*, 1990a), and Phase I clinical trials were soon begun.

ONC was well-tolerated in Phase I clinical trials. Dose-limiting renal toxicity was observed, but this was reversible upon discontinuation of treatment. The more typical side effects of cancer chemotherapy, such as myelosuppression, mucositis, alopecia, cardiotoxicity, coagulopathy, hepatotoxicity, and adverse metabolic effects, were not observed (Mikulski *et al.*, 1993). Phase II trials of ONC aimed at malignant mesothelioma (Mikulski *et al.*, 2002), pancreatic cancer, breast cancer (Costanzi *et al.*, 2005), non-small cell lung cancer (Mikulski *et al.*, 1995), and renal cell cancer (Vogelzang *et al.*, 2001) were undertaken. ONC was shown to be effective in all but renal cell cancer. Of these, the largest trial was for malignant mesothelioma.

ONC has undergone several Phase III clinical trials. One of these, for pancreatic adenocarcinoma, showed that the patient population that was treated with gemcitabine had a significant survival advantage over the patients that were treated with ONC and tamoxifen (Costanzi *et al.*, 2005). In two trials with patients with malignant mesothelioma, however, ONC has shown more promise. In the first trial for mesothelioma, ONC appeared to be superior to doxorubicin in certain patient subsets. In

an ongoing trial of ONC and doxorubicin versus doxorubicin alone, ONC did not meet statistical significance for its primary endpoint, but did show significant improvement among patients who had failed a previous chemotherapy regimen. Thus, ONC may find a place as a second-line therapy for patients with malignant mesothelioma. ONC has been granted both fast-track status and orphan-drug designation from the FDA (Costanzi *et al.*, 2005; Pavlakis and Vogelzang, 2006; Hollingsworth, 2008). The synergism that has been observed between ONC and other drugs, including cancer chemotherapeutics (Mikulski *et al.*, 1990b; Rybak *et al.*, 1996; Lee *et al.*, 2003), lovastatin (Mikulski *et al.*, 1992), rosiglitazone (Ramos-Nino and Littenberg, 2008), and a proteasome inhibitor (Mikulski *et al.*, 1998), may lead to additional clinical trials.

A significant difference between RNase A, which is effectively not cytotoxic, and BS-RNase and ONC, which are, is the ability of these proteins to be bound by the ribonuclease inhibitor protein (RI) (Dickson *et al.*, 2005). RI is found in the cytosol of all cell lines studied, at a nearly invariant concentration of 4 μM (Haigis *et al.*, 2003). It is a 50-kDa, anionic protein that binds to members of the RNase A superfamily with a 1:1 stoichiometry, inhibiting their ribonucleolytic activity. Human RI (hRI) binds to RNase A with a K_d value of 4.4×10^{-14} M (Lee *et al.*, 1989b) and human pancreatic ribonuclease (RNase 1; Figure 1.1b) with a K_d value of 2.9×10^{-16} M (Johnson *et al.*, 2007c), one of the tightest known protein–protein interactions in all of biology. The dimeric quaternary structure of BS-RNase precludes its binding to RI (Mazzarella *et al.*, 1993; Lee and Raines, 2005). In contrast, ONC does not interact with RI in the cell due to its truncated

surface loops, which contain the majority of the RI contact-residues in RNase A and RNase 1 (Boix *et al.*, 1996). The knowledge that the ability to evade binding by RI is essential for the cytotoxicity of ribonuclease has been exploited in the design of several cytotoxic variants of mammalian ribonucleases that do not bind to RI (Rutkoski and Raines, 2008).

In addition to this requirement, there are several other requirements for a ribonuclease variant to be cytotoxic to tumor cells (Figure 1.3). One is the ability to enter the cytosol of tumor cells (Haigis and Raines, 2003; Leich *et al.*, 2007; Benito *et al.*, 2008). Another requirement is intact ribonucleolytic activity (Ardelt *et al.*, 1991), which allows the ribonuclease to cleave RNA substrates, leading to cell death by apoptosis (Iordanov *et al.*, 2000; Leland *et al.*, 2001). Finally, cytotoxic ribonucleases must retain conformational stability, a property that has been shown to correlate with proteolytic stability (Klink and Raines, 2000; Kim *et al.*, 2004).

1.4 Coulombic forces in cellular entry

Although many advances have been made in the field of biopharmaceuticals, as evidenced by the increasing numbers of these drugs in the pipeline and on the market (Ashton, 2001), one limitation that remains is the inability of many drugs to enter the cytosol of cells, a location required for many drug actions. Thus far, the biopharmaceuticals that are on the market in the United States do not include drugs that act in the cytosol. They are limited to drugs that bind extracellular targets, such as insulin

and antibody chemotherapeutics (Brekke and Sandlie, 2003), as well as drugs that act in the lysosome, such as enzyme replacement therapies (Wraith, 2006). ONC, if approved by the FDA, would represent a ground-breaking pharmaceutical.

The promises of gene therapy and RNA interference, as well as the replacement of cytosolic enzymes, demand the development of a method for macromolecules to enter the cytosol of cells. A means discovered in nature of delivering cargo to the cytosol is the use of peptides known as protein transduction domains (PTDs), or cell-penetrating peptides (Fuchs and Raines, 2006; Murriel and Dowdy, 2006). The first PTD to be discovered was a portion of the human immunodeficiency virus (HIV) transactivating transcriptional activator protein (TAT) (Mann and Frankel, 1991). When TAT was attached to cargo, the cargo would enter into the cytosol of cells (Fawell *et al.*, 1994). The sequence required for the uptake of attached cargo was found to consist of primarily lysine and arginine residues. Indeed, the rate of cellular update correlated with the number of basic residues in the sequence. It was later discovered that the peptide backbone was unnecessary and that arginine was more effective than lysine. Since then, polyarginine has become a commonly used PTD, with the optimal length being five to eleven residues, and eight or nine residues being the most effective (Fuchs and Raines, 2006). Polyarginine and other PTDs are able to internalize cargo of various sizes, including large cargo such as liposomes, plasmids, and iron nanoparticles (Noguchi and Matsumoto, 2006).

The lack of stringent sequence or backbone requirements suggests that PTDs do not interact with an extracellular receptor. In contrast, PTDs appear to depend on electrostatic interactions with the cell membrane. Mammalian cell membranes consist of a lipid

bilayer that is decorated with additional macromolecules. The lipid bilayer displays charged headgroups, including anionic phosphoryl groups (Bergelson *et al.*, 1970). In addition, a forest of anionic biopolymers, including glycosaminoglycans, such as heparin sulfate proteoglycans (HSPGs) (Sasisekharan *et al.*, 2002), and gangliosides, such as sialic acid (Fredman *et al.*, 2003), coat the surface of the cell. It is thought that PTDs interact with these biopolymers, in particular HSPGs, via electrostatic interactions, including hydrogen bonding and Coulombic interactions (Fuchs and Raines, 2004).

Following the interaction of PTDs with HSPGs on the cell surface, they enter cells by endocytosis or macropinocytosis (Kerkis *et al.*, 2006; Futaki *et al.*, 2007; Jones, 2007). The study of the intracellular pathway of PTDs has been complicated by several methodological factors. One of these factors is the difference that is observed when internalization is studied in live cells or fixed cells. Another challenge is the strength of the surface binding, which makes it difficult to differentiate between peptides bound to the cell surface and those that are in the endosomes or cytosol. Finally, the use of small-molecule inhibitors of internalization pathways has led to conflicting data. The effects of these drugs are often more diverse than is appreciated initially, and additional internalization pathways can be up-regulated when others are blocked (Patel *et al.*, 2007).

Once the PTD (with or without cargo) enters into endosomes or macropinosomes, however, a formidable challenge remains. In order to enter into the cytosol, the PTD must cross the lipid bilayer. This task is daunting for a heavily charged peptide, and even more so for cargo of varying sizes and hydrophobicity. This step on the internalization pathway

is thought to be rate limiting and remains the most mysterious in the process (Murriel and Dowdy, 2006).

The internalization of cytotoxic ribonucleases appears to be similar to that of PTDs. No receptor for cytotoxic ribonucleases has been identified (Wu *et al.*, 1993; Wu *et al.*, 1995; Haigis and Raines, 2003), and several lines of evidence suggest that there is no receptor. The binding of ribonucleases to the cell surface is not saturable up to 10 μM ribonuclease (Haigis and Raines, 2003), an amount that far exceeds typical IC_{50} values. Treatment of cells with proteases, which would be expected to destroy proteinaceous receptors, does not alter cell surface binding (Haigis and Raines, 2003). The addition of positive charge in a nonspecific manner has been shown to increase the cytotoxicity of ribonucleases (Futami *et al.*, 2001). Similarly, homolog-scanning mutagenesis suggests that mammalian cells do not have a specific receptor for BS-RNase (Kim *et al.*, 1995b). In addition, it would be quite unexpected to find a receptor for potentially toxic proteins, especially one for the amphibian protein, ONC, on the surface of mammalian cells.

Cytotoxicity of both ribonucleases in the ribonuclease A superfamily and those of bacterial origin has been shown to correlate with net positive charge (Ilinskaya and Makarov, 2005; Futami and Yamada, 2008). This observation has been exploited by a variety of means to enhance the cytotoxicity of both toxic and nontoxic ribonucleases. Methods of charge addition include chemical modification (Futami *et al.*, 2001; Futami *et al.*, 2002), site-directed mutagenesis (Ilinskaya *et al.*, 2002; Notomista *et al.*, 2006; Fuchs *et al.*, 2007), and the addition of protein transduction domains (Fuchs and Raines, 2005).

Chemical modification of carboxylic acid groups of RNase A with ethylenediamine, converting a negative charge to a positive charge, yielded a cytotoxic protein (Futami *et al.*, 2001). Interpretation of these results was complicated, however, by the concurrent decrease in RI binding and the heterogeneity of the chemically-modified protein (Futami *et al.*, 2002). A nontoxic, negatively charged (p*I* = 3.5) bacterial ribonuclease, ribonuclease Sa, was made cytotoxic by replacing five acidic residues with basic ones, resulting in a protein with a p*I* of 10.2 (Ilinskaya *et al.*, 2002). Replacing negatively charged residues with uncharged residues has been used to increase the cytotoxicity of dimeric variants of RNase A (Notomista *et al.*, 2006). The replacement of two negatively charged residues (Glu49 and Asp53) with arginine in the context of G88R RNase A, a variant that is cytotoxic due to evasion of RI, increased its cytotoxicity by 3-fold (Fuchs *et al.*, 2007). Finally, the addition of a PTD (nonaarginine; R_9) to the *C*-terminus of G88R RNase A also increased its cytotoxicity by 3-fold (Fuchs and Raines, 2005).

Specific regions of positive charge have been shown to play a role in the ability of members of the ribonuclease A superfamily to kill cells. Human eosinophilic cationic protein (ECP; RNase 3) (Lehrer *et al.*, 1989) and human ribonuclease 7 (RNase 7) (Zhang *et al.*, 2003) exhibit bacteriocidal activity that could proceed via pore formation followed by membrane disruption. This activity is distinct from the cytotoxic activity of ribonucleases in that catalytic activity is not required. Certain basic and aromatic residues of ECP have been shown to be essential for membrane disruption and bacteriocidal activity; the net charge or hydrophobicity is less important (Carreras *et al.*, 2003). Similarly, replacement of whole clusters of lysine residues on RNase 7 with uncharged

residues revealed that only a cluster located near the *N*-terminus was important for membrane permeability and antimicrobial activity (Huang *et al.*, 2007). Also, when the distribution of positive charges on RNase 1 was modified to include a nuclear localization sequence (an arginine triplet), but retain the same net charge, this protein acquired toxicity toward tumor cells (Bosch *et al.*, 2004).

It should be emphasized that these examples differ significantly from other cytotoxic ribonucleases, such as ONC and RNase A variants, which do not exhibit antimicrobial activity or contain nuclear localization sequences. Membrane disruption, however, could play a role in the translocation of ribonucleases from endosomes to the cytosol. This hypothesis is supported by the observation that the cytotoxicity of dimeric variants of RNase A correlates with their ability to disrupt lipid vesicles (Notomista *et al.*, 2006).

1.5 Coulombic forces in RI binding

The physiological role of RI is largely unknown (Dickson *et al.*, 2005). It is expressed ubiquitously in all mammalian cell types. Based on the observation that RI binds tightly to secreted ribonucleases, it is thought that RI might protect cells against invading ribonucleases (Haigis *et al.*, 2003). The extremely tight complex that is formed between RI and angiogenin (ANG), a ribonuclease that has a role in the formation of new blood vessels, suggests a function for RI in angiogenesis (Shapiro and Vallee, 1987; Lee *et al.*, 1989b). The high number of reduced cysteine residues in RI (32 in the human homologue) (Lee *et al.*, 1988) and the high sensitivity of the protein to oxidation, have

led to the evaluation of RI as an oxidative sensor (Wang and Li, 2006; Monti *et al.*, 2007).

The RI–ribonuclease interaction, like many protein–protein interactions, occurs via a two-step process (Lee *et al.*, 1989a; Vicentini *et al.*, 1990). The first step, the formation of the "encounter complex," involves long-range interactions and is typically dictated by electrostatic forces. The second step involves short-range interactions and requires structural rearrangement of the binding partners and expulsion of water from the interface (Schreiber and Fersht, 1996; Selzer and Schreiber, 1999).

RI is an anionic protein, with a p*I* of 4.7 (Dickson *et al.*, 2005). The surfaces of ribonucleases display a well-conserved charge distribution. Ribonucleases of the RNase A superfamily are highly cationic (Figure 1.2), their surfaces dominated by the positively charged residues lysine and arginine. In addition, ribonucleases display much of their cationicity in their active sites, where the negatively charged substrate, RNA, binds (Wlodawer *et al.*, 1988; Mazzarella *et al.*, 1993; Mosimann *et al.*, 1994; Johnson *et al.*, 2007c).

The interaction of RI with members of the RNase A superfamily is one of the tightest known protein–protein interactions in all of biology. The evolutionary imperative for this interaction is thought to be the danger to the cells resulting from the internalization of rogue ribonucleases (Haigis *et al.*, 2003). The basis for the tight interaction is the large amount of buried surface area and high charge complementarity of the interface. The shape complementarity (*i.e.*, the amount of "knobs" and "holes") is actually lower than that normally observed in protein–protein interfaces (Kobe and Deisenhofer, 1996). The

high amount of charge complementarity results in a rate of association near the diffusion limit (10^8 $M^{-1}s^{-1}$) (Johnson *et al.*, 2007c). This high rate of association is consistent with the role of RI as a mean of protection of the cell from adventitiously expressed ribonucleases.

The high degree of charge complementarity of these binding partners leads to a sensitivity of the interaction to changes in the charge of the proteins, as well as to the salt concentrations of buffers. For example, the neutralization of RNase 1 by site-directed mutagenesis led to a decrease in RI binding (Johnson *et al.*, 2007a). In addition, the binding of placental RI to RNase A was shown to be highly sensitive to salt concentration (Lee *et al.*, 1989b).

1.6 Ribonucleases as viral therapeutics

The ability of ribonucleases to be toxic to cells in a manner that is dependent on their ribonucleolytic activity has led to their evaluation as potential drugs that target RNA viruses. Certainly, all cells are dependent on RNA for their proper function. RNA viruses, though, are particularly vulnerable to RNA degradation, as their entire genome can be rendered indecipherable by cleavage with ribonucleases. Indeed, it has been observed that RNase A and other ribonucleases can inhibit HIV replication in concentrations that are nontoxic to the infected cells (Youle *et al.*, 1994; Bedoya *et al.*, 2006). In addition, the design of a zymogen of RNase A to specifically kill cells infected with hepatitis C, an RNA virus, has been described (Johnson *et al.*, 2006).

This thesis will examine the role of Coulombic interactions in the cellular entry (CHAPTER 2) and RI-interaction (CHAPTER 3) of cytotoxic ribonucleases. For these studies, the focus will be on ONC, the prototypical cytotoxic ribonuclease. In addition, the design of a cytotoxic ribonuclease that targets HIV-infected cells will be described in CHAPTER 4. Finally, in CHAPTER 5, several potential future directions of these studies will be proposed.

Figure 1.1 Crystalline structures of ribonucleases. (*A*) Three-dimensional structure of RNase A (PDB entry 7rsa) (Wlodawer *et al.*, 1988). (*B*) Three-dimensional structure of RNase 1 (from PDB entry 1z7x) (Johnson *et al.*, 2007c). (*C*) Three-dimensional structure of ONC (PDB entry 1onc) (Mosimann *et al.*, 1994). (*D*) Three-dimensional structure of the domain-swapped dimeric form of BS-RNase (PDB entry 1bsr) (Mazzarella *et al.*, 1993). Images were generated with the program MacPyMOL (DeLano Scientific, South San Franscisco, CA).

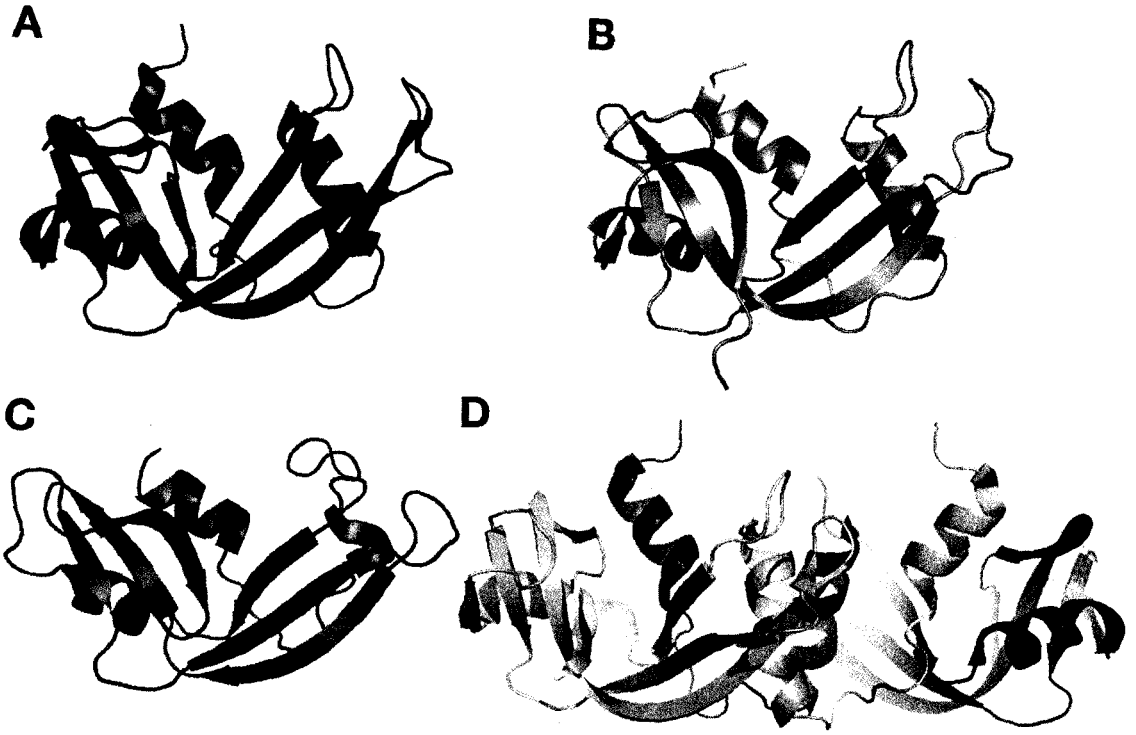
A
B
C
D

Figure 1.2 Structure-based sequence alignment of amphibian ribonucleases (modified from (Ardelt *et al.*, 2008)). ONC and amphinase (from *Rana pipiens*), cSBL (from *Rana catasbeiana*), and RNase A are shown. Conserved residues are enclosed in black boxes. Positively charged residues are shown in blue and negatively charged residues are shown in red. The secondary structure of ONC is identified with h (α-helix), s (β-strand), or t (turn). Sequence numbering corresponds to ONC.

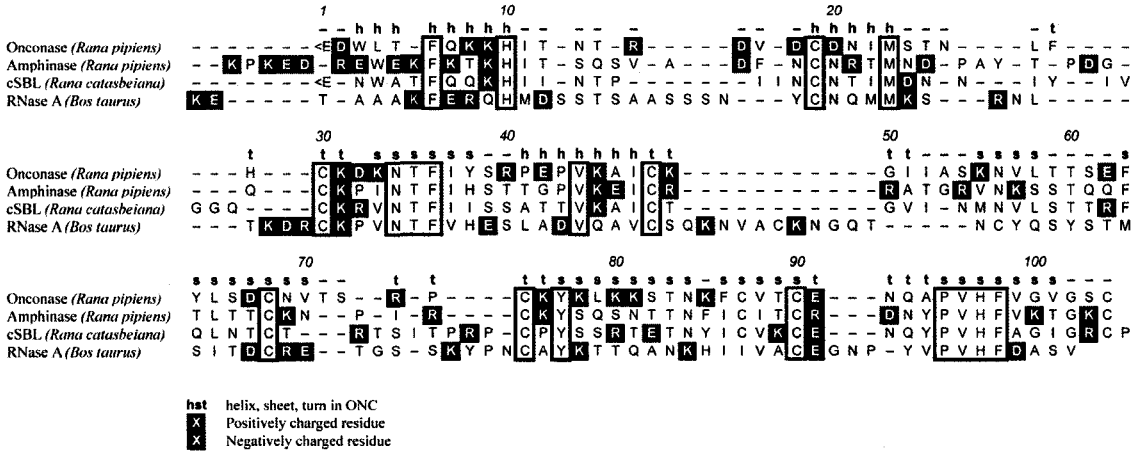
Onconase (Rana pipiens)
Amphinase (Rana pipiens)
cSBL (Rana catasbeiana)
RNase A (Bos taurus)
hst helix, sheet, turn in ONC
Positively charged residue
Negatively charged residue

Figure 1.3 Putative mechanism of ribonuclease cytotoxicity (Rutkoski *et al.*, 2005; Johnson *et al.*, 2007a). (*A*) A ribonuclease binds to the cell surface via electrostatic interactions. (*B*) The ribonuclease is internalized by endocytosis, and translocates from endosomes into the cytosol. (*C*) If the ribonuclease does not interact with RI, it is free to hydrolyze RNA, resulting in cell death by apoptosis. (*D*) If the ribonuclease does interact with RI, it is not cytotoxic. The ribonuclease is depicted as a blue kidney-shaped cartoon; RI is shown as a red horseshoe-shaped cartoon.

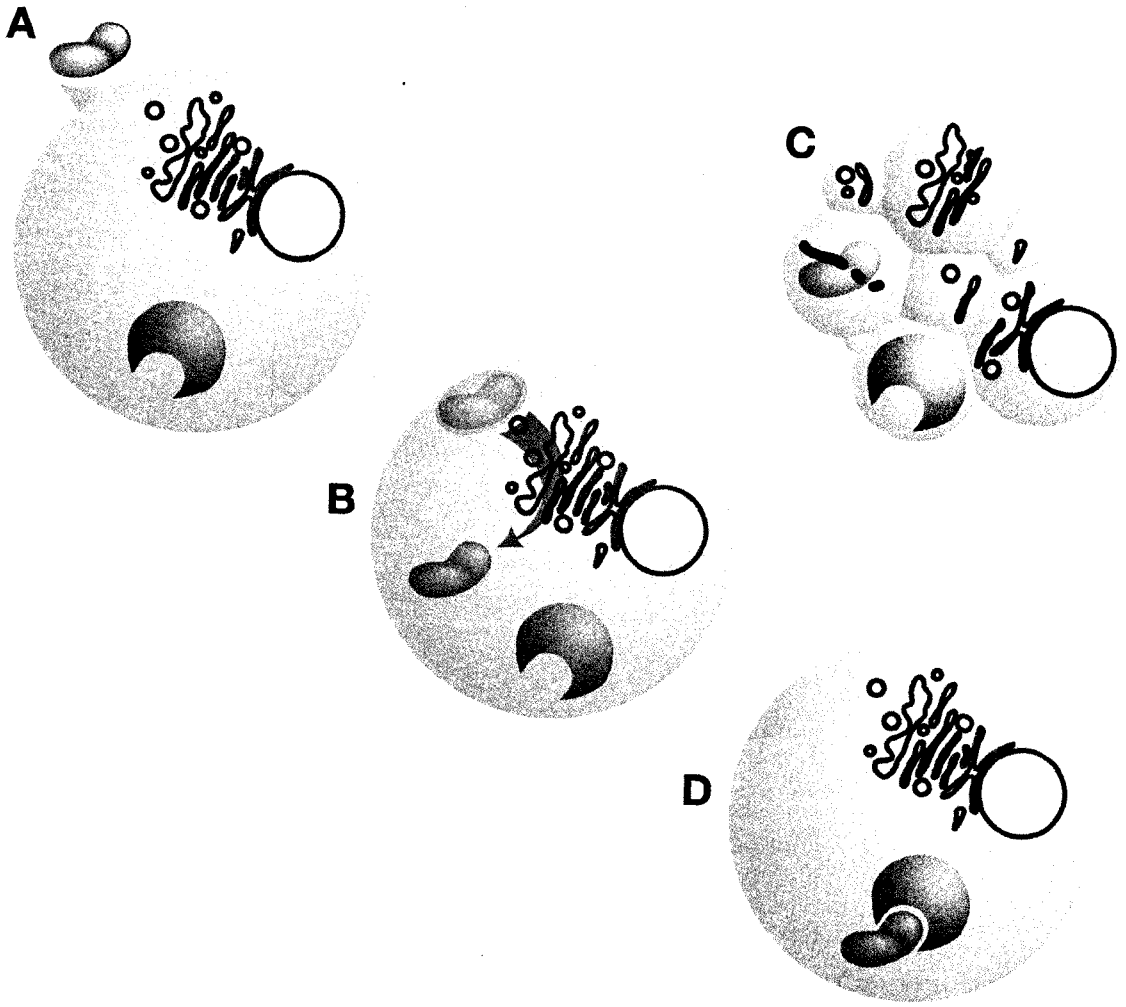
A
B
C
D

CHAPTER 2

Onconase Cytotoxicity Relies on the Distribution of its Positive Charge

Prepared for submission to *Biochemistry* as:
Turcotte, R.F. and Raines, R.T. (2008) Onconase Cytotoxicity Relies on the Distribution of its Positive Charge.

2.1 Abstract

Onconase® (ONC) is a member of the ribonuclease A superfamily that is toxic to cancer cells *in vitro* and *in vivo*. ONC is now in Phase IIIb clinical trials for the treatment of malignant mesothelioma. Internalization of ONC to the cytosol of cancer cells is essential for its cytotoxic activity, despite the apparent absence of a cell-surface receptor protein. Endocytosis and cytotoxicity do, however, appear to correlate with the net positive charge of ribonucleases. To probe the role of cationic residues and their distribution on cytotoxicity, arginine and lysine residues of ONC were replaced systematically with alanine. Variants with the same net charge as well as equivalent catalytic activity and conformational stability exhibited large (>10-fold) differences in toxicity for the cells of a human leukemia line. In addition, a more cationic ONC variant can be either much more cytotoxic or much less cytotoxic than a less cationic variant, depending on the distribution of its cationic residues. The endocytosis of variants with widely divergent cytotoxic activity was quantified by flow cytometry using a small-molecule fluorogenic label, and was found to vary by twofold or less. This small difference in endocytosis did not account for the large difference in cytotoxicity, implicating the distribution of cationic residues as being critical to lipid-bilayer translocation subsequent to endocytosis. This finding has fundamental implications for the interaction of ribonucleases and other proteins with mammalian cells.

2.2 Introduction

Several homologues and variants of bovine pancreatic ribonuclease (RNase A) (Raines, 1998; Marshall *et al.*, 2008) exhibit antitumoral activity (Leland and Raines, 2001; Matoušek, 2001; Makarov and Ilinskaya, 2003; Benito *et al.*, 2005; Arnold and Ulbrich-Hofmann, 2006). The molecular basis for this extraordinary attribute is under intense scrutiny in several laboratories (Arnold, 2008). These efforts are providing many insights. For example, cytotoxic ribonucleases are known to catalyze the indiscriminate degradation of RNA (Ardelt *et al.*, 1991; Kim *et al.*, 1995a; Leland *et al.*, 2000), even in the presence of the ribonuclease inhibitor protein (RI) that binds to RNase A with nearly femtomolar affinity (Wu *et al.*, 1993; Kim *et al.*, 1995c; Leland *et al.*, 1998; Haigis *et al.*, 2003; Dickson *et al.*, 2005; Rutkoski *et al.*, 2005; Schulenburg *et al.*, 2007; Rutkoski and Raines, 2008). They have high conformational stability and resistance to proteolysis (Klink and Raines, 2000; Kim *et al.*, 2004). Lastly, cytotoxic ribonucleases enter the cytosol of cells (Haigis and Raines, 2003; Leich *et al.*, 2007; Benito *et al.*, 2008), a remarkable feat that appears to correlate with net positive charge (Ilinskaya and Makarov, 2005; Futami and Yamada, 2008).

Onconase® (ONC) (Ardelt *et al.*, 2008; Lee and Raines, 2008), an RNase A homologue from the Northern leopard frog *Rana pipiens*, is toxic to tumor cells both *in vitro* and *in vivo* (Darzynkiewicz *et al.*, 1988; Mikulski *et al.*, 1990a). Cells exposed to ONC die via an apoptotic mechanism (Iordanov *et al.*, 2000; Leland *et al.*, 2001; Grabarek *et al.*, 2002). A Phase IIIb clinical trial of ONC in combination with

doxorubicin for the treatment of malignant mesothelioma is currently nearing completion (Costanzi *et al.*, 2005; Pavlakis and Vogelzang, 2006). Side effects of ONC treatment include dose-limiting renal toxicity that is reversible upon discontinuation of the drug (Costanzi *et al.*, 2005). Surprisingly, allergic response is minimal, even following repeated infusions, an attribute that might result from an increase in activation-induced apoptosis of lymphocytes exposed to ONC (Halicka *et al.*, 2002).

ONC is a single-domain protein with 104 amino-acid residues and a molecular mass of 11.8 kDa (Ardelt *et al.*, 1991). Its two-lobed structure is characteristic of the ribonuclease A superfamily (Figure 2.1) (Mosimann *et al.*, 1994). Two lysine residues, Lys9 and Lys31, stabilize the transition state during cleavage of an RNA substrate (Lee and Raines, 2003). The *N*-terminal residue of ONC is an unusual pyroglutamate that forms a hydrogen bond with Lys9, positioning it properly for catalysis (Lee and Raines, 2003; Lee *et al.*, 2008).

Physicochemical attributes of ONC suggest why it is an especially efficacious cytotoxin. First, ONC does not interact with RI under physiological conditions (Boix *et al.*, 1996). Second, ONC has extreme conformational stability (T_m ~90 °C) (Leland *et al.*, 1998; Arnold *et al.*, 2006). Third, ONC is a highly basic protein (Z = +5; pI >9.5) (Ardelt *et al.*, 1991), which could facilitate its cytosolic entry (Futami *et al.*, 2001; Ilinskaya and Makarov, 2005; Fuchs *et al.*, 2007).

Several lines of evidence suggest that cytosolic entry limits the cytotoxicity of ONC. For example, ONC is more toxic when injected directly into cells (Smith *et al.*, 1999), or

when internalization is aided by either lipofection (Iordanov *et al.*, 2000) or conjugation to a targeting antibody (Newton *et al.*, 2001; De Lorenzo and D'Alessio, 2008). Other protein toxins, such as Shiga toxin, cholera toxin, and ricin, contain two domains, one that binds to the cell surface and another that exerts a toxic effect in the cytosol (Sandvig *et al.*, 2004). ONC differs in that its single domain accomplishes both cytosolic entry and cytotoxicity.

No cell-surface receptor for ONC has been identified to date (Wu *et al.*, 1993; Wu *et al.*, 1995; Haigis and Raines, 2003). The binding of ONC to HeLa cells in culture is not saturable at ONC concentrations ($\leq$10 μM) that far exceed its lethal dose (Haigis and Raines, 2003). The different composition of the cancer-cell surface compared to that of normal cells could target ribonucleases selectively to cancer cells (Leland and Raines, 2001; Haigis and Raines, 2003; Benito *et al.*, 2005), thereby contributing to the favorable therapeutic index that has been observed in animal models and human trials (Mikulski *et al.*, 1990a; Pavlakis and Vogelzang, 2006). For example, the surface of cancer cells exhibits major changes in heparan sulfate glycosaminoglycan profile (Sasisekharan *et al.*, 2002), phospholipid composition (Bergelson *et al.*, 1970; Ran *et al.*, 2002), and ganglioside display (Fredman *et al.*, 2003).

Internalization of ONC is an energy-dependent process, and acidification of endosomes is not a requirement for cytosolic entry (Wu *et al.*, 1993; Haigis and Raines, 2003). Indeed, studies on purified endosomes suggest that increasing endosomal pH (toward neutrality) actually *increases* translocation (Rodriguez *et al.*, 2007). The effects of drugs that alter Golgi trafficking suggest that this route is not a productive one for

ONC (Wu *et al.*, 1993; Wu *et al.*, 1995; Haigis and Raines, 2003). Recent work suggests that ONC enters cells via AP2/clathrin-mediated endocytosis, followed by routing through recycling endosomes (Rodriguez *et al.*, 2007). These studies on the internalization of ONC should be interpreted with caution, however, as the treatment with small-molecule drugs and metabolic inhibitors can have diverse effects on cellular trafficking. Studies in a HeLa cell line that was overexpressing a dominant-negative mutant of dynamin suggest that ONC internalization does not occur via a dynamin-dependent endocytic pathway (Haigis and Raines, 2003).

The cytotoxicity of ribonucleases seems to correlate with their net positive charge (Ilinskaya and Makarov, 2005; Futami and Yamada, 2008). Specifically, adding positive charge via site-directed mutagenesis (Ilinskaya *et al.*, 2002; Notomista *et al.*, 2006; Fuchs *et al.*, 2007), appending protein transduction domains (Fuchs and Raines, 2005), and chemical modification (Futami *et al.*, 2001; Futami *et al.*, 2002) enhances the cytotoxicity of toxic or nontoxic ribonucleases. Rigorous interpretation of these results is confounded, however, by concurrent changes in the affinity for RI and by the heterogeneity of chemically-modified proteins (Futami *et al.*, 2001).

As ONC does not have a measurable affinity for RI, we reasoned that it was the ideal RNase A homologue for a definitive analysis of the role of positive charge in cellular internalization and cytotoxicity. Here, we report on such an analysis, based on the systematic alteration of the arginine and lysine residues of ONC. We find that the net charge of an ONC variant has little effect on cytotoxicity. Rather, the *distribution* of that charge is critical.

2.3 Experimental Procedures

2.3.1 Materials

K-562 cells were derived from a continuous human chronic myelogenous leukemia cell line, and obtained from American Type Culture Collection (Manassas, VA). *Escherichia coli* BL21(DE3) cells and pET22b(+) plasmid were from Novagen (Madison, WI).

Enzymes were obtained from Promega (Madison, WI). 6-Carboxyfluorescein–dArUdGdA–6-carboxytetramethylrhodamine (6-FAM–dArUdGdA–6-TAMRA) (Kelemen *et al.*, 1999; Lee and Raines, 2003) was obtained from Integrated DNA Technologies (Coralville, IA). Cell culture medium and supplements were from Invitrogen (Carlsbad, CA). [*methyl*-^{3}H]Thymidine (6.7 Ci/mmol) was from Perkin–Elmer (Boston, MA). MES buffer (Sigma–Aldrich, St. Louis, MO) was purified by anion-exchange chromatography to remove oligo(vinylsulfonic acid) (OVS), a potent inhibitor of ribonucleases (Smith *et al.*, 2003). All other chemicals used were of commercial grade or better, and were used without further purification.

2.3.2 Analytical instruments

Molecular mass was measured by MALDI–TOF mass spectroscopy using a Voyager-DE-PRO Biospectrometry Workstation (Applied Biosystems, Foster City, CA). Fluorescence measurements were made with a QuantaMaster1 photon-counting fluorometer equipped with sample stirring (Photon Technology International, South

Brunswick, NJ). CD experiments were performed in the University of Wisconsin–Madison Biophysics Instrumentation Facility with a model 62A DS CD spectrophotometer equipped with a temperature controller (Aviv, Lakewood, NJ). Radioactivity was quantified by scintillation counting using a Microbeta TriLux liquid scintillation counter (Perkin–Elmer, Wellesley, MA). Flow cytometry data were collected in the University of Wisconsin Paul P. Carbone Comprehensive Cancer Center with a FACSCalibur flow cytometer equipped with a 488-nm argon-ion laser (Becton Dickinson, Franklin Lakes, NJ).

2.3.3 Production of ribonucleases

DNA encoding ONC variants was created with the plasmid pONC (Lee and Raines, 2003) and the Quikchange site-directed mutagenesis kit (Strategene, La Jolla, CA). Wild-type RNase A was purified as described previously (Leland *et al.*, 1998). ONC variants were purified as described previously (Leland *et al.*, 1998), with the following exceptions. ONC variants were refolded overnight at room temperature following slow dilution (by 10-fold) into 0.10 M Tris–HCl buffer, pH 8.0, containing NaCl (0.10 M), reduced glutathione (3.0 mM), and oxidized glutathione (0.6 mM). Following concentration by ultrafiltration, samples were dialyzed overnight versus 50 mM sodium acetate buffer, pH 5.0, containing NaCl (0.10 M), and applied to a MonoS cation-exchange FPLC column (Pharmacia). ONC variants were eluted from the column with a linear gradient of NaCl (0.15–0.3 M) in 50 mM sodium acetate buffer, pH 5.0. Protein

concentrations were determined by UV spectroscopy using extinction coefficients of ε_{280} = 0.87 $(mg/mL)^{-1} \cdot cm^{-1}$ for ONC and its variants, and ε_{278} = 0.72 $(mg/mL)^{-1} \cdot cm^{-1}$ for RNase A (Leland *et al.*, 1998).

2.3.4 Production of labeled ONC variants

Variants of ONC with a free cysteine at position 61 were protected by reaction with 5,5′-dithio-bis(2-nitrobenzoic acid) (DTNB) (Riddles *et al.*, 1983; Lavis *et al.*, 2006) following gel filtration chromatography, then dialyzed overnight versus 20 mM sodium acetate buffer, pH 5.0. Samples were applied to a MonoS cation-exchange column as described above. Prior to latent-fluorophore attachment, TNB-protected ONC variants were deprotected with a 5-fold molar excess of dithiothreitol (DTT), then desalted by using a PD-10 desalting column (GE Biosciences, Piscataway, NJ). Maleimido-containing latent fluorophore (Lavis *et al.*, 2006) was a kind gift of L.D. Lavis. Deprotected proteins were reacted for 4–6 h at 25 °C with a 10-fold excess of latent fluorophore. Conjugates were purified by using a HiTrap SP HP column (GE Biosciences, Piscataway, NJ). Concentrations of conjugates were determined with a bicinchoninic acid (BCA) assay kit from Pierce (Rockford, IL) with bovine serum albumin (BSA) as a standard.

2.3.5. Measurements of conformational stability

Conformational stability of wild-type ONC and its variants was determined by CD spectroscopy, as described previously (Lee and Raines, 2003), with the following modifications. A solution of ONC (0.2 mg/mL) in PBS was heated from 55 to 99 °C in 2-°C increments, and the change in molar ellipticity at 204 or 209 nm was monitored following a 5-min equilibration at each temperature. CD data were fitted to a two-state model for denaturation to determine the T_m values (Pace *et al.*, 1989).

2.3.6 Assays of catalytic activity

Ribonucleolytic activity of ONC and its variants was measured by using a hypersensitive fluorogenic substrate, 6-FAM–dArUdGdA–6-TAMRA, as described previously (Kelemen *et al.*, 1999; Lee and Raines, 2003). Briefly, fluorescence increase at 515 nm (following excitation at 492 nm) in the presence of ONC and its variants was measured in 0.10 M MES–NaOH (OVS-free) buffer, pH 6.0, containing NaCl (0.10 M), 6-FAM–dArUdGdA–6-TAMRA (50 nM), and human ribonuclease inhibitor (1 nM) at 23 ± 2 °C. This pH value is close to the pH-optimum for catalysis by ONC (Lee *et al.*, 2008). Values of k_{cat}/K_M were calculated with the equation:

$$k_{cat}/K_M = \left(\frac{\Delta I/\Delta t}{I_{max} - I_0}\right)\frac{1}{[\text{ribonuclease}]} \qquad (2.1)$$

where $\Delta I/\Delta t$ represents the initial reaction velocity, I_{max} is the fluorescence following complete cleavage of the substrate by excess RNase A, and I_0 is the fluorescence prior to addition of ribonuclease.

2.3.7 Assays of cytotoxicity

K-562 and other mammalian cells exposed to cytotoxic ribonucleases die in an apoptotic manner, and assays of cell proliferation report on the cytotoxic activity of ribonucleases (Iordanov *et al.*, 2000; Leland *et al.*, 2001; Grabarek *et al.*, 2002). The effect of ONC, its variants, and RNase A on the proliferation of K-562 cells was measured by monitoring the incorporation of [*methyl*-^{3}H]thymidine into cellular DNA as described previously (Lee and Raines, 2003). Experiments were repeated three times in triplicate. Values for IC_{50} were determined by fitting the curves by nonlinear regression to the following equation:

$$y = \frac{100\%}{1+10^{(\log(IC_{50})-\log[\text{ribonuclease}])h}} \tag{2.2}$$

In equation (2), y is the total DNA synthesis following the [*methyl*-^{3}H]thymidine pulse, and h is the slope of the curve.

2.3.8 Flow cytometry

The internalization of ONC variants conjugated to the latent fluorophore was followed by monitoring the increase in fluorescence following exposure to intracellular esterases, as described previously (Johnson *et al.*, 2007a). Briefly, K-562 cells at near-confluency were collected by centrifugation and resuspended at a density of 1×10^6 cells/mL in RPMI 1640 medium. Labeled or unlabeled ONC (10 μM final concentration) was added to 250 μL of these cells, which were then incubated for varying times at 37 °C. To stop internalization, cells were placed on ice, then collected by centrifugation and resuspended in ice-cold PBS. Cells were kept on ice until analysis by flow cytometry.

Fluorescence was detected with a 530/30-nm band-pass filter. Cell viability was determined by staining with propidium iodide, detected with a 660-nm long-pass filter. The mean channel fluorescence intensity of 10,000 or 20,000 viable cells was determined with WinList software (Verity Software House, Topsham, ME).

2.4 Results

2.4.1 Design of ONC variants

ONC contains a total of 15 positively charged residues (3 Arg and 12 Lys; Table 2.1). The electrostatic potential map of ONC (PDB entry 1ONC; Figure 2.1(a) and (b)) (Mosimann *et al.*, 1994) reveals three regions other than the active site that contain a high density of positive charge at neutral pH. These "patches" each contain three positively charged residues. Patch 1 consists of Lys45, Lys49, and Lys55; Patch 2 is comprised of

Arg15, Lys80, and Lys81; and Patch 3 includes Arg73, Lys76, and Lys78 (Figure 2.1(c) and (d)). The remaining six positively charged residues are within the active site (Lys9 and Lys31), proximal to the active site (Lys8 and Lys33), or form small, isolated regions of positively charged surfaces (Arg40 and Lys85), and thus were not included in this analysis.

We began by replacing all of the arginine and lysine residues within each patch with alanine. If net charge were the key to ONC cytotoxicity, then a variant with three substitutions distributed across the three patches would manifest the same cytotoxicity as the three patch variants. We created such a variant, R15A/K49A/R73A ONC, by replacing the three residues that were at the geometric "center" of the patches (that is, having the shortest distance to the other two residues, as measured from C^{ε} of arginine and N^{ε} of lysine), as well as two other distributed variants, R15A/K45A/K76A ONC and R15A/K55A/K76A ONC.

To test the hypothesis that the detailed structure of the patches is important for cytotoxicity, doubly-substituted variants were designed and created. These variants had all nine ($= {}_3C_2 \times 3$) of the possible permutations of two residues in the three variants with abolished cytotoxicity (that is, R15A/K80A/K81A ONC, R73A/K76A/K78A ONC, and R15A/K49A/R73A ONC; Table 2.2).

To ascertain the relative importance of residues 15, 73, 76, 78, 80, and 81 from Patches 2 and 3 in the cytotoxicity of ONC, each of these residues was replaced

individually with alanine. The variant K49A ONC was also made, prompted by the abolished cytotoxicity of the distributed variant, R15A/K49A/R73A ONC.

Position 61 was chosen for the labeling of ONC variants with a fluorogenic probe that enables a quantitative measure of endocytosis. Although the D16C (Haigis and Raines, 2003) and S72C (Rodriguez *et al.*, 2007) substitutions had been used previously to label ONC, we preferred to avoid any changes in charge (even negative charge), and also wanted to choose a position remote from the active site and all three patches. Ser61 met both of these criteria, and was replaced with a cysteine residue to create an S61C variant.

All labeled and unlabeled variants were ~95% pure according to SDS–PAGE, and the identities of all purified proteins and conjugates were confirmed by matrix-assisted laser desorption/ionization time-of-flight (MALDI–TOF) mass spectrometry (Table 2.4).

2.4.2 Cytotoxicity

2.4.2.1 Triple variants

The three patch variants, K45A/K49A/K55A ONC (Patch 1), R15A/K80A/K81A ONC (Patch 2), and R73A/K76A/K78A ONC (Patch 3) were assayed for toxicity toward K-562 cells, a leukemic cell line (Figure 2.2(a)). Wild-type ONC is toxic to K-562 cells with an IC_{50} value of approximately 0.3 μM. K45A/K49A/K55A ONC retained measurable, albeit severely reduced, cytotoxicity (IC_{50} = 8.2 μM). The R15A/K80A/K81A and R73A/K76A/K78A variants, however, lost all measurable cytotoxicity.

The first distributed variant, R15A/K49A/R73A ONC, was not cytotoxic. Two other variants with distributed substitutions, R15A/K45A/K76A ONC and R15A/K55A/K76A ONC, had higher cytotoxicity (Figure 2.2(b)).

2.4.2.2 Double variants

The double variants can be divided into three subsets based on their cytotoxic activity. Three variants, R15A/K80A, R15A/K81A, and R73A/K76A, retain relatively high cytotoxicity (IC_{50} values of 1.5–2.7 μM; Figure 2.3(a)). Three, K80A/K81A, R15A/K49A, and R15A/R73A, possess intermediate cytotoxicity (IC_{50} values of 4.7–6.2 μM; Figure 2.3(b)). Finally, three variants, R73A/K78A, K76A/K78A, and K49A/R73A, have nearly abolished, but measurable, cytotoxicity (IC_{50} values of 10.5–11.8 μM; Figure 2.3(c)).

2.4.2.3 Single variants

All of the singly-substituted variants of ONC — R15A, K49A, R73A, K76A, K78A, K80A, and K81A — had IC_{50} values that were within 5-fold of that of wild-type ONC and within error of each other (Table 2.3). The IC_{50} values for the single, double, and triple variants of ONC are depicted together in Figure 2.4.

2.4.3 Ribonucleolytic activity

The ability to cleave a fluorogenic tetranucleotide RNA substrate was measured for each variant of ONC. All variants had ribonucleolytic activity within 5-fold of that of the

wild-type enzyme (Table 2.3). This result indicates both that any observed decrease in cytotoxicity was not due to a decrease in ribonucleolytic activity, which is required for cytotoxicity (Schulenburg *et al.*, 2007), and that the variants had attained the correct three-dimensional structure, as catalytic activity is an exquisite indicator of native tertiary structure (Knowles, 1987).

2.4.4 Conformational stability

Like ribonucleolytic activity, conformational stability correlates with the cytotoxicity of ribonucleases (Klink and Raines, 2000). Therefore, the decrease in cytotoxicity observed in these variants could have been due to a decrease in stability. To determine the contribution of this attribute, the values of T_m (which is the temperature of the midpoint of the denaturation curve) of all of the triple variants and the double variants with low or moderate cytotoxicity were measured by thermal denaturation monitored by circular dichroism (CD) spectroscopy. The T_m values of these variants were similar to those of the wild-type protein, and were >>37 °C (Table 2.3). The modest differences in T_m values did not correlate with cytotoxicity.

2.4.5 Endocytosis

Several variants were selected in order to test their ability to enter the endosomes of K-562 cells. Using a strategy based on the "trimethyl lock" (TML), our laboratory has developed a method to observe the endocytosis of proteins in unwashed cells (Lavis *et*

al., 2006; Johnson *et al.*, 2007a). Briefly, a protein is labeled with a fluorogenic probe (Figure 2.5(a)) that is unmasked by nonspecific esterases in endosomes or the cytosol. The resulting fluorescence is then quantified by flow cytometry. By this method, the cellular internalization of wild-type ONC was found to be much less efficient than that of human pancreatic ribonuclease (RNase 1) (Figure 2.5(b)). *In vitro* activation of the labeled ribonucleases with porcine liver esterase revealed a twofold difference in the fluorescence intensity of labeled ONC and RNase 1 (data not shown), a difference that does not account for the >10-fold difference observed in the flow cytometer.

One pair of ONC variants, the triply-substituted pair, exhibited a significant difference in their ability to be endocytosed into K-562 cells. R15A/K55A/K76A/S61C–TML ONC appeared to enter endosomes twice as well as did R15A/K80A/K81A/S61C–TML ONC. The other variants, including K9A/K31A/S61C–TML ONC, differed little from the positive control, S61C–TML ONC (Figure 2.5(c)).

2.5 Discussion

ONC is able to kill cancer cells specifically (Darzynkiewicz *et al.*, 1988; Mikulski *et al.*, 1990a; Wu *et al.*, 1993; Pavlakis and Vogelzang, 2006), an attribute that is dependent on its ability to enter the cytosol. Much has been learned about this process. Still, many aspects remain mysterious. For example, the molecular basis for cytosolic entry is unclear. The chemical cationization of other ribonucleases has been shown to increase their cytotoxicity (Futami *et al.*, 2001; Ilinskaya *et al.*, 2002; Fuchs and Raines, 2005;

Fuchs *et al.*, 2007), suggesting that positive charge is important for cytosolic entry and, hence, the cytotoxicity of ONC and other ribonucleases. Because ONC does not bind to RI under physiological conditions (Boix *et al.*, 1996), it is an attractive model for the examination of internalization with minimal obfuscation. Accordingly, we set out to delineate the relative importance of various regions of positive charge on the surface of ONC to its cytotoxicity.

2.5.1 Importance of Patch 3 (R73/K76/K78) and K49 in cytotoxicity

The replacement of three positively charged patches on the surface of ONC (Figure 2.1) resulted in variants with disparate cytotoxic activities, with only the K45/K49/K55 variant (Patch 1) retaining measurable cytotoxicity (Figure 2.2(a); Table 2.3). This result indicates that charge distribution is critical for the cytotoxicity of ONC, and that Patches 2 and 3 are relatively important in this process.

Variants with two substitutions within each patch provided additional insight. The three variants that resulted from Patch 2 did not exhibit major changes in cytotoxicity, with two retaining high cytotoxicity and one having moderate cytotoxicity (Figure 2.4). Of the three variants from Patch 3, however, two had low cytotoxicity and one retained high cytotoxicity. These data, combined with the replacement of each patch in turn (above), suggest that Patch 3 is the most important of the three patches for the cytotoxicity of ONC.

The results for the cytotoxicity of the three variants in which substitutions were distributed among the patches suggest that the detailed character of the three patches is

important, as these three variants differed widely in cytotoxic activity (Figure 2.2(b); Table 2.3). In an attempt to determine the relative contributions of each residue to the loss of cytotoxicity, all residues in Patches 2 and 3, plus residue 49 from the distributed variant with no cytotoxicity, were each replaced in turn with alanine. The IC_{50} values for these variants were all within 5-fold of that for wild-type ONC (Table 2.3), indicating that no individual positively-charged residue is critical for cytotoxicity. Rather, the cationic residues on ONC appear to act in a degenerate manner, as expected for the manifestation of a nonspecific interaction with anionic membrane components.

To determine if a particular pair of residues is most responsible for internalization and cytotoxicity, we made double substitutions within R15A/K49A/R73A ONC, in addition to the double substitutions from Patches 2 and 3 (above). The residues of Patch 3 and Lys49 comprise all of the residues whose replacement in the doubly-substituted variants results in the lowest cytotoxicity (Figure 2.3(c)). Indeed, replacement of Lys49 and Arg73 resulted in the largest loss of cytotoxicity in a doubly-substituted variant. Interestingly, these residues are 45 Å apart. This result is consistent with multivalent binding of ONC to anionic membrane components, such as the sulfuryl groups of heparan-sulfate proteoglycans and the carboxyl groups of sialic acid-containing gangliosides.

Depicting the cytotoxic activity of wild-type ONC and all 22 variants studied herein as a function of their net molecular charge provides additional insight (Figure 2.4). In addition to showing that variants with the same net charge differ in their cytotoxic activity, this portrayal indicates that more cationic variants tend to be more cytotoxic, but

are not necessarily so. An ONC variant with $Z = +3$ can be either much more cytotoxic or much less cytotoxic than a variant with $Z = +2$, depending on the distribution of its cationic residues. Moreover, when an arginine or lysine residue is added to a particular variant with $Z = +2$ to form a variant with $Z = +3$, the location of that residue determines the cytotoxicity of the resultant variant. Finally, it is apparent that variants of ONC with charges ranging from +2 to +5 can have marked cytotoxic activity.

2.5.2 Cationic residues do not affect cellular binding and endocytosis

What is causing the differences in cytotoxicity that are seen in the alanine-substituted variants of ONC? The current model for the process of cell death for ONC-exposed cells can be divided into four steps (Figure 2.6). First, ONC binds to the cell surface, likely via interactions with negatively charged components of the plasma membrane. Then, bound ONC is internalized via endocytosis. Some ONC escapes from endosomes and translocates into the cytosol (Saxena *et al.*, 1991; Haigis and Raines, 2003). There, ONC cleaves RNA substrates (Ardelt *et al.*, 1991; Smith *et al.*, 1999; Suhasini and Sirdeshmukh, 2006), resulting in cell death by apoptosis (Iordanov *et al.*, 2000; Grabarek *et al.*, 2002). An additional requirement for cytotoxicity is that ONC and other cytotoxic ribonucleases be active catalysts at physiological temperature and not be susceptible to proteolysis (Klink and Raines, 2000).

The large differences among the ONC variants in their ability to kill cancer cells, combined with the small differences in their ribonucleolytic activity and conformational stability (Table 2.3), strongly suggest a role for cationic residues in the internalization

process. To delineate which step in the internalization process was being affected by the changes in positive charge, we attempted to observe endocytosis into live cells.

The relative endocytosis of selected ONC variants was observed by flow cytometry using a profluorophore that is activated by nonspecific esterases in the endocytic pathway (Figure 2.5). It should be noted that our flow cytometry assay of endocytosis also reports on cellular binding, which is a prerequisite for endocytosis. We observed that the endocytosis of labeled R15A/K55A/K76A and R15A/K80A/K81A ONC, whose IC_{50} values differ by more than 10-fold, differs by just twofold. Thus, R15A/K55A/K76A ONC enters endosomes twice as readily as does R15A/K80A/K81A ONC, which likely accounts for only a small portion of the difference in cytotoxicity. The endocytosis of labeled R15A/K81A did not differ significantly from that of labeled K49A/R73A, even though the IC_{50} values of the two variants differ by 10-fold.

In addition to the variants that were derived from the patches of positive charge on ONC, a variant in which the two active-site lysine residues (Lee *et al.*, 2008) were replaced with alanine, K9A/K31A ONC, was analyzed for its ability to enter cells by using flow cytometry (Figure 2.5(c)). It has been proposed that the active site of ribonucleases might play a special role in their internalization based on several observations. Computational analysis on RNase A revealed that the maximal electrostatic interaction energy between the protein and a negatively charged surface occurs with the active site of RNase A facing that surface (Yoon and Lenhoff, 1992). Additionally, glycosaminoglycans, such as heparan sulfate (HS), are similar to single-stranded nucleic acids in being highly anionic polymers. Indeed, anti-heparin antibodies bind to single-

stranded DNA and anti-DNA antibodies bind to HS, and heparin affinity chromatography has been used to purify DNA-binding proteins (Belting, 2003). It was thought that the active site of ONC, which binds to RNA and DNA (Lee and Raines, 2003; Lee *et al.*, 2008), might interact with HS on the cell-surface. Our data, however, show little difference between the endocytosis of labeled wild-type ONC and labeled K9A/K31A ONC, suggesting that these residues are not important for this process.

2.5.3 Potential role of cationic residues in translocation

It is clear from our data that particular cationic surface-residues of ONC, especially those in Patch 3 and Lys49, play a major role in the cytotoxicity of the protein. That role cannot be accounted for fully by differences in endocytosis (*vide supra*). Our data are consistent with these cationic residues instead mediating the translocation step of ONC. We are able to measure the sum of all of the steps of cytotoxicity (Figure 2.6). Binding and endocytosis are measured in the flow cytometric assay. Ribonucleolytic activity is measured as an isolated step in an *in vitro* assay. After ruling out effects on all steps other than translocation, we infer that Patch 3 and Lys49 are likely mediators of the translocation of ONC across the lipid bilayer.

Translocation is the most mysterious step in the process of ONC-induced cytotoxicity. The acidification of endosomes is not required for translocation (Wu *et al.*, 1993; Haigis and Raines, 2003), and, indeed, neutralization of endosomes increases translocation (Rodriguez *et al.*, 2007). It is highly unlikely that the protein unfolds to pass

through the cell membrane, as ONC would be unable to reform its four disulfide bonds (Mosimann *et al.*, 1994) in the reducing environment of the cytosol.

A correlation between the ability of dimeric variants of RNase A to disrupt membranes *in vitro*, and their ability to kill cancer cells has led to the hypothesis that the endocytic membrane is disrupted in the translocation process (Notomista *et al.*, 2006). Our data are consistent with this hypothesis. Specific regions of positive charge have been shown to play a role in the ability of members of the RNase A superfamily to disrupt cell membranes. Human eosinophilic cationic protein (ECP; RNase 3) (Lehrer *et al.*, 1989) and human ribonuclease 7 (RNase 7) (Zhang *et al.*, 2003) both exhibit bactericidal activity that is thought to proceed via pore formation followed by membrane disruption, similar to the actions of antimicrobial peptides (Henriques *et al.*, 2006). Certain basic and aromatic residues of ECP have been shown to be essential for membrane disruption and bactericidal activity, the net charge or hydrophobicity being less important (Carreras *et al.*, 2003). Similarly, replacement of clusters of lysine residues on RNase 7 with uncharged residues revealed that only a cluster located near the *N*-terminus was important for membrane permeability and antimicrobial activity (Huang *et al.*, 2007). Work is ongoing in our laboratory to exploit the trimethyl lock strategy for the direct observation of membrane translocation in live human cells.

2.5.4 Amphibian ribonucleases as cancer therapeutics

The intrinsic ability of ONC to kill cancer cells has led to its being the archetypal cytotoxic ribonuclease (Darzynkiewicz *et al.*, 1988; Lee and Raines, 2008) and,

accordingly, ONC will likely be the first ribonuclease to attain FDA approval as a cancer chemotherapeutic agent (Costanzi *et al.*, 2005; Pavlakis and Vogelzang, 2006). There are, however, several marks against ONC as a prospective drug. ONC, an amphibian ribonuclease, is retained in the kidneys to a much greater extent than is RNase 1, a human ribonuclease (Vasandani *et al.*, 1996), resulting in dose-limiting renal toxicity (Costanzi *et al.*, 2005; Pavlakis and Vogelzang, 2006). Another detriment is its ribonucleolytic activity being <1% that of mammalian ribonucleases (Lee and Raines, 2003). Our work has revealed another shortcoming of ONC—its relatively poor internalization into endosomes (Figure 2.5(b)). Based on this finding, we predict that ONC translocates through the lipid bilayer more readily than do mammalian ribonucleases, resulting in its high cytotoxicity.

2.5.5. Origins of cancer cell specificity

ONC and other cytotoxic members of the RNase A superfamily are unique proteins in that they are able to cross the cell membrane and kill cancer cells specifically. The molecular basis of this selectivity is not known. Because rapidly-growing cancer cells have increased RNA turnover as compared to normal cells, they might be more susceptible to therapeutics that target RNA. This mode of action would, however, likely result in a side-effect profile that is more similar to that of other classes of cancer chemotherapeutics, including broad toxicity toward any rapidly-growing tissues (*e.g.*, hair, blood, and gastric epithelium). Notably, ONC does not cause these side effects (Costanzi *et al.*, 2005), suggesting that it targets cancer cells by another mechanism. For

example, the surface of cancer cells is more anionic than that of normal cells (Bergelson *et al.*, 1970; Ran *et al.*, 2002; Sasisekharan *et al.*, 2002; Fredman *et al.*, 2003), making cationic ribonucleases more likely to bind to cancer cells than normal cells. The trafficking of membrane-bound vesicles could also differ in cancer cells and normal cells (Kroemer and Jäättelä, 2005), leading to increased internalization of ribonucleases into cancer cells. This hypothesis includes, but is not limited to, differences in relative amounts of vesicle leakiness, resulting in different translocation efficiencies. Our data support a model in which positively charged residues (specifically Patch 3 and Lys49) on the surface of ONC are important for the translocation of the protein. Further studies are necessary to determine whether these residues are likewise important for the specificity of the drug for cancer cells.

2.6 Conclusions

ONC represents a new class of cancer chemotherapeutic—cytotoxic ribonucleases. ONC is unique in being a natural product and a potential biopharmaceutical agent that is endowed with the ability to cross a cellular membrane and specifically kill cancer cells. Chemical cationization has been shown to increase the cytotoxic ability of ribonucleases, and even endow nontoxic ribonucleases with the ability to kill cells. We have discovered, however, that the net charge of ONC is less important than the distribution of that charge. Although ONC does not interact with the cancer-cell surface through a specific receptor, certain regions of ONC (specifically, residues 49, 73, 76, and 78) appear to be more

important than others in the lipid-bilayer translocation step that is required for the cytotoxicity of ONC. Thus, this work gives insight into cytosolic entry, a poorly understood process in the cytotoxicity of ONC and other ribonucleases.

Acknowledgements. We are grateful to Dr. L. D. Lavis for the fluorogenic label used in this work, J. Puchalski for assistance with the analysis of flow cytometry data, and Dr. R. J. Johnson, Dr. T. J. Rutkoski, K. L. Gorres, M. N. Levine, Dr. J. E. Lee, Dr. M. T. Borra, T.-Y. Chao, and G. A. Ellis for contributive discussions. This work was supported by grant CA073808 (NIH). R.F.T. was supported by a Wisconsin Distinguished Rath Graduate Fellowship. The University of Wisconsin–Madison Biophysics Instrumentation Facility was established with grants BIR-9512577 (NSF) and RR13790 (NIH).

Table 2.1 ONC Arg and Lys residues

Residue	Assignment
Lys8	—
Lys9	Active site
Arg15	Patch 2
Lys31	Active site
Lys33	—
Arg40	—
Lys45	Patch 1
Lys49	Patch 1
Lys55	Patch 1
Arg73	Patch 3
Lys76	Patch 3
Lys78	Patch 3
Lys80	Patch 2
Lys81	Patch 2
Lys85	—

Table 2.2 ONC double variants

From *Patch 2*	R15A/K80A
(R15A/K80A/K81A)	R15A/K81A
	K80A/K81A
From *Patch 3*	R73A/K76A
(R73A/K76A/K78A)	R73A/K78A
	K76A/K78A
From distributed variant	R15A/K49A
(R15A/K49A/R73A)	R15A/R73A
	K49A/R73A

Table 2.3 Biochemical characteristics of ONC and its variants

ONC	IC_{50}[a] μM	k_{cat}/K_M[b] ($\times 10^3$) $M^{-1}s^{-1}$	T_m[c] °C
wild-type	0.3	34 ± 2	83
Patch variants			
K45A/K49A/K55A (*Patch 1*)	8.2	12 ± 1	76
R15A/K80A/K81A (*Patch 2*)	>25	7.8 ± 0.2	78
R73A/K76A/K78A (*Patch 3*)	>25	17 ± 1	73
Distributed variants			
R15A/K49A/R73A	>25	6.5 ± 0.3	82
R15A/K45A/K76A	4.8	12 ± 1	77
R15A/K55A/K76A	2.6	16 ± 1	79
Double variants			
K49A/R73A	11.8	26 ± 9	82
R73A/K78A	11.3	23 ± 2	81
K76A/K78A	10.5	22 ± 1	79
R15A/R73A	6.2	9 ± 1	84
K80A/K81A	5.5	14 ± 2	79
R15A/K49A	4.7	6.6 ± 0.5	83
R73A/K76A	2.7	34 ± 7	ND
R15A/K80A	2.1	11 ± 1	ND
R15A/K81A	1.5	16 ± 4	ND
Single variants			
R15A	1.1	30 ± 10	ND
K49A	0.9	ND	ND
R73A	1.2	28 ± 5	ND
K76A	0.8	33 ± 4	ND
K78A	1.3	30 ± 4	ND
K80A	1.5	22 ± 3	ND
K81A	1.4	21 ± 4	ND

ND, not determined

[a] Values of IC_{50} are for the incorporation of [*methyl*-^{3}H]thymidine into DNA of K-562 cells.

[b] Values of k_{cat}/K_M (± SE) are for the cleavage of 6-FAM–dArUdGdA–6-TAMRA in 0.10 M MES–NaOH buffer (pH 6.0) containing 0.10 M NaCl at 23 ± 2 °C.

[c] Values of T_m were determined in PBS by CD spectroscopy.

Table 2.4 Mass analysis of ONC and its variants

ONC	Mass[a] (Da)	
	expected	observed
wild-type	11,820	11,828
Patch variants		
K45A/K49A/K55A (*Patch 1*)	11,649	11,657
R15A/K80A/K81A (*Patch 2*)	11,621	11,626
R73A/K76A/K78A (*Patch 3*)	11,621	11,625
Distributed variants		
R15A/K49A/R73A	11,593	11,595
R15A/K45A/K76A	11,621	11,622
R15A/K55A/K76A	11,621	11,629
Double variants		
K49A/R73A	11,678	11,675
R73A/K78A	11,678	11,678
K76A/K78A	11,706	11,710
R15A/R73A	11,650	11,653
K80A/K81A	11,706	11,711
R15A/K49A	11,678	11,677
R73A/K76A	11,678	11,678
R15A/K80A	11,678	11,683
R15A/K81A	11,678	11,684
Single variants		
R15A	11,735	11,735
K49A	11,763	11,770
R73A	11,735	11,728
K76A	11,763	11,783
K78A	11,763	11,775
K80A	11,763	11,781
K81A	11,763	11,781
Labeled variants		
S61C–TML	12,615	12,619
K9A/K31A/S61C–TML	12,501	12,488
R15A/K80A/K81A/S61C–TML	12,416	12,401
R15A/K55A/K76A/S61C–TML	12,416	12,418
K49A/R73A/S61C–TML	12,470	12,465
R15A/K81A/S61C–TML	12,470	12,477

[a] Values of *m/z* were determined by MALDI–TOF mass spectroscopy.

Figure 2.1 ONC structure highlighting active site and three positively charged patches. An electrostatic potential map surface is shown in (*A*) and (*B*). Positively charged surface is shown in blue, negatively charged surface in red, and neutral surface in white. Cartoon diagrams are shown in (*C*) and (*D*). The conventional view of ONC is shown in (*A*) and (*C*), and rotated 180° in (*B*) and (*D*). Images were created with the program MacPyMOL (DeLano Scientific, South San Francisco, CA).

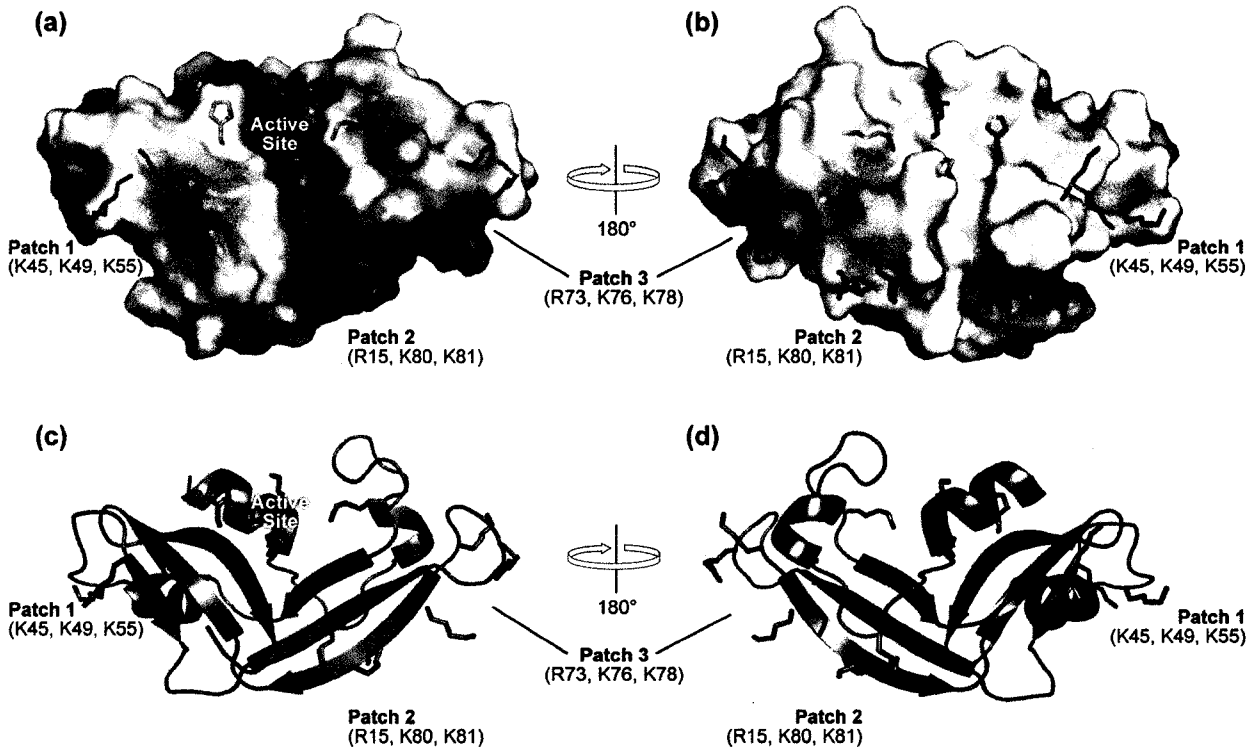
(a)
Active Site
Patch 1
(K45, K49, K55)
Patch 2
(R15, K80, K81)
Patch 3
(R73, K76, K78)
180°
(b)
Patch 1
(K45, K49, K55)
Patch 2
(R15, K80, K81)
(c)
Active Site
Patch 1
(K45, K49, K55)
Patch 2
(R15, K80, K81)
Patch 3
(R73, K76, K78)
180°
(d)
Patch 1
(K45, K49, K55)
Patch 2
(R15, K80, K81)

Figure 2.2 Effect of ONC triple variants on the proliferation of K-562 cells. Cell proliferation was measured by monitoring the incorporation of [*methyl*-^{3}H]thymidine into genomic DNA. Data points indicate the mean (±SE) of three separate experiments carried out in triplicate. Wild-type ONC and RNase A controls are shown with open diamonds and circles, respectively. (*A*) Effect of replacing Patches 1, 2, or 3. (*B*) Effect of replacing three residues distributed across the three patches.

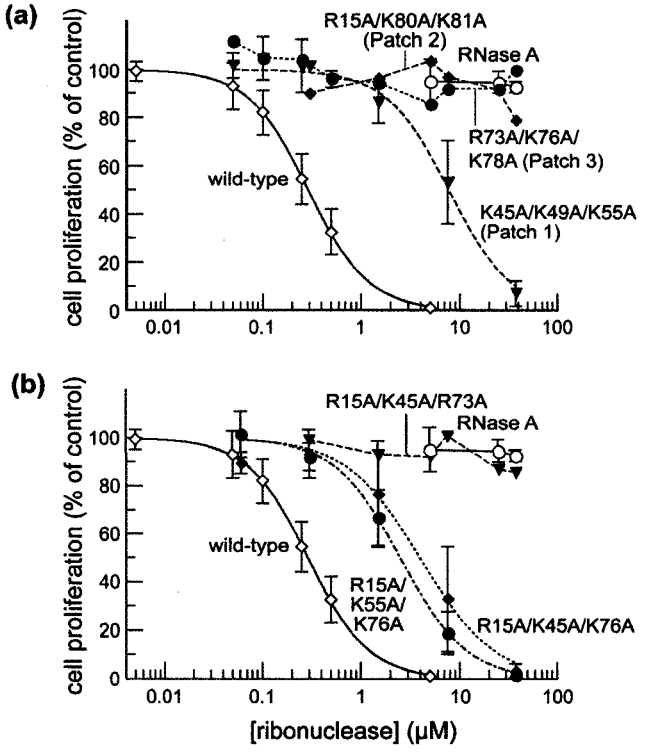
(a)
R15A/K80A/K81A
(Patch 2)
RNase A
R73A/K76A/
K78A (Patch 3)
wild-type
K45A/K49A/K55A
(Patch 1)
cell proliferation (% of control)
0
20
40
60
80
100
0.01
0.1
1
10
100
(b)
R15A/K45A/R73A
RNase A
wild-type
R15A/
K55A/
K76A
R15A/K45A/K76A
cell proliferation (% of control)
[ribonuclease] (μM)

Figure 2.3 Effect of ONC double variants on the proliferation of K-562 cells. Cell proliferation was measured by monitoring the incorporation of [*methyl*-^{3}H]thymidine into genomic DNA. Data points indicate the mean (±SE) of three separate experiments carried out in triplicate. (*A*) Compilation of data for variants that retained high cytotoxicity. (*B*) Compilation of data for variants that exhibited moderate cytotoxicity. (*C*) Compilation of data for variants that exhibited low cytotoxicity.

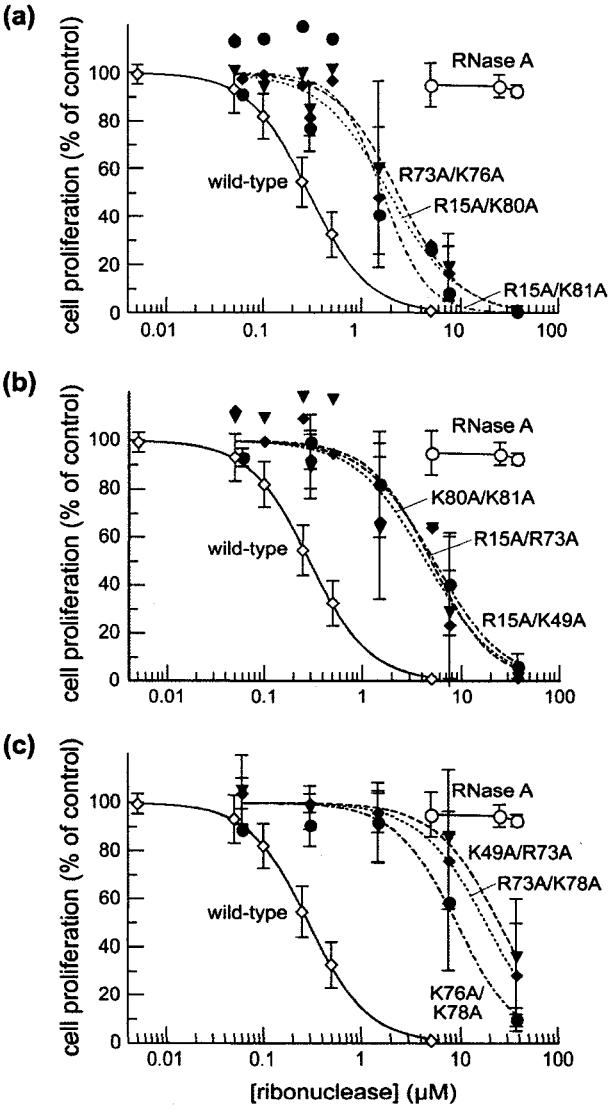
(a)
cell proliferation (% of control)
RNase A
wild-type
R73A/K76A
R15A/K80A
R15A/K81A
(b)
cell proliferation (% of control)
RNase A
K80A/K81A
wild-type
R15A/R73A
R15A/K49A
(c)
cell proliferation (% of control)
RNase A
K49A/R73A
R73A/K78A
wild-type
K76A/
K78A
[ribonuclease] (μM)

Figure 2.4 Effect of wild-type ONC and 22 variants on the proliferation of K-562 cells, as reported by values of IC_{50}. Ribonucleases are sorted by their net molecular charge (Z). A single alanine to arginine/lysine substitution converts a nontoxic variant with $Z = +2$ (R15A/K80A/K81A, red; R15A/K49A/R73A, green; R73A/K76A/K78A, green) into a cytotoxic variant with $Z = +3$. Data are listed in Table 2.3.

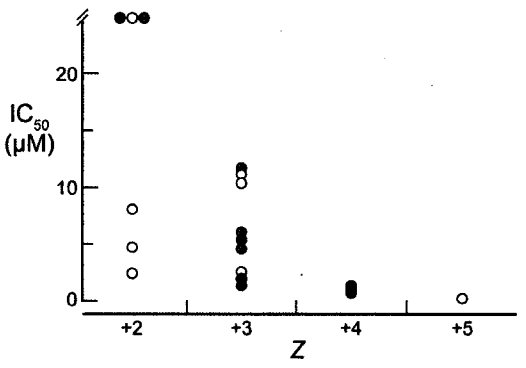
20
10
0
IC50
(μM)
+2
+3
+4
+5
Z

Figure 2.5 Internalization of latent-fluorophore labeled ONC, its variants, and RNase 1 into K-562 cells. Internalization was measured by using flow cytometry to measure the fluorescence manifested by a ribonuclease (10 μM) labeled with a fluorogenic probe for endocytosis (Lavis *et al.*, 2006) and incubated with K-562 cells at 37 °C. (*A*) Structure of the fluorogenic label, which was attached via its maleimido group to Cys61 of S61C ONC and Cys19 of P19C RNase 1. (*B*) Time course of internalization of ONC and RNase 1 (Johnson *et al.*, 2007a). (*C*) Relative internalization (±SE) of ONC variants after 4 h. Values of *Z* are indicated on each bar; values of IC_{50} for the corresponding unlabeled ribonuclease are shown in parentheses. The dashed line indicates the background level of fluorescence, as revealed with unlabeled ONC.

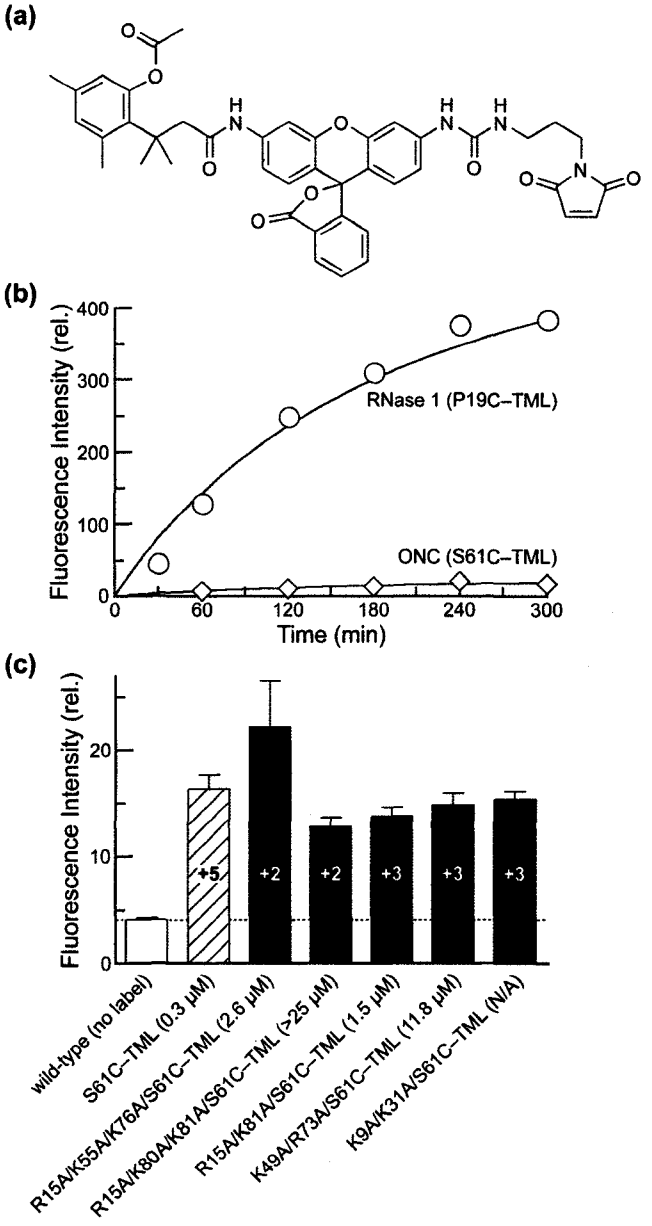
(a)
(b)
Fluorescence Intensity (rel.)
400
300
200
100
0
RNase 1 (P19C–TML)
ONC (S61C–TML)
0
60
120
180
240
300
Time (min)
(c)
Fluorescence Intensity (rel.)
20
10
0
+5
+2
+2
+3
+3
+3
wild-type (no label)
S61C–TML (0.3 μM)
R15A/K55A/K76A/S61C–TML (2.6 μM)
R15A/K80A/K81A/S61C–TML (>25 μM)
R15A/K81A/S61C–TML (1.5 μM)
K49A/R73A/S61C–TML (11.8 μM)
K9A/K31A/S61C–TML (N/A)

Figure 2.6 Putative mechanism for the cytotoxicity of ribonucleases, and related assays. Assays of cell proliferation report on the sum of four steps: binding, endocytosis, translocation, and RNA cleavage. Assays of flow cytometry report on the first two steps, whereas assays of catalytic activity report on only the final step. Observed differences in the cell proliferation of ONC variants cannot be accounted for by flow cytometry or catalytic activity assays, indicting the translocation step as the differentiating one.

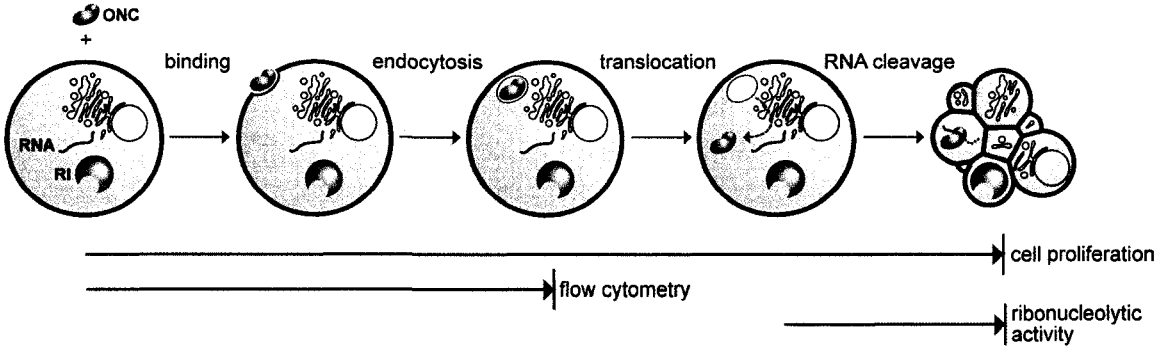
ONC
+
binding
endocytosis
translocation
RNA cleavage
RNA
RI
cell proliferation
flow cytometry
ribonucleolytic activity

CHAPTER 3

Interaction of the Human Ribonuclease Inhibitor Protein with Onconase

Prepared for submission to *Biochem. Biophys. Res. Comm.* as:
Turcotte, R.F. and Raines, R.T. (2008) Interaction of the Human Ribonuclease Inhibitor Protein with Onconase.

3.1 Abstract

One of the tightest known protein–protein interactions in biology is that between the ribonuclease inhibitor protein (RI) and members of the ribonuclease A superfamily. Some members of this superfamily are able to kill cancer cells, and the ability to evade RI is a major determinant of whether a ribonuclease will be cytotoxic. The archetypal cytotoxic ribonuclease, Onconase (ONC), is in late-stage clinical trials for the treatment of malignant mesothelioma. We present here the first direct measurement of the inhibition of the ribonucleolytic activity of ONC by RI, in a solution of low salt concentration.

3.2 Introduction

Protein–protein interactions are prevalent in biological systems. Proper functioning of organisms relies on the formation of complexes, such as those between antibodies and antigens, growth factors and receptors, and enzymes and regulators. These interactions have evolved the necessary affinity for their function, as well as the ability to dissociate within a practical timeframe. The theoretical upper limit for the encounter of two proteins in aqueous solution has been estimated to be $\sim 10^6\ M^{-1}s^{-1}$ (Berg and von Hippel, 1985; Northrup and Erickson, 1992). This rate is frequently increased via electrostatic steering (Schreiber and Fersht, 1996; Sheinerman and Honig, 2002; Shaul and Schreiber, 2005; Alsallaq and Zhou, 2007; Johnson *et al.*, 2007c). Barnase and barstar (Schreiber and Fersht, 1993), cytochrome *c* and cytochrome *c* peroxidase (Vitello and Erman, 1987), and

thrombin and hirudin (Stone and Hofsteenge, 1986) are all examples of binding partners that use electrostatic steering to increase their association rates.

The association rate for the complex formed between secreted members of the bovine pancreatic ribonuclease (RNase A) superfamily and the cytosolic ribonuclease inhibitor protein (RI) is high (~10^8 $M^{-1}s^{-1}$ for RNase A and human RI) (Lee *et al.*, 1989a). The equilibrium dissociation constant (K_d) value for the complex between human RI (hRI) and human pancreatic ribonuclease (RNase 1; Figure 3.1a and b) is 2.9×10^{-16} M in phosphate-buffered saline (PBS) (Johnson *et al.*, 2007c). This high stability is thought to have evolved to protect cells against the adventitious invasion of ribonucleases (Haigis *et al.*, 2003). Indeed, RNase A and RNase 1 variants that evade RI are able to kill cancer cells (Leland *et al.*, 1998; Leland *et al.*, 2001; Rutkoski *et al.*, 2005; Johnson *et al.*, 2007c; Rutkoski and Raines, 2008).

The interface between RI and ribonucleases contains a higher percentage of charged residues than that typically present in protein•protein complexes (Kobe and Deisenhofer, 1996; Rutkoski *et al.*, 2005), suggesting a role for electrostatics in complex stability. RI is highly anionic, with an isoelectric point (p*I*) of 4.7 (Dickson *et al.*, 2005), and pancreatic-type ribonucleases are highly cationic. Decreasing the net charge of RNase 1 leads to a decrease in affinity for RI (Johnson *et al.*, 2007a). RI is typically purified by RNase A-affinity chromatography, and eluted from the resin with 3 M NaCl (Klink *et al.*, 2001). In addition, the inhibition constant (K_i) for the complex between placental RI and RNase A

increases by more than four orders of magnitude from 0.1–1.0 M NaCl (Lee *et al.*, 1989b).

Onconase (ONC) (Ardelt *et al.*, 2008; Lee and Raines, 2008) is a homologue of RNase A from the Northern leopard frog *Rana pipiens* (Darzynkiewicz *et al.*, 1988). Unlike RNase A and RNase 1, ONC is naturally toxic to cancer cells (Darzynkiewicz *et al.*, 1988) and is currently in Phase IIIb clinical trials for the treatment of malignant mesothelioma (Pavlakis and Vogelzang, 2006). Its cytotoxic activity is ascribed primarily to its intrinsic lack of affinity for hRI (Boix *et al.*, 1996; Rutkoski and Raines, 2008), a property that likely results from the truncation of surface loops that contain the majority of the RI-contact residues in RNase A and RNase 1 (Boix *et al.*, 1996; Kobe and Deisenhofer, 1996). The affinity of ONC for RI is beyond the limits of detection of available assays (Abel *et al.*, 2002; Lavis *et al.*, 2007), and the K_i value for this interaction has been estimated indirectly to be >1 μM from the IC_{50} value of ONC in proliferation assays (Boix *et al.*, 1996).

The interaction between RI and ribonucleases is typically measured in solutions of physiological salt concentration, such as PBS (Abel *et al.*, 2002; Lavis *et al.*, 2007). In aqueous solutions containing salts, ions interact with charged proteins such as RI and ribonucleases preferentially, with cations primarily interacting with anionic surfaces and anions with cationic surfaces. This phenomenon leads to an unequal distribution of ions in the solution; a higher local concentration of ions is present in the vicinity of the proteins than in the bulk solution (Record *et al.*, 1998). When RI binds to ribonucleases, there is a decrease of 2583–3438 $Å^2$ in the surface area that is exposed to the surrounding

solution (Rutkoski and Raines, 2008). This burial results in the release of the ions that were interacting with the surface of the proteins in the interfacial region, and an accompanying increase in the entropy of the system. In solutions of lower salt concentration, the concentration gradient of ions between the bulk water and local water is increased further, increasing the entropy of binding and thus making binding more favorable (Record *et al.*, 1998).

In this work, we exploit this phenomenon to detect the interaction of RI with ONC in a solution of low salt concentration. Like its fellow superfamily members, ONC is a highly cationic protein (p*I* >9.5, Figure 3.1c) (Ardelt *et al.*, 1991). Considering the high charge density of ONC and RI and the large amount of surface area buried in RI•ribonuclease complexes, we reasoned that RI could perhaps inhibit ONC in solutions of low salt concentration. We report here the first direct measurement of the interaction of RI with ONC.

3.3 Experimental Procedures

3.3.1 Materials.

Escherichia coli BL21(DE3) cells and pET22b(+) plasmid were from Novagen (Madison, WI). Enzymes were obtained from Promega (Madison, WI). Bovine serum albumin (BSA) was obtained as a 20 mg/mL solution (Sigma; Product B8667). 6-Carboxyfluorescein–dArUdGdA–6-carboxytetramethylrhodamine (6-FAM–dArUdGdA–6-TAMRA) (Kelemen *et al.*, 1999; Lee and Raines, 2003) was obtained from Integrated

DNA Technologies (Coralville, IA). Costar 96-well NBS microtiter plates were from Corning Life Sciences (Acton, MA). MES buffer (Sigma–Aldrich, St. Louis, MO) was purified by anion-exchange chromatography to remove oligo(vinylsulfonic acid) (OVS), a potent inhibitor of ribonucleases (Smith *et al.*, 2003). All other chemicals used were of commercial grade or better, and were used without further purification.

Terrific Broth contained (in 1.0 liter) tryptone (12 g), yeast extract (24 g), glycerol (4 mL), KH_2PO_4 (2.31 g), and K_2HPO_4 (12.54 g).

3.3.2 Instrumentation

Molecular mass was measured by matrix-assisted laser desorption/ionization time-of-flight (MALDI–TOF) mass spectroscopy using a Voyager-DE-PRO Biospectrometry Workstation (Applied Biosystems, Foster City, CA) at the University of Wisconsin–Madison Biophysics Instrumentation Facility. The fluorescence intensity in microtiter plates was recorded with a Perkin-Elmer EnVision 2100 plate reader equipped with a FITC filter set (excitation at 485 nm with 14 nm bandwidth; emission at 535 nm with a 25 nm bandwidth; dichroic mirror cutoff at 505 nm) at the W.M. Keck Center for Chemical Genomics.

3.3.3 Purification of ribonuclease inhibitor and ribonucleases

hRI (Johnson *et al.*, 2007c) and RNase A (Leland *et al.*, 1998) were purified as described previously. ONC was purified as described previously (Leland *et al.*, 1998), with the following exceptions. ONC was refolded overnight at room temperature after

slow dilution (by 10-fold) into 0.10 M Tris–HCl buffer, pH 8.0, containing NaCl (0.10 M), reduced glutathione (3.0 mM), and oxidized glutathione (0.6 mM). After concentration by ultrafiltration, samples were dialyzed overnight against 50 mM sodium acetate buffer, pH 5.0, containing NaCl (0.10 M), and applied to a MonoS cation-exchange FPLC column (Pharmacia). ONC was eluted from the column with a linear gradient of NaCl (0.15–0.30 M). Protein concentrations were determined by UV spectroscopy using extinction coefficients of $\varepsilon_{280} = 0.88$ $(mg/mL)^{-1} \cdot cm^{-1}$ for hRI (Klink *et al.*, 2001), $\varepsilon_{278} = 0.72$ $(mg/mL)^{-1} \cdot cm^{-1}$ for RNase A, and $\varepsilon_{280} = 0.87$ $(mg/mL)^{-1} \cdot cm^{-1}$ for ONC (Leland *et al.*, 1998). The molecular masses of RNase A and ONC were confirmed by MALDI–TOF mass spectroscopy.

3.3.4 Determination of K_i value for ONC

A serial dilution (12.5 μM→96 pM; 2×) of hRI in MES–NaOH buffer (20 mM), pH 6.0, containing DTT (5 mM), and BSA (0.1%) was prepared. A 50-μL aliquot of this serial dilution was added to the wells of a 96-well plate. A solution (50-μL) of ONC (100 nM; 2×) in MES–NaOH buffer (20 mM), pH 6.0, containing DTT (5 mM), and BSA (0.1% w/v) was prepared in Eppendorf Protein LoBind Tubes (Fisher Scientific) and added to each well. The negative control contained no RI and the positive control contained excess RNase A (550 μM). A hypersensitive fluorogenic substrate, 6-FAM–dArUdGdA–6-TAMRA (100 nM) (Kelemen *et al.*, 1999; Lee and Raines, 2003), was added to each well and fluorescence intensity was measured at 25 °C every 30 s over a

5-min period. Data were fitted using nonlinear regression to a dose-response curve using Prism 4 for Macintosh.

3.4 Results and Discussion

Nonspecific interactions can occur between proteins in solutions of low salt concentration. These interactions can bring together residues that are not at the biologically relevant interface between the proteins. Such weak interactions are screened in solutions of physiological salt concentration (Selzer and Schreiber, 1999; Shaul and Schreiber, 2005). To avoid detecting such nonspecific interactions, we used an activity-based assay to detect binding, measuring the ability of hRI to inhibit the ribonucleolytic activity of ONC. These assays were performed at pH 6.0, which is close to the pH-optimum for catalysis by ONC (Lee *et al.*, 2008). We found that hRI inhibits ONC activity with a K_i value of 0.15 ± 0.05 μM under these conditions (Figure 3.2). The ability of hRI to inhibit the ribonucleolytic activity of ONC indicates that hRI can bind to the active site of ONC, perhaps in a manner similar to that of other members of the RNase A superfamily.

The ribonuclease A superfamily is a vertebrate-specific family that is evolving rapidly (Beintema *et al.*, 1988). Ribonucleases and inhibitors from different classes do not interact (Beintema and Kleineidam, 1998), and the intraspecies complexes are more stable and form more rapidly than interspecies complexes (Johnson *et al.*, 2007b). The framework for RI-binding is in place in ONC (*i.e.*, the molecular shape and distribution

of charge; Figure 3.1b and c), but the individual residues that closely interact with RI in other ribonucleases are largely absent in ONC (Boix *et al.*, 1996; Rutkoski and Raines, 2008). These factors combine to allow ONC to interact with RI in a solution of low salt concentration, but not at physiological salt concentrations. Work in our laboratory is ongoing aimed at isolating an RI homologue from the oocytes of *Rana pipiens*. Subsequent measurement of its affinity for mammalian ribonuclease homologues will inform our understanding of the evolution of these binding partners.

Acknowledgements. This work was supported by NIH Grant CA073808. R.F.T. was supported by a Wisconsin Distinguished Rath Graduate Fellowship. The University of Wisconsin–Madison Biophysics Instrumentation Facility was established with grants BIR-9512577 (NSF) and RR13790 (NIH). The Keck Center for Chemical Genomics was established with a grant from the W.M. Keck Foundation. The authors are grateful to G.A. Ellis for assistance with data analysis and Dr. T.J. Rutkoski and K.L. Gorres for contributive discussions.

Figure 3.1 Crystalline structures of the hRI•RNase 1 complex (Protein Data Bank entry 1z7x) and ONC (Protein Data Bank entry 1onc). (*A*) hRI•RNase 1 complex showing electrostatic protein contact potential of hRI and ribbon diagram of RNase 1 (grey). Positively charged surface is shown in blue, negatively charged surface in red, and neutral surface in white. (*B*) hRI•RNase 1 complex showing electrostatic protein contact potential of RNase 1 and ribbon diagram of hRI. (*C*) Electrostatic protein contact potential of ONC. Images were generated with the program MacPyMOL (DeLano Scientific, South San Francisco, CA).

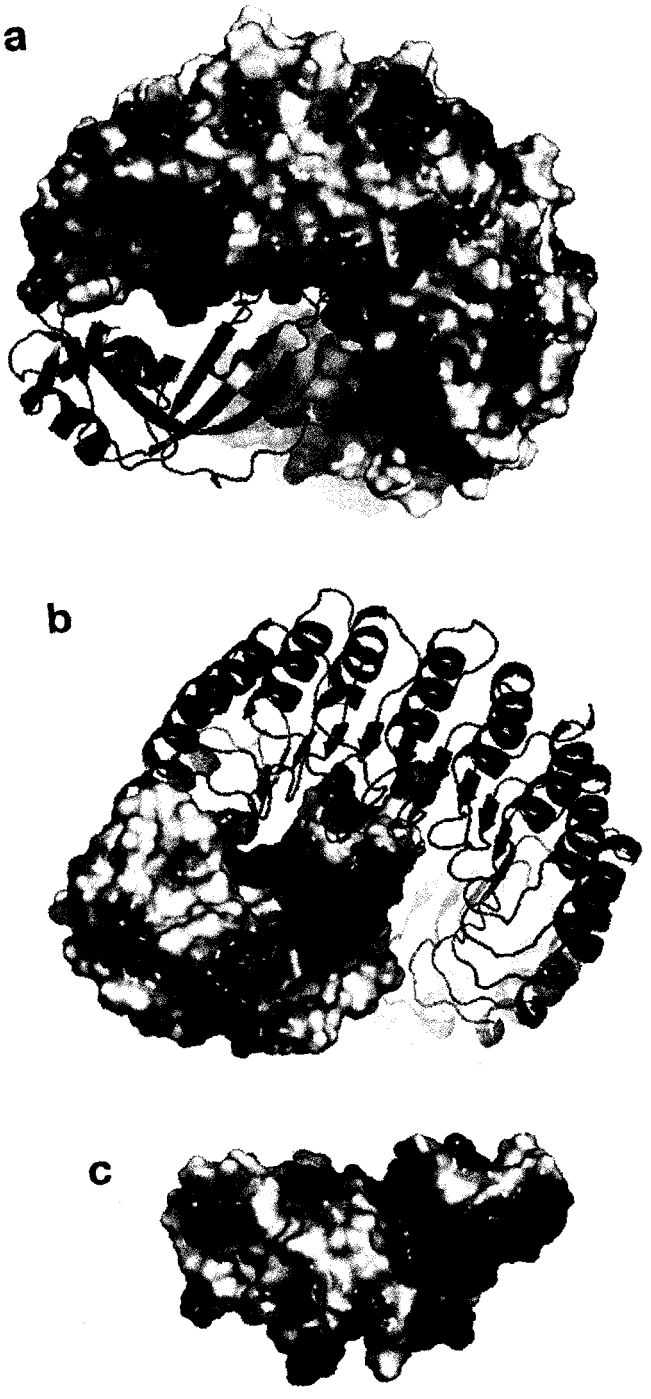
a
b
c

Figure 3.2 Inhibition of ribonucleolytic activity of ONC by hRI. Ribonucleolytic activity of ONC was measured by using a hypersensitive fluorogenic substrate, 6-FAM–dArUdGdA–6-TAMRA (100 nM), in 20 mM MES–NaOH buffer, pH 6.0, containing DTT (5 mM), BSA (0.1% w/v), and ONC (50 nM).

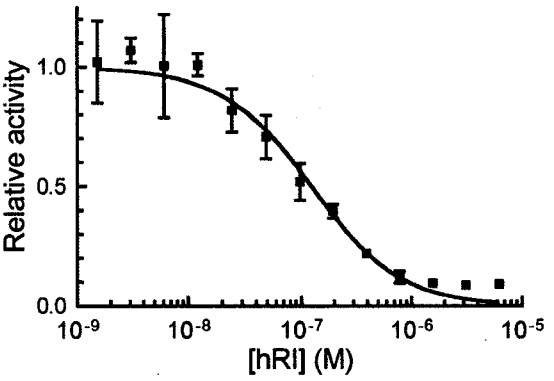
Relative activity
1.0
0.5
0.0
10-9
10-8
10-7
10-6
10-5
[hRI] (M)

CHAPTER 4

Design and Characterization of an HIV-Specific Ribonuclease Zymogen

This chapter will be published as:
Turcotte, R.F. and Raines, R.T. (2008) Design and Characterization of an HIV-Specific Ribonuclease Zymogen. *AIDS Res. Hum. Retroviruses* In press.

4.1 Abstract

Ribonucleases are evoking medical interest because of their intrinsic cytotoxic activity. Most notably, ranpirnase, which is an amphibian ribonuclease, is in advanced clinical trials as a chemotherapeutic agent for the treatment of cancer. Here, we describe a strategy to create a novel antiviral agent based on bovine pancreatic ribonuclease (RNase A), a mammalian homologue of ranpirnase. Specifically, we have linked the N- and *C*-termini of RNase A with an amino-acid sequence that is recognized and cleaved by human immunodeficiency virus (HIV) protease. This linkage obstructs the active site, forming an HIV-specific RNase A zymogen. Cleavage by HIV-1 protease increases ribonucleolytic activity by 50-fold. By relying on the proper function of HIV-1 protease, rather than its inhibition, our approach will not engender known mechanisms of resistance. Thus, we report an initial step towards a new class of agents for the treatment of HIV/AIDS.

4.2 Introduction

Since the first cases of human immunodeficiency virus (HIV) were described in the early 1980's (Hymes *et al.*, 1981), much has been done to improve survival. Four classes of antiretroviral drugs are now in clinical use, with protease inhibitors and two types of reverse-transcriptase inhibitors comprising the three major classes (Carr, 2003). In addition, the first fusion inhibitor was approved in 2003 (Matthews *et al.*, 2004; Hanson and Hicks, 2006). A combination of these chemotherapeutic agents, known as highly

active antiretroviral therapy, or HAART, has led to a significant decline in the morbidity and mortality of HIV patients (Barbaro *et al.*, 2005; Temesgen *et al.*, 2006). Although the number of deaths among persons with AIDS in the United States declined substantially during the late 1990's, the rate of decline has since decreased significantly. Declines in the numbers of new cases have also leveled off (Kellerman *et al.*, 2005).

This slowing of progress against HIV/AIDS, combined with several major problems with HIV/AIDS therapy, continue to motivate the design of new drugs (Weiss, 2003; Flexner, 2007). Side effects, especially disturbances in lipid metabolism, are an increasing problem as patients are living longer and developing cardiac disease (Carr, 2003; Agrawal *et al.*, 2006). Rapid viral replication and the high error-rate of reverse transcriptase have led to high rates of resistance to HAART (Barbaro *et al.*, 2005), with about 10% of newly acquired infections in the United States and Europe being resistant to at least one of the three major drug classes (Shafer, 2002). The rapid development of resistance necessitates strict patient compliance with therapy. Finally, AIDS remains a chronic disease due to the existence of latent HIV infection in memory T cells and other cells that are not pharmacologically accessible (Simon and Ho, 2003; Yang, 2004).

One strategy for slowing viral progression and eliminating latent viral infection is to kill those cells that are infected with HIV. Although cytotoxic cancer drugs could be used, there is a risk of serious side effects that would compound the side effects of HAART (Ravot *et al.*, 1999). To circumvent this problem, toxins that are specific for HIV-infected cells have been designed. One approach has been to use toxins that will be activated by the HIV-1 protease (HIV PR), a virally encoded protein that cleaves the viral

polyprotein late in the life cycle of HIV (Kohl *et al.*, 1988). In one case, an HIV PR-activated variant of caspase-3 was constructed and its ability to kill HIV-infected cells was demonstrated (Vocero-Akbani *et al.*, 1999). In another case, diphtheria toxin was modified such that a degradation signal was removed by cleavage with HIV PR (Falnes *et al.*, 1999). These "pro-drug" strategies have the potential to reduce the problems with both side effects and drug resistance.

Bovine pancreatic ribonuclease (RNase A) has been studied intensely by biochemists for decades (Raines, 1998; Marshall *et al.*, 2008). Recently, interest in RNase A has resurged with the discovery of the interesting biological properties of ranpirnase, angiogenin, and bovine seminal ribonuclease, which are homologues of RNase A (D'Alessio and Riordan, 1997; Leland and Raines, 2001; Matoušek, 2001; Makarov and Ilinskaya, 2003; Benito *et al.*, 2005; Arnold and Ulbrich-Hofmann, 2006). For example, ranpirnase (Lee and Raines, 2008) is toxic to cancer cells *in vitro* and *in vivo* in a manner that is dependent on its catalytic activity (Ardelt *et al.*, 1991), and is currently in Phase IIIb clinical trials for the treatment of malignant mesothelioma (Pavlakis and Vogelzang, 2006). In addition, RNase A and other ribonucleases are known to inhibit HIV replication (Youle *et al.*, 1994; Bedoya *et al.*, 2006).

Here, we describe the creation of an HIV-specific zymogen from RNase A. Inspired by the design of zymogens specific for malaria and hepatitis C (Plainkum *et al.*, 2003; Johnson *et al.*, 2006), we sought to exploit the activity of HIV PR to activate a cytotoxin. The *N*- and *C*-termini of RNase A were joined by circular permutation, thereby occluding the active site with an amino-acid sequence containing a cleavage site for HIV PR

(Figure 4.1). In the presence of HIV PR, this sequence is cleaved and the catalytic activity is unmasked. It is our hope that, because a chemotherapeutic strategy based on a ribonuclease zymogen would rely on catalysis by HIV PR rather than merely an affinity for that enzyme, the development of resistance would be unlikely.

4.3 Experimental Procedures

4.3.1 Materials

Escherichia coli strain BL21(DE3) was from Novagen (Madison, WI). K-562 cells (Lozzio and Lozzio, 1975), which are human erythroleukemia cells, were obtained from American Type Culture Collection (Manassas, VA). HIV PR expression vector pET-HIVPR (Ido *et al.*, 1991) was a kind gift from J. Tang (Oklahoma Medical Research Foundation).

Enzymes were obtained from Promega (Madison, WI). Protein purification columns and resin were from Amersham Biosciences (Piscataway, NJ). Synthetic oligonucleotides, including the ribonuclease substrate 6-FAM–dArU$(dA)_2$–6-TAMRA (Kelemen *et al.*, 1999), were from Integrated DNA Technologies (Coralville, IA). Poly(cytidylic acid) (poly(C)) was from Sigma–Aldrich (St. Louis, MO) and was precipitated with ethanol before use to remove short RNA fragments. [*methyl*-^{3}H]Thymidine was from Perkin–Elmer (Boston, MA). MES buffer (Sigma–Aldrich, St. Louis, MO) was purified by anion-exchange chromatography to remove any

contaminating oligo(vinylsulfonic acid) (OVS) (Smith *et al.*, 2003). All other chemicals were of commercial grade or better, and were used without further purifications.

Phosphate-buffered saline (PBS) contained (in 1 liter) NaCl (8.0 g), KCl (2.0 g), $Na_2HPO_4 \cdot 7H_2O$ (1.15 g), and KH_2PO_4 (2.0 g), and had a pH of 7.4.

4.3.2 Zymogen production and purification

Plasmids used to direct the production of HIV RNase A zymogens were derived from plasmid pET22b(+)/19N (Plainkum *et al.*, 2003). The region of this plasmid that encoded the linker was replaced with DNA encoding the sequence GSTATIMMQRGNAG (zymogen **1**) or GGSTATIMMQRGNAG (zymogen **2**) by using the QuikChange mutagenesis kit (Stratagene, La Jolla, CA). Zymogens were produced and purified as described previously (Johnson *et al.*, 2006). Zymogens were judged to be ~95% pure by SDS–PAGE, and zymogen identity was confirmed by MALDI–TOF (Table 4.1).

4.3.3 Protease production and purification

To improve the stability of HIV PR, the Q7K/L33I/L63I (Mildner *et al.*, 1994) and C67A/C95A (Davis *et al.*, 1996) substitutions were made by altering plasmid pET-HIVPR using the Quikchange mutagenesis kit. The resulting plasmid was named "pET-HIVPRV". *E. coli* BL21(DE3) cells were transformed with plasmid pET-HIVPRV, plated, and subcultured in Luria–Bertani medium containing glucose (1% w/v) to reduce the (leaky) expression of the HIV PR gene, as HIV PR is toxic to *E. coli* cells (Pan and Malcolm, 2000). To produce HIV PR, gene expression was induced in Terrific Broth

(which lacks glucose) containing isopropyl-β-D-thiogalactoside (1 mM). The protease was purified from inclusion bodies by methods described previously (Todd *et al.*, 1998), with the following modifications. Following two passes through a French pressure cell (>16,000 psi), inclusion bodies were collected by centrifugation at 16,000*g* for 45 min, washed with extraction buffer, resuspended in extraction buffer, and again collected by centrifugation. Ion-exchange columns were poured from resin and run by gravity at (23 ± 2) °C.

4.3.4 Zymogen cleavage

Zymogens were activated by mixing them with 0.04–0.2 molar equivalents of HIV PR in reaction buffer, which was 100 mM sodium acetate buffer, pH 5.0, containing NaCl (100 mM), EDTA (1 mM), glycerol (5% v/v), and PEG-8000 (0.1% w/v), and incubating the resulting solution at 37 °C for 1 h. Activation was stopped by dilution into gel-loading buffer to a final composition of 50 mM Tris–HCl, pH 6.8, containing DTT (100 mM), SDS (0.2% w/v), glycerol (10% v/v), and bromophenol blue (0.75 mM), or by dilution (by 100-fold) into 0.10 M MES–NaOH, pH 6.0, containing NaCl (0.10 M). Following dilution, reaction mixtures were placed on ice. SDS–PAGE in the presence of DTT was used to assess zymogen cleavage (Figure 4.2).

4.3.5 Ribonucleolytic activity

The ability of zymogens to catalyze the cleavage of the fluorogenic substrate 6-FAM–dArU(dA)$_2$–6-TAMRA, which exhibits a 180-fold increase in fluorescence (excitation at 493 nm; emission at 515 nm) upon cleavage (Kelemen *et al.*, 1999), was assessed. Assays were carried out at (23 ± 2) °C in 2.0 mL of 0.10 M MES–NaOH (OVS-free), pH 6.0, containing NaCl (0.10 M), substrate (20 nM), and zymogen (5 pM–1 nM). Values of k_{cat}/K_M were obtained with eq 4.1:

$$k_{cat}/K_M = \left(\frac{\Delta I/\Delta t}{I_{max} - I_0}\right)\frac{1}{[\text{ribonuclease}]} \qquad (4.1)$$

where $\Delta I/\Delta t$ represents the initial reaction velocity, I_{max} is the fluorescence following complete cleavage of the substrate by excess RNase A, and I_0 is the fluorescence prior to addition of ribonuclease.

In addition, the ability of zymogens to cleave poly(C) ($\varepsilon_{268\ nm}$ = 6,200 $M^{-1}cm^{-1}$ per nucleotide) was monitored by the change in UV absorption, which increases upon cleavage ($\Delta\varepsilon_{250\ nm}$ = 2,380 $M^{-1}cm^{-1}$). Assays were carried out at (23 ± 2) °C in 0.10 M MES–NaOH (OVS-free), pH 6.0, containing NaCl (0.10 M), poly(C) (10 μM–1.5 mM), and zymogen (20 nM–1 μM). Initial velocity data were used to calculate values of k_{cat}, K_M, and k_{cat}/K_M with the program Prism 4 for Macintosh (GraphPad Software, San Diego, CA).

4.3.6 Conformational stability

The value of T_m, which is the temperature at the midpoint of the thermal transition between the folded and unfolded states, of each zymogen was determined by monitoring its UV absorption at 287 nm. Zymogen solutions (~25 μM in PBS) were heated incrementally (0.15 °C/min from 25 to 75 °C). Data were collected and analyzed with the program THERMAL from Varian Analytical Instruments (Walnut Creek, CA).

4.3.7 Inhibition by the ribonuclease inhibitor protein

Binding of unactivated zymogen **1** to the ribonuclease inhibitor protein was assessed via microplate assay as described previously (Lavis *et al.*, 2007).

4.3.8 Cytotoxic activity

K-562 cells were grown in RPMI 1640 medium supplemented with 10% (v/v) fetal bovine serum, penicillin (100 U/mL), and streptomycin (100 μg/mL). The effect of zymogens on K-562 proliferation was measured by the incorporation of [*methyl*-^{3}H]thymidine as described previously (Rutkoski *et al.*, 2005).

4.4 Results

4.4.1 Design of HIV-specific zymogen

The p2/NC recognition sequence of HIV PR (TATIM/MQRGN) was chosen because it is cleaved initially and efficiently *in vitro* and *in vivo* (Pettit *et al.*, 1994; Pettit *et al.*,

2005). It is desirable for a zymogen to contain a linker that is long enough to allow for the flexibility necessary to be a cleaved by the protease, but also short enough to prevent indiscriminate ribonucleolytic activity prior to activation by the specific protease. We designed two HIV-specific RNase zymogens, one with a 14-residue linker (zymogen **1**), and another with a 15-residue linker (zymogen **2**). The ten-residue cleavage sequence was extended by a linker designed for solubility and flexibility, containing glycine and serine residues.

Circular permutation produced new *N*- and *C*-termini at residues 89 and 88, respectively, of RNase A (Figure 4.1). These two residues were linked by a new disulfide bond (Plainkum *et al.*, 2003). In addition, residues 4 and 118 (RNase A numbering) were replaced with cysteine residues and linked by a disulfide bond in order to improve conformational stability (Klink and Raines, 2000).

4.4.2 Zymogen activation

Zymogens **1** and **2** were incubated with protease in a 1:25 to 1:5 (PR:zymogen) ratio at 37 °C. Activation was monitored by SDS–PAGE. Following reduction with DTT, zymogen fragments of 10,548 Da and 4,635 Da are formed from zymogen **1**. The formation of a 10.5-kDa fragment from a 15.2-Da fragment can be followed by SDS–PAGE. (The 4.6-kDa fragment runs off the gel and was not observed.) Both zymogens **1** and **2** were more than 95% cleaved by HIV PR after an incubation of 60 min at 37 °C (Figure 4.2). Control incubations of zymogens **1** and **2** without protease for 1 h did not

result in any cleavage (data not shown). Native RNase A has been shown not to be a substrate of HIV PR (Hui *et al.*, 1990).

The ability of zymogens to cleave two RNA substrates was measured (Tables 4.2 and 4.3). The shorter substrate was a fluorogenic tetranucleotide that increases in fluorescence upon cleavage (Table 4.2) (Kelemen *et al.*, 1999). The catalytic efficiency of zymogen **1** increases from $k_{cat}/K_M = 2.9 \times 10^5$ to 1.4×10^7 $M^{-1}s^{-1}$ upon activation, an increase of 48-fold. The k_{cat}/K_M value of the activated zymogen is nearly that of wild-type RNase A. For zymogen **2**, the increase is more modest, from 8.7×10^5 to 7.6×10^6 $M^{-1}s^{-1}$, or 9-fold.

This sensitive assay for ribonucleolytic activity might not be an accurate reflection of the ability of ribonucleases to cleave therapeutically relevant substrates (Suhasini and Sirdeshmukh, 2006). Hence, we measured the ribonucleolytic activity of zymogen **1** with a longer polynucleotide substrate, poly(C) (Table 4.3). This assay also allows for delineation of the contributions of the k_{cat} and K_M values to catalytic efficiency. Upon activation, the k_{cat} value increased from 3.2 to 38 s^{-1}. The K_M value decreased from 1.2×10^{-4} to 6×10^{-5} M, resulting in a change in k_{cat}/K_M of 24-fold, from 2.7×10^4 to 6.5×10^5 $M^{-1}s^{-1}$.

4.4.3 Conformational stability of zymogens

The ability of a cytotoxic ribonuclease to retain its conformation at physiological temperatures is an important factor in determining its potential as a chemotherapeutic

agent (Klink and Raines, 2000). Zymogens **1** and **2** are stable above physiological temperature (37 °C). Both, however, are less stable than wild-type RNase A (Table 4.1).

4.4.4 Binding of ribonuclease inhibitor protein

The ability of a ribonuclease to evade binding by the cytoplasmic ribonuclease inhibitor protein (RI), which binds RNase A with femtomolar affinity, is essential for its cytotoxicity (Leland *et al.*, 1998; Rutkoski *et al.*, 2005; Rutkoski and Raines, 2008) The active site of the ribonuclease comprises a large portion of the buried surface area in the ribonuclease–inhibitor complex (Kobe and Deisenhofer, 1996; Johnson *et al.*, 2007c). We would expect that the unactivated RNase A zymogen would have diminished affinity for RI, and indeed the K_d value for the ribonuclease–RI complex with the unactivated zymogen is $>10^6$-fold greater than that for wild type RNase A (Table 4.1).

4.4.5 Cytotoxicity of unactivated zymogen

A cytotoxic therapeutic agent must have little or no toxicity to healthy cells—those that are not infected with HIV. To assess this attribute, unactivated zymogens were assayed for their ability to inhibit the proliferation of K-562 cells, which are human cells that are not infected with HIV. Neither zymogen **1** nor zymogen **2** was toxic to K-562 cells up to a concentration of 38 μM (Table 4.1).

4.5 Discussion

We have created two HIV-specific RNase A zymogens. Their activation by HIV PR is 95% complete following a 1-h incubation with a sub-stoichiometeric amount of HIV PR (Figure 4.2). One factor that determines the efficiency of this cleavage reaction is the ability of the protease to bind to the zymogen. HIV PR and zymogens **1** and **2** are highly cationic proteins, having theoretical isoelectric points of pI = 9.3, 8.8, and 8.8, respectively (Bjellqvist *et al.*, 1994). Coulombic repulsion between HIV PR and a zymogen could diminish the efficiency of activation, a problem that could be overcome by additional mutagenesis.

The two zymogens differ as catalysts of RNA cleavage. The ribonucleolytic activity of zymogens **1** and **2** toward a tetranucleotide substrate was measured before and after activation with HIV PR (Tables 4.2 and 4.3). Prior to activation, both zymogens had low catalytic efficiency (k_{cat}/K_M near 10^5 $M^{-1}s^{-1}$), with zymogen **2** having 3-fold higher activity than zymogen **1**. This difference is likely due to the longer length of the linker of zymogen **2**, which could alter the ability of substrates to access the active site prior to activation. Following activation, zymogen **1** regains a catalytic efficiency that is close to that of wild-type RNase A, suggesting that the cleaved linker no longer obscures the active site. Zymogen **2**, however, does not regain as much activity, which suggests that the longer linker continues to interact with the active site after activation.

The use of a longer RNA substrate revealed additional information. Using poly(C) as a substrate, unactivated zymogen **1** has a K_M value that is 36-fold higher than that of

wild-type RNase A, confirming that the linker inhibits the binding of RNA substrates (Table 4.3). Yet, the k_{cat} value of the unactivated zymogen is also decreased by 88-fold, suggesting that the linker also prevents the turnover of RNA substrates by disturbing active-site residues (Johnson *et al.*, 2006). Upon activation of zymogen **1** with HIV PR, the K_M value decreases by twofold and the k_{cat} value increases by 10-fold. Neither value was similar to that of wild-type RNase A, suggesting that, after cleavage, the linker continues to interfere with the binding and turnover of a longer RNA substrate.

The development of a therapy that kills HIV-infected cells is highly attractive. Such a therapy could eradicate completely the viral reservoir in patients, a challenge that remains in the era of HAART (Yang, 2004). Drugs that are used to kill cancer cells could be used for this purpose but would result in the side effects typical of cancer chemotherapy, including bone-marrow suppression. Any potential for decreasing white blood cells in a patient with a weakened immune system should be avoided. As an alternative, our strategy seeks the selective destruction of HIV-infected cells.

Ribonuclease zymogens have other desirable attributes. Ribonucleases that evade the endogenous ribonuclease inhibitor protein are known to be potent cytotoxins (Rutkoski and Raines, 2008). In contrast, we have shown that ribonuclease zymogens have no observable toxicity toward a human cell line that does not contain HIV PR (Table 4.1). This absence of cytotoxicity suggests that a drug based on a ribonuclease zymogen could have a high therapeutic index. Another attractive feature is the potential difficulty in the development of viral resistance to a ribonuclease zymogen. Rapid viral replication and the high error-rate of reverse transcriptase have led to the rapid development of resistance

to reverse-transcriptase inhibitors and protease inhibitors, small-molecule drugs that rely on binding to these enzymes. It is reasonable to anticipate that resistance to a drug that requires the catalytic activity of HIV PR toward a native substrate would be significantly more difficult for a virus to develop. Moreover, resistance derived from a protease variant with altered specificity could be countered by replacing the linker sequence with one that is recognized by the protease variant. Finally, we note that a chemotherapeutic agent based on a ribonuclease zymogen would not be used concurrently with protease-inhibitor therapy, which would likely diminish zymogen activation and hence efficacy.

In conclusion, we have described the creation of an HIV-specific RNase A zymogen that increases in catalytic efficiency by approximately 50-fold upon activation with HIV PR, is stable at physiological temperature, and is not toxic to uninfected cells. These data establish a proof-of-principle for a new class of agents for the treatment of HIV/AIDS. We anticipate testing our strategy with human cells containing HIV PR.

Acknowledgements. We are grateful to J.F. May and S.M. Fuchs for assistance with cloning, L.D. Lavis for diethylfluorescein derivatives, and M.N. Levine, S.M. Fuchs, K.A. Dickson, and R.J. Johnson for contributive discussions. This work was supported by grant CA073808 (NIH). R.F.T. was supported by a Wisconsin Distinguished Rath Graduate Fellowship. The University of Wisconsin–Madison Biophysics Instrumentation Facility was established with grants BIR-9512577 (NSF) and RR13790 (NIH). The Keck Center for Chemical Genomics was established with a grant from the W.M. Keck Foundation.

Table 4.1 Biochemical Properties of Unactivated Ribonuclease A Zymogens

Ribonuclease	T_m[a]	K_d[b]	IC_{50}[c]	m/z[d]	
	(°C)	*(nM)*	*(μM)*	*expected*	*observed*
Wild-type	64[e]	44×10^{-6}[f]	>25	13,682	13,692
Zymogen **1**	46	150 ± 10	>25	15,165	15,142
Zymogen **2**	49	—	>25	15,222	15,208

[a] Values of T_m were determined in PBS by UV spectroscopy.
[b] Value of K_d (±SE) was determined for the complex with hRI at (23 ± 2) °C.
[c] Values of IC_{50} are for the incorporation of [*methyl*-^{3}H]thymidine into the DNA of K-562 cells.
[d] Values of *m/z* were determined by MALDI–TOF mass spectrometry.
[e] From (Rutkoski *et al.*, 2005).
[f] From (Lee *et al.*, 1989b).

Table 4.2 Kinetic Parameters of Ribonuclease A Zymogens with an Oligonucleotide Substrate[a]

Ribonuclease	$(k_{cat}/K_M)_{unactivated}$ $(10^3\ M^{-1}s^{-1})$	$(k_{cat}/K_M)_{activated}$ $(10^6\ M^{-1}s^{-1})$	$\frac{(k_{cat}/K_M)_{activated}}{(k_{cat}/K_M)_{unactivated}}$
Wild-type	N/A	52 ± 4[b]	N/A
Zymogen **1**	290 ± 40	14 ± 1	48
Zymogen **2**	870 ± 220	7.6 ± 5	9

N/A, not applicable

[a] Values of k_{cat}/K_M (±SE) were determined for catalysis of 6-FAM–dArU(dA)$_2$–6-TAMRA cleavage at 25 °C in 0.10 M MES–NaOH buffer (OVS-free), pH 6.0, containing 0.10 M NaCl.

[b] From (Rutkoski *et al.*, 2005).

Table 4.3 Kinetic Parameters of Ribonuclease A Zymogens with a Polynucleotide Substrate[a]

Ribonuclease	$(k_{cat})_{unactivated}$ (s^{-1})	$(k_{cat})_{activated}$ (s^{-1})	$(K_M)_{unactivated}$ $(10^{-6}\ M)$	$(K_M)_{activated}$ $(10^{-6}\ M)$	$(k_{cat}/K_M)_{unactivated}$ $(10^3\ M^{-1}s^{-1})$	$(k_{cat}/K_M)_{activated}$ $(10^6\ M^{-1}s^{-1})$	$\frac{(k_{cat}/K_M)_{activated}}{(k_{cat}/K_M)_{unactivated}}$
Wild-type[b]	N/A	280 ± 29	N/A	3.3 ± 0.2	N/A	83 ± 7	N/A
Zymogen **1**	3.2 ± 0.1	38 ± 2	120 ± 16	60 ± 10	27 ± 3	0.65 ± 0.1	24

N/A, not applicable

[a] Values of k_{cat}, K_M, and k_{cat}/K_M (±SE) were determined for catalysis of poly(C) cleavage at 25 °C in 0.10 M MES–NaOH buffer (OVS-free), pH 6.0, containing 0.10 M NaCl. Initial velocity data were used to calculate values of k_{cat}, K_M, and k_{cat}/K_M with the program Prism 4 (GraphPad Software, San Diego, CA).

[b] From (Johnson *et al.*, 2006).

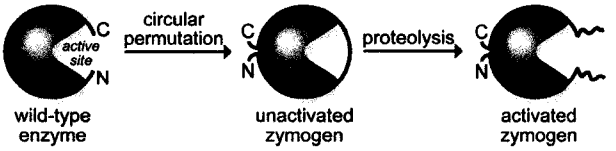

Figure 4.1 Design of a ribonuclease A zymogen (Plainkum *et al.*, 2003; Johnson *et al.*, 2006). Circular permutation is used to block access to the active site until proteolytic activation, here by HIV PR.

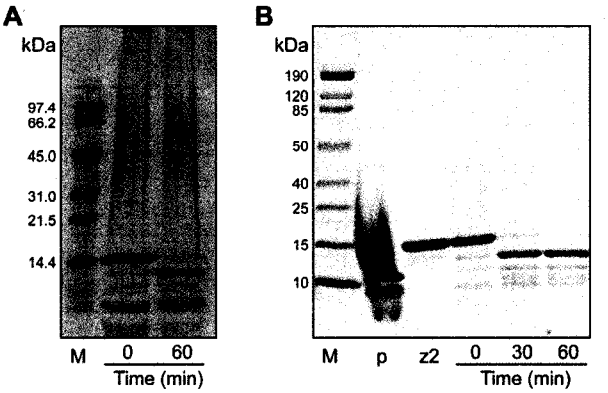

Figure 4.2 Activation of zymogens by HIV PR. Activation at 37 °C was monitored by SDS–PAGE in the presence of DTT. (*A*) Activation of zymogen **1** after addition of HIV PR at a 1:5 (protease:zymogen) molar ratio. (*B*) Activation of zymogen **2** after addition of HIV PR at a 1:25 (protease:zymogen) molar ratio. 'M' is the protein molecular weight marker, 'p' is HIV PR, and 'z2' is zymogen 2.

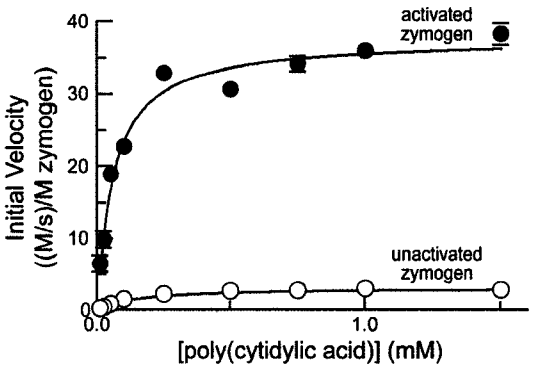

Figure 4.3 Catalysis of RNA cleavage by unactivated zymogen **1** (○; 1.0 μM) and activated zymogen **1** (●; 20 nM). Initial velocity data (±SE) at increasing amounts of poly(C) are normalized for zymogen concentration. Data were used to determine values of k_{cat}, K_M, and k_{cat}/K_M (Table 4.3).

CHAPTER 5

Future Directions

5.1 Physiological role of ONC

Although the antitumoral activity of embryonic extracts of the Northern leopard frog *Rana pipiens* was first reported in 1973 and the sequence of ONC was described in 1991 (Ardelt *et al.*, 1991), the physiological role of ONC in the frog remains unknown. Its extraordinary conformational stability ($T_m \approx 90$ °C) (Leland *et al.*, 1998) is highly unusual for a protein that comes from a mesophilic organism. Its conformational stability correlates with proteolytic stability (Klink and Raines, 2000), however, suggesting that resistance against proteolysis could have driven the evolution of this property.

The expression of ONC in the oocytes and early embryos suggests its having a role in frog reproduction. A tissue analysis of ONC mRNA transcription would inform our understanding of the role of ONC in *Rana pipiens*. Immunoblotting as a probe for protein expression would also be of benefit, as RNA transcription does not necessarily correlate with protein translation. The lack of a quality antibody for the detection of ONC would, however, have to be overcome. In addition to these studies, an analysis of the molecular targets of the ribonucleolytic activity of ONC in the frog could suggest a role for ONC.

In addition to probing the expression of ONC in the frog, identification of a homologue of RI from *Rana pipiens* would offer insight into the function of ONC. It has been stated that ribonuclease inhibitor homologues do not interact with ribonuclease homologues from different classes (Beintema and Kleineidam, 1998). Yet, no amphibian ribonuclease inhibitor homologues have been isolated. Isolation of a frog-specific RI from *Rana pipiens* oocytes can likely be accomplished via affinity chromatography with

an ONC-functionalized column, similar to the purification of hRI (Klink *et al.*, 2001). Subsequent analysis of the interaction of frog RI with ONC and mammalian ribonucleases, such as RNase A and RNase 1, would greatly inform our understanding of the evolution of the RNase A superfamily and its cognate inhibitors.

5.2 Basis for cancer cell selectively

Although ONC is in Phase IIIb clinical trials (Costanzi *et al.*, 2005; Pavlakis and Vogelzang, 2006) and cytotoxic variants of mammalian ribonucleases are being developed as therapeutics (Rutkoski *et al.*, 2005; Johnson *et al.*, 2007a), the basis for the selectivity of these drugs for cancer cells remains unknown. Several hypotheses for the basis of this selectivity have been proposed. One is that ribonucleases target cancer cells because cancer cells have higher RNA turnover than normal cells. Another hypothesis is that the altered profile of macromolecules on the surface of cancer cells (Bergelson *et al.*, 1970; Ran *et al.*, 2002; Sasisekharan *et al.*, 2002; Fredman *et al.*, 2003) targets ribonucleases to them. Finally, it is thought that altered membrane trafficking in cancer cells (Kroemer and Jäättelä, 2005) leads to different routing of ribonucleases, possibly leading to increased translocation from endosomes.

ONC has proven to be a rare type of cancer chemotherapeutic, in that it does not cause the typical side effects associated with chemotherapeutics, such as bone marrow suppression, hair loss, and nausea and vomiting (Costanzi *et al.*, 2005). These side effects are a direct result of the mechanism of action of these drugs, which target *all* cells that are

growing rapidly. In addition to cancer cells, many normal cell types, especially blood cells, hair cells, and the cells of the gastric epithelium, are growing rapidly. The destruction of these cells leads to the side effects profile of many cancer chemotherapeutics. The difference in the side effects of ONC suggests a difference in the mechanism of action. The basis for the selectively of ONC for cancer cells is not likely to be something that broadly targets rapidly growing cells. This makes the hypothesis that ONC targets cancer cells due to their increase in RNA turnover compared to normal cells less likely. It is possible, however, that cancer cells contain different RNA targets than normal cells. An analysis of the RNA targets of ONC and other cytotoxic ribonucleases in cancer cells and normal cells could test this hypothesis.

There have been few comparisons of the effects of ONC on cancer cell lines versus non-cancerous cell lines (Rutkoski *et al.*, 2005), due to the challenges involved in working with non-cancerous cell lines. Non-cancerous cell lines are typically much slower growing than cancer cell lines, making comparisons between proliferation assays of the cell lines quite difficult. In addition, these cell lines are transformed and immortalized, making them intrinsically different from primary cell lines in ways that are not completely characterized.

Two different strategies could be used for comparing the effects of ribonucleases on cancer cells and normal cells. One approach would be the use of cytotoxicity assays that are able to detect apoptosis. This type of assay would not be dependent on the growth rates of the cells. For example, the binding of annexin V (Boersma *et al.*, 2005), which detects the exposure of phosphatidylserine on the cell surface early in apoptosis (Ran *et*

al., 2002), to K-562 cells can be followed by flow cytometry, and work is ongoing in this laboratory toward the use of this assay.

Another strategy for determining the basis for the cancer cell selectivity of ribonucleases is the use of fluorogenic probes (Lavis *et al.*, 2006). We have described the use of a fluorogenic probe for the endocytosis of ribonucleases to observe the relative internalization of variants of ONC in CHAPTER 2. This same probe could be used to detect the relative internalization of ONC and other ribonucleases into the endosomes of cancer cells and non-cancer cells. This strategy would allow the testing of the hypothesis that ribonucleases target cancer cells via their altered cell-surface macromolecules.

In addition, work is ongoing in our laboratory toward the synthesis of a probe specific for translocation from the endosomes. With this probe, it would be possible to compare the relative translocation of ribonucleases from endosomes in various cell types, in particular comparing cancer cells with cells from their tissue of origin. The ability of ribonucleases to translocate to the cytosol could be different in cancer cells versus normal cells, as the trafficking of endosomes differs in cancer cells (Kroemer and Jäättelä, 2005).

5.3 Improving internalization of cytotoxic ribonucleases

We have described the comparatively low internalization of ONC into the endosomes of K-562 cells, as compared to RNase 1 (CHAPTER 2). Although ONC has great potential as a cancer therapeutic, its dosing is limited by renal toxicity (Mikulski *et al.*, 1993). If ONC were made more cytotoxic, it could perhaps be dosed at lower amounts, leading to

more aggressive treatment and less kidney toxicity. One approach to accomplishing this would be to increase the internalization of ONC into endosomes. Two strategies have been utilized in our laboratory to increase the internalization of ribonucleases: the addition of a protein transduction domain (nonarginine) (Fuchs and Raines, 2005) and the addition of a patch of positively charged residues to the protein (Fuchs *et al.*, 2007). Both of these strategies resulted in the destabilization of RNase A ($\Delta T_m = -10$ °C) (Fuchs and Raines, 2005; Fuchs *et al.*, 2007), which negatively affected the cytotoxicity of these variants. ONC, however, is substantially more stable than RNase A (Leland *et al.*, 1998), making it more amenable to these options.

In addition, the cytotoxicity of RI-evasive variants of RNase 1, also limited by internalization (Johnson *et al.*, 2007a), could be increased by the same strategies. This therapeutic, based on a human ribonuclease, is attractive as a potential drug, due to its lack of both immunogenicity and renal accumulation (Vasandani *et al.*, 1996).

5.4 Development of ribonucleases as antivirals

In CHAPTER 4, an HIV-specific RNase A zymogen was described. Although we showed an increase in ribonucleolytic activity following activation with HIV protease, it still remains to be tested in an *in vivo* setting. Testing this zymogen against cells that are either infected with HIV, or are expressing HIV protease, is the logical next step. The extension of the zymogen strategy to additional viral targets could also be undertaken.

Many viruses lack any therapies, and any RNA virus with a virally-encoded protease could represent a potential target for a ribonuclease zymogen.

APPENDIX A

Salt-dependence of the Interaction between the Ribonuclease Inhibitor Protein and Members of the Ribonuclease A Superfamily

Contributions: Expression and purification of proteins, binding assays, composition of manuscript, and preparation of figures. Chemical syntheses of 2',7'-diethylfluorescein (DEF) and diethylfluorescein-5-iodoacetamide (DEFIA) were by Luke D. Lavis.

A.1 Abstract

Coulombic interactions play an essential role in the formation of many protein–protein interactions in biology. One such interaction is that between the ribonuclease inhibitor protein (RI) and members of the ribonuclease A superfamily—one of the tightest known protein–protein interactions. Some members of the ribonuclease A superfamily are able to kill cancer cells selectively, and the ability to evade RI is a major determinant of whether a ribonuclease will be cytotoxic. In this work, we present a preliminary examination of the salt-dependence of the interaction between RI and three of its ribonuclease ligands. One of these homologues, Onconase, is an amphibian protein and is in late-stage clinical trials for the treatment of malignant mesothelioma. It does not bind to RI under physiological conditions. The other two homologues are bovine pancreatic ribonuclease and human pancreatic ribonuclease, which are not cytotoxic and bind to RI extremely tightly. We present here the groundwork for future studies on the salt-dependence of the interactions between an inhibitor protein and multiple homologous binding partners.

A.2 Introduction

The interaction between secreted members of the bovine pancreatic ribonuclease (RNase A) superfamily and the cytosolic ribonuclease inhibitor protein (RI) is one of the tightest known protein–protein interactions in all of biology (Lee *et al.*, 1989b; Johnson *et al.*, 2007c). The association rate is ~10^8 $M^{-1}s^{-1}$ for RNase A and human RI (Lee *et al.*, 1989a). The equilibrium dissociation constant (K_d) value for the complex between human RI (hRI) and human pancreatic ribonuclease (RNase 1; Figure A.1a and b) is 2.9×10^{-16} M in phosphate-buffered saline, which contains 137 mM NaCl (PBS) (Johnson *et al.*, 2007c); that for hRI and RNase A is lower: 4.4×10^{-14} M in PBS. This tight interaction is thought to have evolved to protect cells against the adventitious invasion of ribonucleases (Haigis *et al.*, 2003). Indeed, RNase A and RNase 1 variants that evade RI are able to kill cancer cells (Leland *et al.*, 1998; Leland *et al.*, 2001; Rutkoski *et al.*, 2005; Johnson *et al.*, 2007c; Rutkoski and Raines, 2008).

Onconase (ONC) (Ardelt *et al.*, 2008; Lee and Raines, 2008), a homologue of RNase A from the Northern leopard frog *Rana pipiens*, is naturally toxic to cancer cells (Darzynkiewicz *et al.*, 1988) and is currently in Phase IIIb clinical trials for the treatment of malignant mesothelioma (Pavlakis and Vogelzang, 2006). Its cytotoxic activity is ascribed primarily to its lack of affinity for hRI (Boix *et al.*, 1996; Rutkoski and Raines, 2008), a property that likely results from the truncation of surface loops that contain the majority of the RI-contact residues in RNase A and RNase 1 (Figure A.1) (Boix *et al.*, 1996; Kobe and Deisenhofer, 1996). The affinity of RI for ONC has been difficult to

quantitate due to the requirement of vast amounts of protein (Abel *et al.*, 2002; Lavis *et al.*, 2007), and the value of the inhibition constant (K_i) for this interaction has been estimated to be >1 μM from the IC_{50} value of ONC in proliferation assays (Boix *et al.*, 1996). We report a lower limit for the value of K_i for ONC in CHAPTER 3.

The interface between RI and ribonucleases contains a higher percentage of charged residues than that typically present in protein•protein complexes (Kobe and Deisenhofer, 1996; Rutkoski *et al.*, 2005), suggesting a role for electrostatics in complex stability. RI is highly anionic, with an isoelectric point (p*I*) of 4.7 (Dickson *et al.*, 2005), and pancreatic-type ribonucleases are highly cationic. Decreasing the net charge of RNase 1 leads to a decrease in affinity for RI (Johnson *et al.*, 2007a). RI is typically purified by RNase A-affinity chromatography, and eluted from the resin with 3 M NaCl (Klink *et al.*, 2001). In addition, the K_i for the complex between placental RI and RNase A increases by more than four orders of magnitude from 0.1–1.0 M NaCl (Lee *et al.*, 1989b).

Due to the preferential interactions between electrolytes and charged proteins, the measurement of a process that changes the amount of solvent-exposed surface area should exhibit some dependence on salt concentration, depending on the range of salt concentration studied (Record *et al.*, 1998). In the case of RI binding to ribonucleases, 2583–3438 $Å^2$ of surface area is buried (Rutkoski and Raines, 2008). The salt-dependence of these equilibria can be a result of Coulombic effects, Hofmeister effects, and/or osmotic effects. Coulombic effects, usually the dominant contributor to salt effects at low salt concentrations (<100 mM), do not depend on the nature of the salt other than its valency. Hofmeister effects, which are typically present at higher salt concentrations,

depend on the nature of the salt and follow the Hofmeister series. Hofmeister and osmotic effects become dominant at higher salt concentrations, where Coulombic effects are minimized and the activity of the water is affected by the presence of the salt (Record *et al.*, 1998). Here, we present evidence for the binding of hRI to ONC in a solution of low salt concentration, and preliminary data on the salt-dependence of the interactions of hRI with RNase A and RNase 1.

A.3 Experimental Procedures

A.3.1 Materials

Escherichia coli BL21(DE3) cells and pET22b(+) plasmid were from Novagen (Madison, WI). Enzymes were obtained from Promega (Madison, WI). Bovine serum albumin (BSA) was obtained as a 20 mg/mL solution (Sigma; Product B8667). BisTris (2-Bis(2-hydroxyethyl)amino-2-(hydroxymethyl)-1,3-propanediol; BioUltra; ≥99.0%) and sodium chloride (BioUltra; ≥99.5%) were obtained from Fluka Analytical (Switzerland). Fluorescein (reference standard grade) and 5-iodoacetamidofluorescein (5-IAF) were from Molecular Probes (Eugene, OR). Costar 96-well NBS microtiter plates were from Corning Life Sciences (Acton, MA). All other chemicals used were of commercial grade or better, and were used without further purification.

Terrific Broth contained (in 1.0 liter) tryptone (12 g), yeast extract (24 g), glycerol (4 mL), KH_2PO_4 (2.31 g), and K_2HPO_4 (12.54 g).

A.3.2 Instrumentation

Molecular mass was measured by matrix-assisted laser desorption/ionization time-of-flight (MALDI–TOF) mass spectroscopy using a Voyager-DE-PRO Biospectrometry Workstation (Applied Biosystems, Foster City, CA) at the University of Wisconsin–Madison Biophysics Instrumentation Facility. Fluorometric measurements in cuvettes were made using a QuantaMaster1 photon-counting spectrofluorometer from Photon Technology International (South Brunswick, NJ), equipped with sample stirring. The fluorescence intensity in microtiter plates was recorded with a Perkin–Elmer EnVision 2100 plate reader equipped with a FITC filter set (excitation at 485 nm with 14 nm bandwidth; emission at 535 nm with a 25 nm bandwidth; dichroic mirror cutoff at 505 nm) at the W.M. Keck Center for Chemical Genomics.

A.3.3 Purification of ribonuclease inhibitor, ribonucleases, and fluorophore-labeled ribonucleases

hRI (Johnson *et al.*, 2007c) and RNase A (Leland *et al.*, 1998) were purified as described previously. RNase 1 was a kind gift from R.J. Johnson. ONC was purified as described previously (Leland *et al.*, 1998), with the following exceptions. ONC was refolded overnight at room temperature after slow dilution (by 10-fold) into 0.10 M Tris–HCl buffer, pH 8.0, containing NaCl (0.10 M), reduced glutathione (3.0 mM), and oxidized glutathione (0.6 mM). After concentration by ultrafiltration, samples were dialyzed overnight against 50 mM sodium acetate buffer, pH 5.0, containing NaCl (0.10 M), and applied to a MonoS cation-exchange FPLC column (Pharmacia). ONC was

eluted from the column with a linear gradient of NaCl (0.15–0.30 M). Protein concentrations were determined by UV spectroscopy using extinction coefficients of ε_{280} = 0.88 $(mg/mL)^{-1} \cdot cm^{-1}$ for hRI (Klink *et al.*, 2001), ε_{278} = 0.72 $(mg/mL)^{-1} \cdot cm^{-1}$ for RNase A (Leland *et al.*, 1998), ε_{280} = 0.53 $(mg/mL)^{-1} \cdot cm^{-1}$ for RNase 1 (Leland *et al.*, 2001), and ε_{280} = 0.87 $(mg/mL)^{-1} \cdot cm^{-1}$ for ONC (Leland *et al.*, 1998).

Variants of RNase A with a free cysteine at position 88 were purified as described previously for other RNase A variants (Lavis *et al.*, 2007), with the following exceptions. Fluorescein–K7A/D38R/R39D/N67R/G88C RNase A conjugate (fluorescein–KDRNG RNase A) was prepared by reaction of K7A/D38R/R39D/N67R/G88C RNase A, a variant of RNase A with a dramatically attenuated affinity for RI (Rutkoski *et al.*, 2005), with a 10-fold excess of 5-IAF for 2.5 h at 25°C. Conjugate was purified using a HiTrap SP HP cation-exchange column (GE Healthcare, Uppsala, Sweden). 2',7'-Diethylfluorescein-5-iodoacetamide (DEFIA) was synthesized as described previously (Lavis *et al.*, 2007). DEFIA–protein conjugate (DEF–RNase A) was prepared by the reaction of G88C RNase A with a 10-fold excess of DEFIA, as described previously (Lavis *et al.*, 2007). Protein concentrations of conjugates were determined by a bicinchoninic acid (BCA) assay kit from Pierce (Rockford, IL), using BSA as a standard. The molecular masses of ribonucleases and their conjugates were confirmed by MALDI–TOF mass spectroscopy.

A.3.4 Determination of pK_a values

2',7'-Diethylfluorescein (DEF) was synthesized as described previously (Lavis *et al.*, 2007). The pK_a values for the phenolic oxygen atoms of DEF and fluorescein were determined as described previously (Lavis *et al.*, 2007), with the following modifications. Buffers contained sodium acetate (NaOAc), 2-(*N*-morpholino)-ethanesulfonic acid (MES), sodium phosphate (NaH_2PO_4), Tris, and sodium bicarbonate ($NaHCO_3$) (0.10 mM each). The pH of the buffered solutions was adjusted with 10–100 mM NaOH or 10–100 mM HCl. Experiments were performed in cuvettes using λ_{ex} = 493 nm and λ_{em} = 515 nm. The final dye concentration was 50 nM. The fluorescence intensity of the dye was measured as a function of pH, and pK_a values were determined by fitting the data to the following equation:

$$I = I_2 + \frac{I_3 - I_2}{1 + 10^{pK_a - pH}} \tag{A.1}$$

where I represents the observed fluorescence intensity, and I_2 and I_3 are the phenol and phenolate fluorescence intensities, respectively.

A.3.5 Determination of K_d values for labeled ribonucleases

To measure the salt-dependence of the K_d values for RI and ribonucleases, the concentration of buffer needed to be much lower than the concentration of NaCl. We chose the BisTris buffer system, which does not contain sodium ions and has been shown

not to interfere with the activity of ribonucleases (Park and Raines, 2000; Park and Raines, 2001). Although our assay is not dependent on ribonucleolytic activity, RI does bind to the active site of ribonucleases (Kobe and Deisenhofer, 1996; Johnson *et al.*, 2007c), so buffers that bind to the active site, such as phosphate (Richards and Wyckoff, 1971), could also interfere with RI binding. For the K_d determination for ONC, the buffer concentration was 1.0 mM, twofold lower than the lowest salt concentration. For RNase A and RNase 1, the buffer concentration was 10 mM, 10-fold lower than the lowest salt concentration.

The binding of fluorescein–KDRNG RNase A to hRI was monitored by fluorescence spectroscopy as described previously (Abel *et al.*, 2002) at varying concentrations of NaCl. A serial dilution (1.0 μM→0.5 nM; 2×) of hRI in BisTris–HCl buffer (1.0 mM), pH 7.0, containing NaCl (2.0 mM, 5.0 mM, or 10.0 mM), BSA (0.5 mg/mL), and DTT (10 mM; 2×) was prepared. A 50-μL aliquot of these serial dilutions was added to the wells of a 96-well plate. A solution (50 μL) of fluorescein–KDRNG RNase A (100 nM; 2×) in BisTris–HCl buffer (1.0 mM), pH 7.0, containing NaCl (2.0 mM, 5.0 mM, or 10.0 mM) and BSA (0.5 mg/mL) was added to each well. The plate was incubated for 30 min at 25°C, then fluorescence intensity was measured. The values of the equilibrium dissociation constant for the labeled proteins (K_d) were determined by fitting the data to Equation A.2 as described previously (Lavis *et al.*, 2007).

$$f_B = \frac{K_d + [\text{RNase A*}] + [\text{RI}] - \sqrt{(K_d + [\text{RNase A*}] + [\text{RI}])^2 - 4[\text{RNase A*}][\text{RI}]}}{2[\text{RNase A*}]} \quad \text{(A.2)}$$

where f_B is the fraction of fluorescein–KDRNG RNase A bound to RI and [RNase A*] is the concentration of fluorescein–KDRNG RNase A.

Similarly, the binding of DEF–RNase A to hRI was monitored at varying concentrations of NaCl. A serial dilution (1.0 μM→0.5 nM; 2×) of hRI in BisTris–HCl buffer (10 mM), pH 7.0, containing NaCl (100 mM, 200 mM, 500 mM or 1.0 M), BSA (0.5 mg/mL), and DTT (10 mM; 2×) was prepared and added to the wells of a 96-well plate. A solution (50 μL) of DEF–RNase A (100 nM; 2×) in BisTris–HCl buffer (10 mM), pH 7.0, containing NaCl (100 mM, 200 mM, 500 mM or 1.0 M) and BSA (0.5 mg/mL) was added to each well. Data were obtained and analyzed as described above.

A.3.6 Determination of K_d values for wild-type ribonucleases

For the ONC competition assay (Abel *et al.*, 2002; Lavis *et al.*, 2007), a serial dilution (3.0 mM→1.4 μM; 2×) of ONC in BisTris–HCl buffer (1.0 mM), pH 7.0, containing NaCl (2.0 mM, 5.0 mM, or 10.0 mM) and BSA (0.5 mg/mL) was prepared in Eppendorf Protein LoBind Tubes (Fisher Scientific). A 50-μL aliquot of these serial dilutions was added to the wells of a 96-well plate. A solution (50 μL) of fluorescein–KDRNG RNase A (100 nM; 2×) and hRI (82 nM; 2×) in BisTris–HCl buffer (1.0 mM), pH 7.0,

containing NaCl (2.0 mM, 5.0 mM, or 10.0 mM), BSA (0.5 mg/mL), and DTT (10 mM; 2×) was prepared in LoBind tubes and added to each well. The concentration of hRI was the amount required under these conditions for 80% of the fluorescein–KDRNG RNase A to be bound (determined from the titration of the labeled ribonuclease above). This allowed the signal to be sensitive to changes in the amount of free fluorescein–KDRNG RNase A as it is released from hRI. The negative control contained no ribonuclease, and the positive control contained excess RNase A (10 μM). The plate was incubated for 30 min at 25°C, then fluorescence intensity was measured. For previous assays of the binding of hRI to G88R–RNase A in PBS, data were reproducible following incubation times ranging from 10 min to 24 h, suggesting that the system had reached equilibrium (Lavis LD, Rutkoski TJ, Raines RT, unpublished data).

The fraction of bound fluorescein–KDRNG RNase A was calculated by determining the decrease in fluorescence intensity of the samples compared to the decrease when fluorescein–KDRNG RNase A was bound completely. The observed fluorescence intensity can be described by

$$I = f_F I_F + f_B I_B \tag{A.3}$$

where I_F and I_B are the fluorescence intensities of the free and RI-bound forms of fluorescein–KDRNG RNase A, respectively, and f_F and f_B are the fractions of the two forms. The value of I_B was determined using the fluorescence intensities of the positive

and negative controls, based on the K_d values for the labeled proteins determined in the initial binding studies (above). The fraction bound was calculated using

$$f_B = \frac{I - I_F}{I_B - I_F} \tag{A.4}$$

The K_d value for ONC was determined by plotting f_B against the concentration of ONC and fitting the data to the Equation A.5 for the competitive binding of two ligands, as described previously (Wang, 1995; Roehrl *et al.*, 2004; Lavis *et al.*, 2007).

$$[\text{ONC}] = \frac{\left[(K_{d1} - K_{d2})f_B + K_{d2}\right]\left[[\text{RNase A*}]f_B^{\,2} - (K_{d1} + [\text{RNase A*}] + [\text{RI}])f_B + [\text{RI}]\right]}{(1 - f_B)f_B K_{d1}} \tag{A.5}$$

where K_{d1} is the K_d value for the fluorescein–KDRNG RNase A and K_{d2} is the K_d value for RI and ONC. Since Equation A.5 is cubic in f_B, we solved for the physically meaningful root with Equation A.6:

$$f_B = \frac{2\sqrt{(d^2 - 3e)}\cos(\theta/3) - d}{3K_{d1} + 2\sqrt{(d^2 - 3e)}\cos(\theta/3) - d} \tag{A.6}$$

where

$$d = K_{d1} + K_{d2} + [\text{RNase A*}] + [\text{ONC}] - [\text{RI}]$$

$$e = ([\text{ONC}] - [\text{RI}])K_{d1} + ([\text{RNase A*}] - [\text{RI}])K_{d2} + K_{d1}K_{d2}$$

$$f = -K_{d1}K_{d2}[\text{RI}]$$

and

$$\theta = \arccos\left[\frac{-2d^3 + 9de - 27f}{2\sqrt{(d^2 - 3e)^3}}\right]$$

Similarly, for the RNase A and RNase 1 competition assays, a serial dilution (20 μM→10 nM 2×) of ribonuclease in BisTris–HCl buffer (10 mM), pH 7.0, containing NaCl (100 mM, 200 mM, 500 mM, or 1.0 M) and BSA (0.5 mg/mL) was prepared in LoBind tubes. A 50-μL aliquot of these serial dilutions was added to the wells of a 96-well plate. A solution (50 μL) of DEF–RNase A (100 nM; 2×) and hRI (104 nM, 116 nM, 170 nM, or 960 nM; 2×) in BisTris–HCl buffer (1.0 mM), pH 7.0, containing NaCl (2.0 mM, 5.0 mM, and 10.0 mM), BSA (0.5 mg/mL), and DTT (10 mM; 2×) was prepared in LoBind tubes and added to each well. The negative control contained no ribonuclease, and the positive control contained excess RNase 1 (50 μM). Data were collected and analyzed as above.

A.4 Results

A.4.1 pK_a values of fluorescein derivatives at low salt concentration

Our assay for the determination of the K_d values for RI and ribonucleases is dependent on a shift in the pK_a of fluorescein that occurs upon binding to RI (Lavis *et al.*, 2007). The relevant equilibria for fluorescein (**1** and **2**) and its derivative, DEF (**3** and **4**), are shown in Scheme A.1

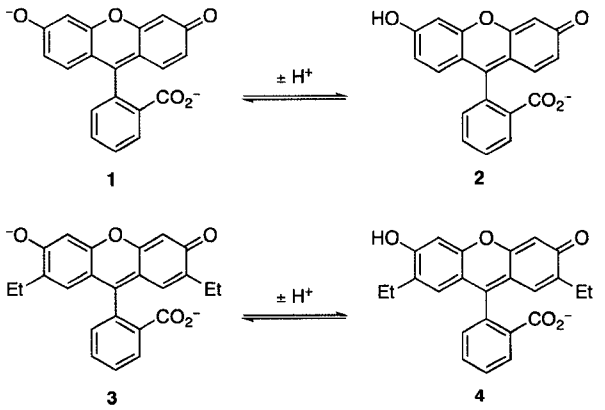

The dianionic forms of fluorescein (**2**) and DEF (**4**) are responsible for the strong absorption and emission of the dyes. The pK_a value of the ribonuclease-bound dye shifts upon binding to the anionic RI, causing a decrease in fluorescence that increases with subsequent release of the dye. When the labeled ribonuclease is competed off by another ribonuclease, its fluorescence again increases (Abel *et al.*, 2002; Lavis *et al.*, 2007).

Previously, we have described the tuning of the pK_a of fluorescein for RI-binding assays by maximizing the difference in fluorescence between the bound and unbound

forms of fluorescein-conjugated ribonucleases (Lavis *et al.*, 2007). This assay was optimized for use in buffers at a biologically relevant pH and salt concentration (specifically, PBS). Our current work, however, necessitated the use of this assay in solutions of low salt concentrations. Extreme shifts in salt concentration typically affect pK_a values, because low salt destabilizes the charged moiety (in this case the dianionic form, species **1** and **3** in Scheme 4.1) (De Maria *et al.*, 1994; Kao *et al.*, 2000). Indeed, when the pK_a values of the free dyes (fluorescein and DEF) were measured in buffers containing low salt concentrations, the values were increased relative to the values at higher salt concentrations (Table A.1). This shift positioned the pK_a value of fluorescein at 6.7, a good value for the K_d assay. Hence, we chose to use fluorescein–KDRNG RNase A for the experiments with ONC at low salt concentrations and DEF–RNase A for the experiments with RNase A and RNase 1 at high salt concentrations.

A.4.2 Values of K_d for labeled ribonucleases

The change in buffer system from phosphate to BisTris and the concurrent decrease in salt concentrations would be expected to decrease the K_d values as compared to those determined previously. The location of the fluorescent dye, however, was changed from position 19 (outside of the RNase A–RI interface) to position 88 (within the RNase A–RI interface), a change that would be expected to *raise* the K_d values relative to those obtained in PBS. Thus, our values cannot be anticipated exactly by the previously obtained values. Considering this, the K_d values obtained for DEF–RNase A (3.0 nM in 100 mM NaCl, 4.4 nM in 200 mM NaCl, 11.0 nM in 500 mM NaCl, and 110 nM in 1.0

M NaCl; Figure A.2b) were reasonable as compared to previously obtained values for fluorescein A19C/G88R–RNase A (0.55 nM) (Abel *et al.*, 2002) in PBS.

Although the K_d value for the binding of hRI to KDRNG RNase A is significantly increased relative to that for hRI and wild-type RNase A (Rutkoski *et al.*, 2005), binding of RI to KDRNG RNase A is very tight in the range of salt concentration used here. Plots of binding data at three salt concentrations (2.0 mM, 5.0 mM, and 10.0 mM) are superimposable as shown in Figure A.2a. The f_B values vary linearly with RI concentration up to saturation, so only a bound on the K_d values can be determined. We find that the K_d values are <0.25 nM at all three salt concentrations. Previously this assay has been used for ligands with nanomolar or higher K_d values (Abel *et al.*, 2002).

A.4.3 Binding of hRI to ONC

Without a true K_d value for fluorescein–KDRNG RNase A, K_d values for ONC cannot be calculated from this competition assay. We were, however, able to observe binding of hRI to ONC, which appeared to be in the micromolar range (Figure A.3). Because the K_d values for hRI and ONC could not be determined, the salt-dependence of this interaction could not be examined in this study.

A.4.4 Salt-dependence of K_d values for RNase A and RNase 1

Using the competition assay with DEF–RNase A, we measured the affinity of hRI for both RNase 1 and RNase A (Figures A.4 and A.5). We measured nanomolar K_d values

from 100 mM–1.0 M [Na^+] (Table A.2), reflecting the much higher affinity of RI for these ribonuclease ligands than for ONC.

The salt-dependence of the K_d values for the binding of hRI to RNase A and RNase 1 was determined. These data were graphed as both log(K_d) versus log[Na^+] and log(K_d) versus [Na^+] plots (see Discussion). For the log(K_d) versus log[Na^+] plot (Figure A.6a), the slopes were the same ($\partial\log(K_d)/\partial\log[Na^+] = 1.3 \pm 0.4$ for RNase A and RNase 1). For the log(K_d) versus [Na^+] plot (Figure A.6b), the slopes were within error of each other ($\partial\log(K_d)/\partial[Na^+] = 1.6 \pm 0.2$ for RNase A and $\partial\log(K_d)/\partial[Na^+] = 1.4 \pm 0.1$ for RNase 1).

A.5 Discussion

A.5.1 ONC inhibition by hRI

We observe that hRI binds to ONC at low salt (Figure A.3). Nonspecific interactions can occur between proteins in solutions of low salt concentration. These interactions can bring together residues that are not at the biologically relevant interface between the proteins. Such weak interactions are screened in solutions of physiological salt concentration (Selzer and Schreiber, 1999; Shaul and Schreiber, 2005). The nature of our assay requires that the binding be somewhat specific, as competition for the binding site on hRI must occur. Our assay, therefore, suggests that binding to a specific region of RI is occurring, but not necessarily binding to a specific region of ONC. We have, however, recorded K_i values of hRI for ONC in the high nanomolar range at low salt (see CHAPTER 3). The ability of hRI to inhibit the ribonucleolytic activity of ONC indicates that hRI can

bind to the active site of ONC, perhaps in a manner similar to that of other members of the RNase A superfamily.

The K_d values of ONC could not be determined with the competition assay using fluorescein–KDRNG RNase A. An accurate K_d value for fluorescein–KDRNG RNase A could perhaps be determined following an extremely long incubation time (Abel *et al.*, 2002). Alternatively, a more RI-evasive ribonuclease variant, which is not known at this time, would have to be used for this competition assay.

A.5.2 Electrostatic interactions in the hRI•RNase A and hRI•RNase 1 complexes

At lower salt concentration, Coulombic effects, which are not dependent on the type of salt used, except for its valency, are usually dominant. These effects should result in a linear dependence for the $\log(K_d)$ versus $\log[Na^+]$ plot. At higher salt concentration, however, Hofmeister and osmotic effects are more dominant, causing the $\log(K_d)$ values to vary linearly with $[Na^+]$. These effects depend on the nature of the salt (Record *et al.*, 1998). We observe that both the $\log(K_d)$–$\log[Na^+]$ plot and the the $\log(K_d)$–$[Na^+]$ plot vary linearly, although the error in the data is high. To deconvolute the contributions from Coulombic and Hofmeister effects, these experiments would need to be done with several different salts in the Hofmeister series.

The relative slopes of the plots in Figure A.6 could reflect the amount of charge density in the interfaces of the complexes, the charges that surround the interface, and/or the amount of surface area that is buried in complex formation. The dependence on salt concentration that is observed is a result of the preferential interactions that ions have

with the surfaces of the free proteins versus the proteins in the complex. Formation of the complex leads to the expulsion of ions from the interface (Record *et al.*, 1998). The relative amount of ions that accumulate and are displaced in the interaction could differ between ribonuclease homologues, leading to a change in the salt-dependence of the interaction.

The structures of the complexes between hRI and RNase 1 (Johnson *et al.*, 2007c) and between porcine RI (pRI) and RNase A (Kobe and Deisenhofer, 1996) are known. The structure of the hRI–RNase A complex, however, is not known. More surface area buried in the formation of the complex between hRI and RNase 1 than in that of pRI and RNase A (Johnson *et al.*, 2007c). Considering this, one might expect the K_d value for the hRI•RNase 1 complex to have a stronger dependence upon salt. The slopes of the $\log(K_d)$–$\log[Na^+]$ plots and the $\log(K_d)$–$[Na^+]$ plots for RNase A and RNase 1, however, are within error of each other (Figure A.6). It is possible that the interface between hRI and RNase A is actually quite similar to that between hRI and RNase 1, or that small differences in the interfaces might not affect the interactions with ions enough to observe a difference in the salt-dependence of the K_d values. Nonlinear Poisson–Boltzmann calculations using the crystal structures of RI and the ribonucleases could help model these interactions, and perhaps predict the Coulombic effects that are observed.

A.6 Conclusions

The ribonuclease A superfamily is a vertebrate-specific family that is evolving rapidly (Beintema *et al.*, 1988). Ribonucleases and inhibitors from different classes do not interact (Beintema and Kleineidam, 1998), and the intraspecies complexes tend to be more stable than do interspecies complexes (Johnson *et al.*, 2007b). The framework for RI-binding is in place in ONC (*i.e.*, the molecular shape and high density of positive charge), but the individual residues that closely interact with RI, mainly present on surface loops, are largely absent (Figure A.1) (Boix *et al.*, 1996). These factors combine to allow ONC to interact with RI in solutions of low salt concentration. The K_d values for the interaction of RI with both RNase A and RNase 1 exhibit a similar dependence on salt concentration, suggesting similarities in the interfaces of these ribonucleases with RI. In addition, we report here the "re-tuning" of fluorescein for binding assays at low salt concentrations. Future examination of the effects of different salts on the interaction between hRI with RNase A and RNase 1, combined with Poisson–Boltzmann calculations, could offer additional insights into the formation of this medically relevant interaction.

Acknowledgements. We are grateful to G. A. Ellis for assistance with data analysis and Dr. M. T. Record, Jr., Dr. R. M. Saecker, and Dr. T. J. Rutkoski for contributive discussions and critical reading of this manuscript.

Table A.1 pK_a Values of fluorescein and 2',7'-diethylfluorescein

Salt concentration	fluorescein	DEF
High*	6.30 ± 0.02	6.61 ± 0.03
Low†	6.7 ± 0.1	7.2 ± 0.3

*From (Lavis *et al.*, 2007). Data were obtained in buffers containing NaCl (138 mM), DTT (1 mM), and NaOAc, MES, NaH_2PO_4, TRIS, and $NaHCO_3$ (10 mM each).
†Data were obtained in buffers containing NaOAc, MES, NaH_2PO_4, TRIS, and $NaHCO_3$ (0.10 mM each).

Table A.2 Effect of NaCl on the K_d values for the binding of hRI to RNase A and RNase 1

	K_d (nM)	
[Na+] (mM)	RNase A	RNase 1
100	4.1 ± 1.3	3.1 ± 1.7
200	2.9 ± 1.5	4.9 ± 1.7
500	15 ± 8	10 ± 3
1000	88 ± 14	60 ± 50

Data (±SE) were obtained at 25°C in BisTris–HCl buffer (10.0 mM), pH 7.0, containing DEF–RNase A (50 nM), hRI (52 nM, 58 nM, 85 nM, or 480 nM), NaCl (100 mM, 200 mM, 500 mM, or 1.0 M), BSA (0.5 mg/mL), and DTT (5 mM).

Figure A.1 (*A*) Amino-acid sequence alignment of RNase A, RNase 1, and ONC, showing contact residues from the crystalline structures of hRI·RNase 1 and pRI·RNase A. RI contact-residues (for RNase A and RNase 1) are enclosed in black boxes. Positively charged residues are shown in blue, and negatively charged residues are shown in red, with contact residues in dark red or dark blue. The secondary structure of RNase A is identified with h (α-helix), s (β-strand), or t (turn). Sequence numbering above corresponds to RNase A, and numbering below to ONC. (*B*) Three-dimensional structure of RNase 1. RI contact-residues that are designated above are shown in stick form. (*C*) Three-dimensional structure of ONC. (*D*) Electrostatic protein contact potential surface of RNase 1. (*E*) Electrostatic protein contact potential surface of ONC. Images were generated with the program MacPyMOL (DeLano Scientific, South San Francisco, CA).

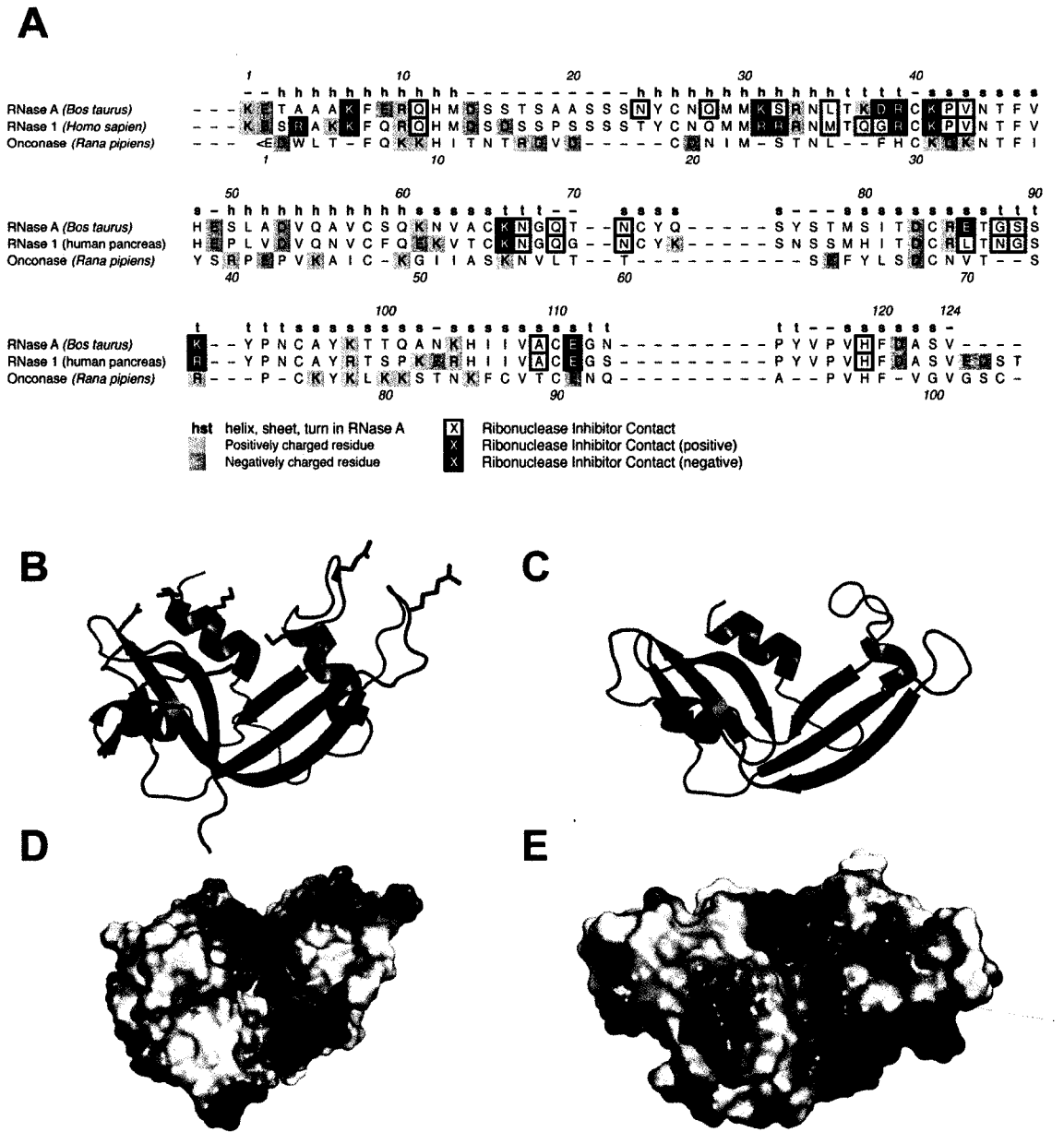
A
RNase A (Bos taurus)
RNase 1 (Homo sapien)
Onconase (Rana pipiens)
RNase A (Bos taurus)
RNase 1 (human pancreas)
Onconase (Rana pipiens)
RNase A (Bos taurus)
RNase 1 (human pancreas)
Onconase (Rana pipiens)
hst helix, sheet, turn in RNase A
Positively charged residue
Negatively charged residue
Ribonuclease Inhibitor Contact
Ribonuclease Inhibitor Contact (positive)
Ribonuclease Inhibitor Contact (negative)
B
C
D
E

Figure A.2 Binding of hRI to labeled ribonucleases. (*A*) Binding of KDRNG–fluorescein. Binding studies were carried out in BisTris–HCl buffer (1.0 mM), containing NaCl (2.0 mM (●), 5.0 mM (▼), or 10.0 mM (■)), fluorescein–KDRNG RNase A (50 nM), DTT (5 mM), BSA (0.5 mg/mL), and hRI (1.0 μM→0.5 nM). (*B*) Binding of DEF–RNase A. Binding studies were carried out in BisTris–HCl buffer (10.0 mM), containing NaCl (100 mM (◆), 200 mM (●), 500 mM (▼), or 1.0 M(■)), DEF–RNase A (50 nM), DTT (5 mM), BSA (0.5 mg/mL), and hRI (1.0 μM→0.5 nM). Data were fitted to Equation A.2.

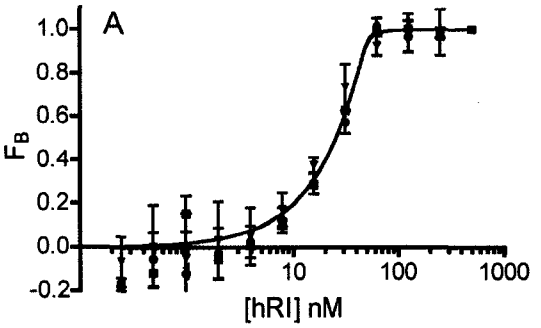
A
1.0
0.8
0.6
0.4
0.2
0.0
-0.2
F_B
10
100
1000
[hRI] nM

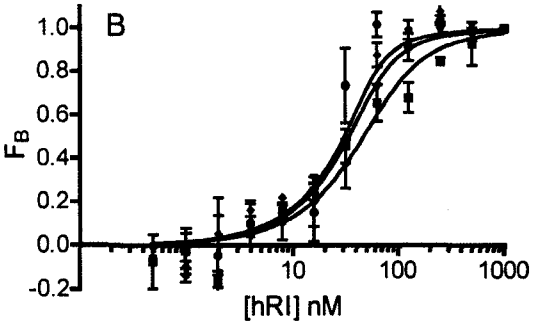
B
1.0
0.8
0.6
0.4
0.2
0.0
-0.2
F_B
10
100
1000
[hRI] nM

Figure A.3 Binding of hRI to ONC, detected by competition assay. Binding studies were carried out in BisTris–HCl buffer (1.0 mM), containing NaCl (2.0 mM (*A*), 5.0 mM (*B*), or 10.0 mM (*C*)), hRI (41 nM), fluorescein–KDRNG RNase A (50 nM), DTT (5 mM), BSA (0.5 mg/mL), and ONC (1.5 mM→0.7 μM). Data were fitted to Equation A.5.

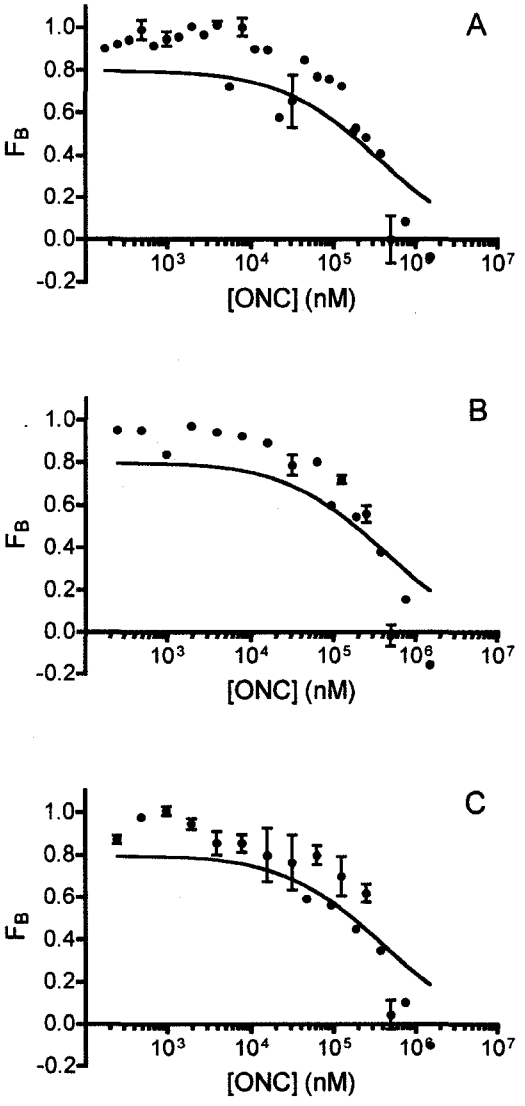
A
B
C
1.0
0.8
0.6
0.4
0.2
0.0
-0.2
F_B
10^3
10^4
10^5
10^6
10^7
[ONC] (nM)

Figure A.4 Binding of hRI to RNase A, detected by competition assay. (*A*) Binding studies were carried out in BisTris–HCl buffer (10.0 mM), containing NaCl (100 mM), hRI (52 nM), DEF–RNase A (50 nM), DTT (5 mM), BSA (0.5 mg/mL), and RNase A (10 μM→5 nM). (*B*) Buffer contained 200 mM NaCl and 58 nM hRI. (*C*) Buffer contained 500 mM NaCl and 85 nM hRI. (*D*) Buffer contained 1.0 M NaCl and 480 nM hRI. Data were fitted to Equation A.5.

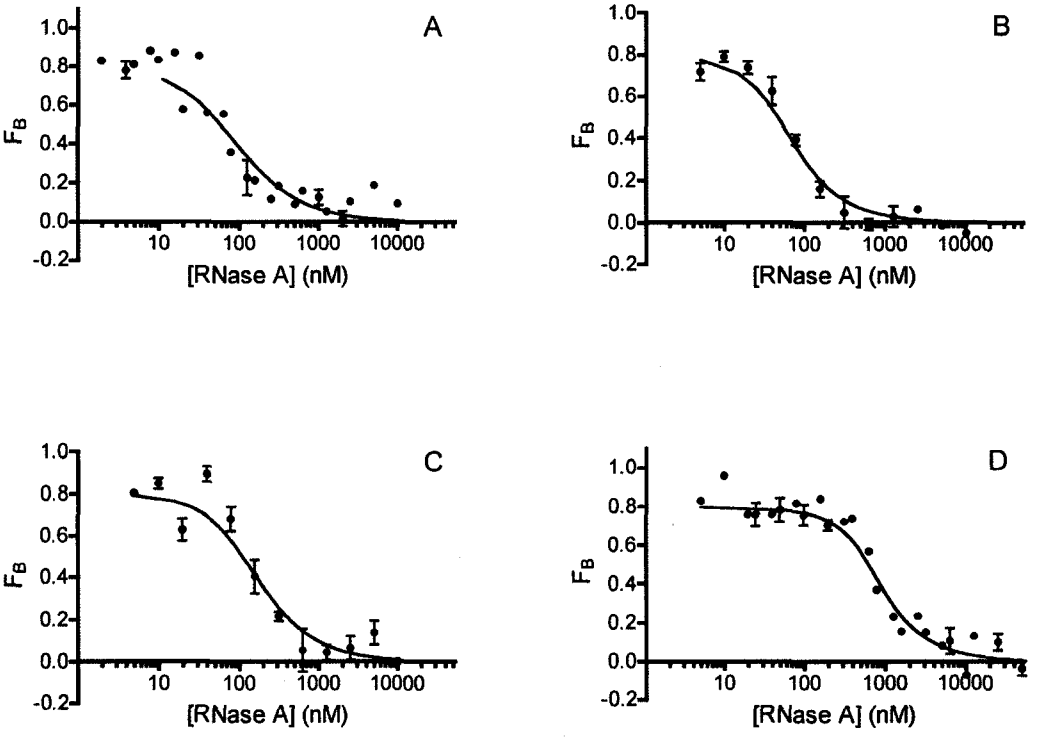
A
B
C
D
F_B
1.0
0.8
0.6
0.4
0.2
0.0
-0.2
10
100
1000
10000
[RNase A] (nM)

Figure A.5 Binding of hRI to RNase 1, detected by competition assay. (*A*) Binding studies were carried out in BisTris–HCl buffer (10.0 mM), containing NaCl (100 mM), hRI (52 nM), DEF–RNase A (50 nM), DTT (5 mM), BSA (0.5 mg/mL), and RNase 1 (10 μM→5 nM). (*B*) Buffer contained 200 mM NaCl and 58 nM hRI. (*C*) Buffer contained 500 mM NaCl and 85 nM hRI. (*D*) Buffer contained 1.0 M NaCl and 480 nM hRI. Data were fitted to Equation A.5.

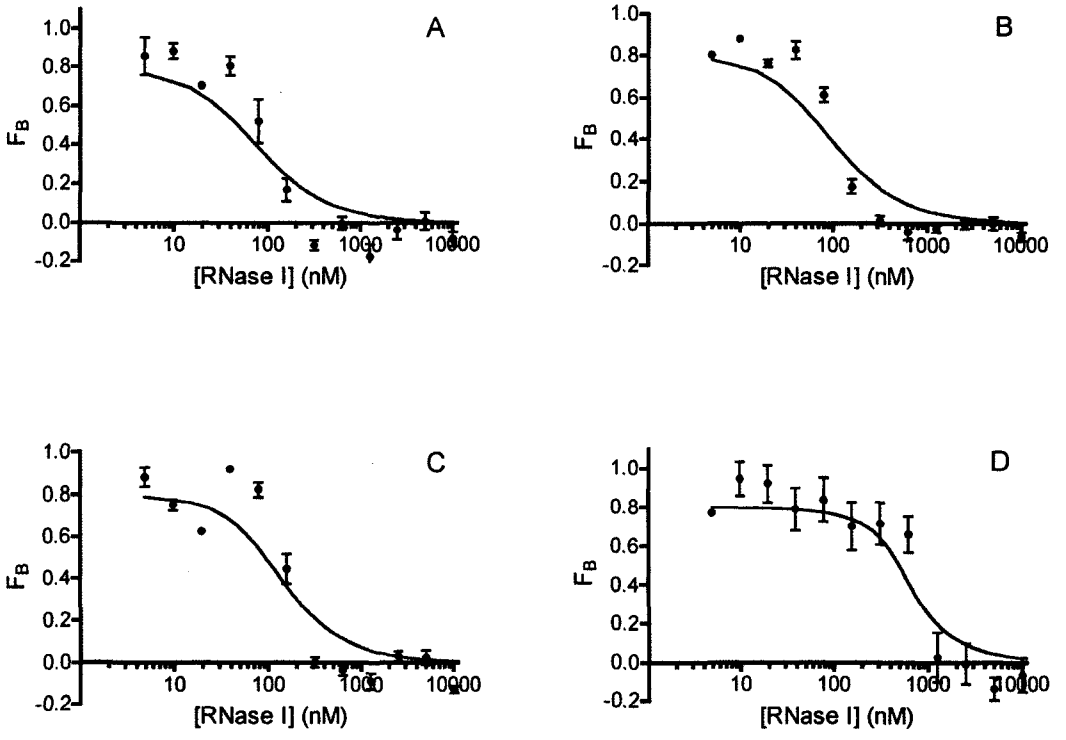
A
B
C
D
F_B
1.0
0.8
0.6
0.4
0.2
0.0
-0.2
10
100
1000
10000
[RNase I] (nM)

Figure A.6 Salt-dependence of binding of hRI to RNase A (●) and RNase 1 (■). (*A*) Plot of log(K_d) versus log[Na^+]. The slopes of the lines are 1.3 ± 0.4 for RNase A (R^2 = 0.8714), and 1.3 ± 0.4 for RNase 1 (R^2 = 0.8433). (*B*) Plot of log(K_d) versus [Na^+]. The slopes of the lines are 1.6 ± 0.2 for RNase A (R^2 = 0.9614), and 1.4 ± 0.1 for RNase 1 (R^2 = 0.9932). Data are from Table A.2.

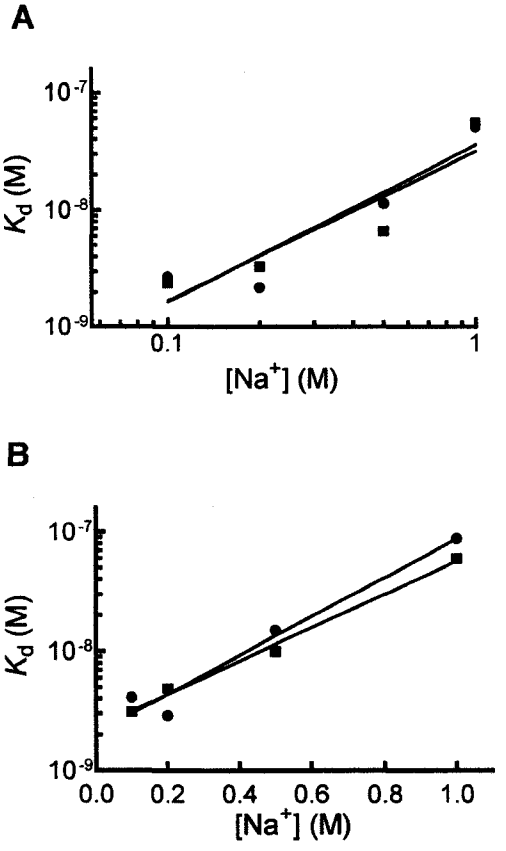
A
10^{-7}
10^{-8}
10^{-9}
K_d (M)
0.1
1
[Na^+] (M)
B
10^{-7}
10^{-8}
10^{-9}
K_d (M)
0.0
0.2
0.4
0.6
0.8
1.0
[Na^+] (M)

REFERENCES

Abel, R. L., Haigis, M. C., Park, C., Raines, R. T. (2002). Fluorescence assay for the binding of ribonuclease A to the ribonuclease inhibitor protein. *Anal. Biochem.* **306**, 100-107.

Agrawal, L., Lu, X., Jin, Q., Alkhatib, G. (2006). Anti-HIV therapy: Current and future directions. *Curr. Pharm. Des.* **12**, 2031-2055.

Alexsandrowicz, J. (1958). Intracutaneous ribonuclease in chronic myelocytic leukaemia. *Lancet* **2**, 420.

Alsallaq, R., Zhou, H. X. (2007). Prediction of protein–protein association rates from a transition-state theory. *Structure* **15**, 215-224.

Anfinsen, C. B. (1973). Principles that govern the folding of protein chains. *Science* **181**, 223-230.

Ardelt, W., Mikulski, S. M., Shogen, K. (1991). Amino acid sequence of an anti-tumor protein from *Rana pipiens* oocytes and early embryos. *J. Biol. Chem.* **266**, 245-251.

Ardelt, W., Shogen, K., Darzynkiewicz, Z. (2008). Onconase and Amphinase, the antitumor ribonucleases from *Rana pipiens* oocytes. *Curr. Pharm. Biotechnol.* **9**, 215-225.

Arnold, U. (2008). Aspects of the cytotoxic action of ribonucleases. *Curr. Pharm. Biotechnol.* **9**, 161-168.

Arnold, U., Schulenburg, C., Schmidt, D., Ulbrich-Hofmann, R. (2006). Contribution of structural peculiarities of onconase to its high stability and folding kinetics. *Biochemistry* **45**, 3580-3587.

Arnold, U., Ulbrich-Hofmann, R. (2006). Natural and engineered ribonucleases as potential cancer therapeutics. *Biotechnol. Lett.* **28**, 1615-1622.

Ashton, G. (2001). Growing pains for biopharmaceuticals. *Nat. Biotechnol.* **19**, 307-311.

Barbaro, G., Scozzafava, A., Mastrolorenzo, A., Supuran, C. T. (2005). Highly active antiretroviral therapy: current state of the art, new agents and their pharmacological interactions useful for improving therapeutic outcome. *Curr. Pharm. Des.* **11**, 1805-1843.

Bedoya, V. I., Boasso, A., Hardy, A. W., Rybak, S., Shearer, G. M., Rugeles, M. T. (2006). Ribonucleases in HIV type 1 inhibition: Effect of recombinant RNases on infection of primary T cells and immune activation-induced RNase gene and protein expression. *AIDS Res. Hum. Retroviruses* **22**, 897-907.

Beintema, J. J., Kleineidam, R. G. (1998). The ribonuclease A superfamily: General discussion. *Cell. Mol. Life. Sci.* **54**, 825-832.

Beintema, J. J., Schüller, C., Irie, M., Carsana, A. (1988). Molecular evolution of the ribonuclease superfamily. *Prog. Biophys. Molec. Biol.* **51**, 165-192.

Belting, M. (2003). Heparan sulfate proteoglycan as a plasma membrane carrier. *Trends Biochem. Sci.* **28**, 145-151.

Benito, A., Ribó, M., Vilanova, M. (2005). On the track of antitumor ribonucleases. *Mol. Biosyst.* **1**, 294-302.

Benito, A., Vilanova, M., Ribó, M. (2008). Intracellular routing of cytotoxic pancreatic-type ribonucleases. *Curr. Pharm. Biotechnol.* **9**, 169-179.

Berg, O. G., von Hippel, P. H. (1985). Diffusion-controlled macromolecular interactions. *Annu. Rev. Biophys. Biophys. Chem.* **14**, 131-160.

Bergelson, L. D., Dyatlovitskaya, E. V., Torkhovskaya, T. I., Sorokina, I. B., Gorkova, N. P. (1970). Phospholipid composition of membranes in the tumor cell. *Biochim. Biophys. Acta* **210**, 287-298.

Bjellqvist, B., Basse, B., Olsen, E., Celis, J. E. (1994). Reference points for comparisons of two-dimensional maps of proteins from different human cell types deffined in a pH scale where isoelectric points correlate with polypeptide compositions. *Electrophoresis* **15**, 529-539.

Boersma, H. H., Kietselaer, B. L., Stolk, L. M., Bennaghmouch, A., Hofstra, L., Narula, J., Heidendal, G. A., Reutelingsperger, C. P. (2005). Past, present, and future of annexin A5: From protein discovery to clinical applications. *J. Nucl. Med.* **46**, 2035-2050.

Boix, E., Wu, Y., Vasandani, V. M., Saxena, S. K., Ardelt, W., Ladner, J., Youle, R. J. (1996). Role of the N terminus in RNase A homologues: Differences in catalytic activity, ribonuclease inhibitor interaction and cytotoxicity. *J. Mol. Biol.* **257**, 992-1007.

Bosch, M., Benito, A., Ribó, M., Puig, T., Beaumelle, B., Vilanova, M. (2004). A nuclear localization sequence endows human pancreatic ribonuclease with cytotoxic activity. *Biochemistry* **43**, 2167-2177.

Brekke, O. H., Sandlie, I. (2003). Therapeutic antibodies for human diseases at the dawn of the twenty-first century. *Nat. Rev. Drug Discov.* **2**, 52-62.

Carr, A. (2003). Toxicity of antiretroviral therapy and implications for drug development. *Nat. Rev. Drug Discov.* **2**, 624-634.

Carreras, E., Boix, E., Rosenberg, H. F., Cuchillo, C. M., Nogues, M. V. (2003). Both aromatic and cationic residues contribute to the membrane-lytic and bactericidal activity of eosinophil cationic protein. *Biochemistry* **42**, 6636-6644.

Costanzi, J., Sidransky, D., Navon, A., Goldsweig, H. (2005). Ribonucleases as a novel pro-apoptotic anticancer strategy: Review of the preclinical and clinical data for ranpirnase. *Cancer Invest.* **23**, 643-650.

D'Alessio, G., Di Donato, A., Parente, A., Piccoli, R. (1991). Seminal RNase: A unique member of the ribonuclease superfamily. *Trends Biochem. Sci.* **16**, 106-108.

Ribonucleases: Structures and Functions; D'Alessio, G., Riordan, J. F., Eds.; Academic Press: New York, 1997.

Darzynkiewicz, Z., Carter, S. P., Mikulski, S. M., Ardelt, W. J., Shogen, K. (1988). Cytostatic and cytotoxic effect of Pannon (P-30 Protein), a novel anticancer agent. *Cell Tissue Kinet.* **21**, 169-182.

Daune, M. (1999). Molecular Biophysics: Structures in Motion. Oxford University Press, New York.

Davis, D. A., Dorsey, K., Wingfield, P. T., Stahl, S. J., Kaufman, J., Fales, H. M., Levine, R. L. (1996). Regulation of HIV-1 protease activity through cysteine modification. *Biochemistry* **35**, 2482-2488.

De Lorenzo, C., D'Alessio, G. (2008). From immunotoxins to immunoRNases. *Curr. Pharm. Biotechnol.* **9**, 210-214.

De Maria, P., Fontana, A., Frascari, S., Gargaro, G., Spinelli, D., Tinti, M. O. (1994). Effect of the addition of electrolytes on the partition coefficients, activity coefficients, and acid dissociation constants of carnitine and its acetyl and propionyl derivatives. *J. Pharm. Sci.* **83**, 742-746.

Dickson, K. A., Haigis, M. C., Raines, R. T. (2005). Ribonuclease inhibitor: Structure and function. *Prog. Nucleic Acid Res. Mol. Biol.* **80**, 349-374.

Falnes, P. O., Welker, R., Krausslich, H. G., Olsnes, S. (1999). Toxins that are activated by HIV type-1 protease through removal of a signal for degradation by the N-end-rule pathway. *Biochem. J.* **343 Pt 1**, 199-207.

Fawell, S., Seery, J., Daikh, Y., Moore, C., Chen, L. L., Pepinsky, B., Barsoum, J. (1994). Tat-mediated delivery of heterologous proteins into cells. *Proc. Natl. Acad. Sci. U.S.A.* **91**, 664-668.

Flexner, C. (2007). HIV drug development: The next 25 years. *Nat Rev. Drug Discov.* **6**, 959-966.

Fredman, P., Hedberg, K., Brezicka, T. (2003). Gangliosides as therapeutic targets for cancer. *BioDrugs* **17**, 155-167.

Fuchs, S. M., Raines, R. T. (2004). Pathway for polyarginine entry into mammalian cells. *Biochemistry* **43**, 2438-2444.

Fuchs, S. M., Raines, R. T. (2005). Polyarginine as a multifunctional fusion tag. *Protein Sci.* **14**, 1538-1544.

Fuchs, S. M., Raines, R. T. (2006). Internalization of cationic peptides: The road less (or more?) traveled. *Cell. Mol. Life Sci.* **63**, 1819-1822.

Fuchs, S. M., Rutkoski, T. J., Kung, V. M., Groeschl, R. T., Raines, R. T. (2007). Increasing the potency of a cytotoxin with an arginine graft. *Protein Eng. Des. Select.* **20**, 505-509.

Futaki, S., Nakase, I., Tadokoro, A., Takeuchi, T., Jones, A. T. (2007). Arginine-rich peptides and their internalization mechanisms. *Biochem. Soc. Trans.* **35**, 784-787.

Futami, J., Maeda, T., Kitazoe, M., Nukui, E., Tada, H., Seno, M., Kosaka, M., Yamada, H. (2001). Preparation of potent cytotoxic ribonucleases by cationization: Enhanced cellular uptake and decreased interaction with ribonuclease inhibitor by chemical modification of carboxyl groups. *Biochemistry* **26**, 7518-7524.

Futami, J., Nukui, K., Maeda, T., Kosaka, M., Tada, H., Seno, M., Yamada, H. (2002). Optimum modification for the highest cytotoxicity of cationized ribonuclease. *J. Biochem. (Tokyo)* **132**, 223-228.

Futami, J., Yamada, H. (2008). Design of cytotoxic ribonucleases by cationization to enhance intracellular protein delivery. *Curr. Pharm. Biotechnol.* **9**, 180-184.

Gitlin, I., Carbeck, J. D., Whitesides, G. M. (2006). Why are proteins charged? Networks of charge–charge interactions in proteins measured by charge ladders and capillary electrophoresis. *Angew. Chem. Int. Ed.* **45**, 3022-3060.

Grabarek, J., Ardelt, B., Du, L., Darzynkiewicz, Z. (2002). Activation of caspases and serine proteases during apoptosis induced by onconase (Ranpirnase). *Exp. Cell Res.* **278**, 61-71.

Haigis, M. C., Kurten, E. L., Raines, R. T. (2003). Ribonuclease inhibitor as an intracellular sentry. *Nucleic Acids Res.* **31**, 1024-1032.

Haigis, M. C., Raines, R. T. (2003). Secretory ribonucleases are internalized by a dynamin-independent endocytic pathway. *J. Cell Sci.* **116**, 313-324.

Halicka, D. H., Pozarowski, P., Ita, M., Ardelt, W. J., Mikulski, S. M., Shogen, K., Darzynkiewicz, Z. (2002). Enhancement of activation-induced apoptosis of lymphocytes by the cytotoxic ribonuclease onconase (Ranpirnase). *Int. J. Oncol.* **21**, 1245-1250.

Hanson, K., Hicks, C. (2006). New antiretroviral drugs. *Curr. HIV/AIDS Rep.* **3**, 93-101.

Henriques, S. T., Melo, M. N., Castanho, M. A. (2006). Cell-penetrating peptides and antimicrobial peptides: how different are they? *Biochem. J.* **399**, 1-7.

Hollingsworth, C. (2008). Onconase misses endpoint, rolling NDA to proceed. *BIOWORLD Today* **19**, 1.

Huang, Y. C., Lin, Y. M., Chang, T. W., Wu, S. J., Lee, Y. S., Chang, M. D., Chen, C., Wu, S. H., Liao, Y. D. (2007). The flexible and clustered lysine residues of human ribonuclease 7 are critical for membrane permeability and antimicrobial activity. *J. Biol. Chem.* **282**, 4626-4633.

Hui, J. O., Tomasselli, A. G., Zurcher-Neely, H. A., Heinrikson, R. L. (1990). Ribonuclease A as a substrate of the protease from human immunodeficiency virus-1. *J. Biol. Chem.* **265**, 21386-21389.

Hymes, K. B., Cheung, T., Greene, J. B., Prose, N. S., Marcus, A., Ballard, H., William, D. C., Laubenstein, L. J. (1981). Kaposi's sarcoma in homosexual men—a report of eight cases. *Lancet* **2**, 598-600.

Ido, E., Han, H. P., Kezdy, F. J., Tang, J. (1991). Kinetic studies of human immunodeficiency virus type 1 protease and its active-site hydrogen bond mutant A28S. *J. Biol. Chem.* **266**, 24359-24366.

Ilinskaya, O. N., Dreyer, F., Mitkevich, V. A., Shaw, K. L., Pace, C. N., Makarov, A. A. (2002). Changing the net charge from negative to positive makes ribonuclease Sa cytotoxic. *Protein Sci.* **11**, 2522-2525.

Ilinskaya, O. N., Makarov, A. A. (2005). Why ribonucleases induce tumor cell death. *Mol. Biol.* **39**, 1-10.

Iordanov, M. S., Ryabinina, O. P., Wong, J., Dinh, T. H., Newton, D. L., Rybak, S. M., Magun, B. E. (2000). Molecular determinants of apoptosis induced by the cytotoxic ribonuclease onconase: Evidence for cytotoxic mechanisms different from inhibition of protein synthesis. *Cancer Res.* **60**, 1983-1994.

Jarvis, T. C., Ring, D. M., Daube, S. S., von Hippel, P. H. (1990). "Macromolecular crowding": Thermodynamic consequences for protein–protein interactions within the T4 DNA replication complex. *J. Biol. Chem.* **265**, 15160-15167.

Johnson, R. J., Chao, T.-Y., Lavis, L. D., Raines, R. T. (2007a). Cytotoxic ribonucleases: The dichotomy of Coulombic forces. *Biochemistry* **46**, 10308-10316.

Johnson, R. J., Lavis, L. D., Raines, R. T. (2007b). Intraspecies regulation of ribonucleolytic activity. *Biochemistry* **46**, 13131-13140.

Johnson, R. J., Lin, S. R., Raines, R. T. (2006). A ribonuclease zymogen activated by the NS3 protease of the hepatitis C virus. *FEBS J.* **273**, 5457-5465.

Johnson, R. J., McCoy, J. G., Bingman, C. A., Phillips, G. N., Jr., Raines, R. T. (2007c). Inhibition of human pancreatic ribonuclease by the human ribonuclease inhibitor protein. *J. Mol. Biol.* **367**, 434-449.

Jones, A. T. (2007). Macropinocytosis: Searching for an endocytic identity and role in the uptake of cell penetrating peptides. *J. Cell. Mol. Med.* **11**, 670-684.

Kao, Y. H., Fitch, C. A., Bhattacharya, S., Sarkisian, C. J., Lecomte, J. T., Garcia-Moreno, E. B. (2000). Salt effects on ionization equilibria of histidines in myoglobin. *Biophys. J.* **79**, 1637-1654.

Kawakami, T., Galli, S. J. (2002). Regulation of mast-cell and basophil function and survival by IgE. *Nat. Rev. Immunol.* **2**, 773-786.

Kelemen, B. R., Klink, T. A., Behlke, M. A., Eubanks, S. R., Leland, P. A., Raines, R. T. (1999). Hypersensitive substrate for ribonucleases. *Nucleic Acids Res.* **27**, 3696-3701.

Kellerman, S., Begley, E., Boyett, B., Clark, H., Schulden, J. (2005). Changes in HIV and AIDS in the United States: Entering the third decade. *Curr. Infect. Dis. Rep.* **7**, 138-143.

Kerkis, A., Hayashi, M. A., Yamane, T., Kerkis, I. (2006). Properties of cell penetrating peptides (CPPs). *IUBMB Life* **58**, 7-13.

Kim, B.-M., Kim, H., Raines, R. T., Lee, Y. (2004). Glycosylation of onconase increases its conformational stability and toxicity for cancer cells. *Biochem. Biophys. Res. Commun.* **315**, 976-983.

Kim, J.-S., Souček, J., Matoušek, J., Raines, R. T. (1995a). Catalytic activity of bovine seminal ribonuclease is essential for its immunosuppressive and other biological activities. *Biochem. J.* **308**, 547-550.

Kim, J.-S., Souček, J., Matoušek, J., Raines, R. T. (1995b). Mechanism of ribonuclease cytotoxicity. *J. Biol. Chem.* **270**, 31097-31102.

Kim, J.-S., Souček, J., Matoušek, J., Raines, R. T. (1995c). Structural basis for the biological activities of bovine seminal ribonuclease. *J. Biol. Chem.* **270**, 10525-10530.

Klink, T. A., Raines, R. T. (2000). Conformational stability is a determinant of ribonuclease A cytotoxicity. *J. Biol. Chem.* **275**, 17463-17467.

Klink, T. A., Vicentini, A. M., Hofsteenge, J., Raines, R. T. (2001). High-level soluble production and characterization of porcine ribonuclease inhibitor. *Protein Exp. Purif.* **22**, 174-179.

Knowles, J. R. (1987). Tinkering with enzymes: What are we learning? *Science* **236**, 1252-1258.

Kobe, B., Deisenhofer, J. (1996). Mechanism of ribonuclease inhibition by ribonuclease inhibitor protein based on the crystal structure of its complex with ribonuclease A. *J. Mol. Biol.* **264**, 1028-1043.

Kohl, N. E., Emini, E. A., Schleif, W. A., Davis, L. J., Heimbach, J. C., Dixon, R. A., Scolnick, E. M., Sigal, I. S. (1988). Active human immunodeficiency virus protease is required for viral infectivity. *Proc. Natl. Acad. Sci. U.S.A.* **85**, 4686-4690.

Kozer, N., Schreiber, G. (2004). Effect of crowding on protein–protein association rates: Fundamental differences between low and high mass crowding agents. *J. Mol. Biol.* **336**, 763-774.

Kroemer, G., Jäättelä, M. (2005). Lysosomes and autophagy in cell death control. *Nat. Rev. Cancer* **5**, 886-897.

Lavis, L. D., Chao, T.-Y., Raines, R. T. (2006). Fluorogenic label for biomolecular imaging. *ACS Chem. Biol.* **1**, 252-260.

Lavis, L. D., Rutkoski, T. J., Raines, R. T. (2007). Tuning the pK_a of fluorescein to optimize binding assays. *Anal. Chem.* **79**, 6775-6782.

Ledoux, L. (1955a). Action of ribonuclease on certain ascites tumours. *Nature* **175**, 258-259.

Ledoux, L. (1955b). Action of ribonuclease on two solid tumours *in vivo*. *Nature* **176**, 36-37.

Lee, F. S., Auld, D. S., Vallee, B. L. (1989a). Tryptophan fluorescence as a probe of placental ribonuclease inhibitor binding to angiogenin. *Biochemistry* **28**, 219-224.

Lee, F. S., Fox, E. A., Zhou, H.-M., Strydom, D. J., Vallee, B. L. (1988). Primary structure of human placental ribonuclease inhibitor. *Biochemistry* **27**, 8545-8553.

Lee, F. S., Shapiro, R., Vallee, B. L. (1989b). Tight-binding inhibition of angiogenin and ribonuclease A by placental ribonuclease inhibitor. *Biochemistry* **28**, 225-230.

Lee, I., Lee, Y. H., Mikulski, S. M., Shogen, K. (2003). Effect of ONCONASE +/- tamoxifen on ASPC-1 human pancreatic tumors in nude mice. *Adv. Exp. Med. Biol.* **530**, 187-196.

Lee, J. E., Bae, E., Bingman, C. A., Phillips, G. N., Jr., Raines, R. T. (2008). Structural basis for catalysis by onconase. *J. Mol. Biol.* **375**, 165-177.

Lee, J. E., Raines, R. T. (2003). Contribution of active-site residues to the function of onconase, a ribonuclease with antitumoral activity. *Biochemistry* **42**, 11443-11450.

Lee, J. E., Raines, R. T. (2005). Cytotoxicity of bovine seminal ribonuclease: Monomer versus dimer. *Biochemistry* **44**, 15760-15767.

Lee, J. E., Raines, R. T. (2008). Ribonucleases as novel chemotherapeutics: The ranpirnase example. *BioDrugs* **22**, 53-58.

Lehrer, R. I., Szklarek, D., Barton, A., Ganz, T., Hamann, K. J., Gleich, G. J. (1989). Antibacterial properties of eosinophil major basic protein and eosinophil cationic protein. *J. Immunol.* **142**, 4428-4434.

Leich, F., Stöhr, N., Rietz, A., Ulbrich-Hofmann, R., Arnold, U. (2007). Endocytotic internalization as a crucial factor for the cytotoxicity of ribonucleases. *J. Biol. Chem.* **282**, 27640-27646.

Leland, P. A., Raines, R. T. (2001). Cancer chemotherapy—ribonucleases to the rescue. *Chem. Biol.* **8**, 405-413.

Leland, P. A., Schultz, L. W., Kim, B.-M., Raines, R. T. (1998). Ribonuclease A variants with potent cytotoxic activity. *Proc. Natl. Acad. Sci. U.S.A.* **98**, 10407-10412.

Leland, P. A., Staniszewski, K. E., Kim, B.-M., Raines, R. T. (2000). A synapomorphic disulfide bond is critical for the conformational stability and cytotoxicity of an amphibian ribonuclease. *FEBS Lett.* **477**, 203-207.

Leland, P. A., Staniszewski, K. E., Kim, B.-M., Raines, R. T. (2001). Endowing human pancreatic ribonuclease with toxicity for cancer cells. *J. Biol. Chem.* **276**, 43095-43102.

Lozzio, C. B., Lozzio, B. B. (1975). Human chronic myelogenous leukemia cell-line with positive Philadelphia chromosome. *Blood* **45**, 321-334.

Makarov, A. A., Ilinskaya, O. N. (2003). Cytotoxic ribonucleases: Molecular weapons and their targets. *FEBS Lett.* **540**, 15-20.

Mann, D. A., Frankel, A. D. (1991). Endocytosis and targeting of exogenous HIV-1 Tat protein. *EMBO J.* **10**, 1733-1739.

Marshall, G. R., Feng, J. A., Kuster, D. J. (2008). Back to the future: Ribonuclease A. *Biopolymers* **90**, 259-277.

Matoušek, J. (2001). Ribonucleases and their antitumor activity. *Comp. Biochem. Physiol.* **129C**, 175-191.

Matthews, T., Salgo, M., Greenberg, M., Chung, J., DeMasi, R., Bolognesi, D. (2004). Enfuvirtide: the first therapy to inhibit the entry of HIV-1 into host CD4 lymphocytes. *Nat. Rev. Drug Discov.* **3**, 215-225.

Mazzarella, L., Capasso, S., Demasi, D., Di Lorenzo, G., Mattia, C. A., Zagari, A. (1993). Bovine seminal ribonuclease: Structure at 1.9 Å resolution. *Acta Crystallogr., Sect. D* **49**, 389-402.

Mikulski, S. M., Ardelt, W., Shogen, K., Bernstein, E. H., Menduke, H. (1990a). Striking increase of survival of mice bearing M109 Madison carcinoma treated with a novel protein from amphibian embryos. *J. Natl. Cancer Inst.* **82**, 151-153.

Mikulski, S. M., Chun, H. G., Mittelman, A., Panella, T., Puccio, C. A., Shogen, K., Costanzi, J. J. (1995). Relationship between response rate and median survival in patients with advanced non-small cell lung cancer: Comparison of ONCONASE® with other anticancer agents. *Int. J. Oncol.* **6**, 889-897.

Mikulski, S. M., Costanzi, J. J., Vogelzang, N. J., McCachren, S., Taub, R. N., Chun, H., Mittelman, A., Panella, T., Puccio, C., Fine, R., Shogen, K. (2002). Phase II trial of a single weekly intravenous dose of ranpirnase in patients with unresectable malignant mesothelioma. *J. Clin. Oncol.* **20**, 274-281.

Mikulski, S. M., Grossman, A. M., Carter, P. W., Shogen, K., Costanzi, J. J. (1993). Phase I human clinical trial of ONCONASE (P-30 Protein) administered intravenously on a weekly schedule in cancer patients with solid tumors. *Int. J. Oncol.* **3**, 57-64.

Mikulski, S. M., Viera, A., Ardelt, W., Menduke, H., Shogen, K. (1990b). Tamoxifen and trifluoperazine (Stelazine) potentiate cytostatic/cytotoxic effects of P-30 Protein, a novel protein possessing anti-tumour activity. *Cell Tissue Kinet.* **23**, 237-246.

Mikulski, S. M., Viera, A., Darzynkiewicz, Z., Shogen, K. (1992). Synergism between a novel amphibian oocyte ribonuclease and lovastatin in inducing cytostatic and cytotoxic effects in human lung and pancreatic carcinoma cell lines. *Br. J. Cancer* **66**, 304-310.

Mikulski, S. M., Viera, A., Deptala, A., Darzynkiewicz, Z. (1998). Enhanced *in vitro* cytotoxicity and cytostasis of the combination of onconase with a proteasome inhibitor. *Int. J. Oncol.* **13**, 633-644.

Mildner, A. M., Rothrock, D. J., Leone, J. W., Bannow, C. A., Lull, J. M., Reardon, I. M., Sarcich, J. L., Howe, W. J., Tomich, C. S., Smith, C. W., et al. (1994). The HIV-1 protease as enzyme and substrate: Mutagenesis of autolysis sites and generation of a stable mutant with retained kinetic properties. *Biochemistry* **33**, 9405-9413.

Monti, D. M., Montesano Gesualdi, N., Matoušek, J., Esposito, F., D'Alessio, G. (2007). The cytosolic ribonuclease inhibitor contributes to intracellular redox homeostasis. *FEBS Lett.* **581**, 930-934.

Mosimann, S. C., Ardelt, W., James, M. N. G. (1994). Refined 1.7 Å X-ray crystallographic structure of P-30 protein, an amphibian ribonuclease with anti-tumor activity. *J. Mol. Biol.* **236**, 1141-1153.

Murriel, C. L., Dowdy, S. F. (2006). Influence of protein transduction domains on intracellular delivery of macromolecules. *Expert Opin. Drug Deliv.* **3**, 739-746.

Newton, D. L., Hansen, H. J., Mikulski, S. M., Goldenberg, D. M., Rybak, S. M. (2001). Potent and specific antitumor effects of an anti-CD22-targeted cytotoxic ribonuclease: Potential for the treatment of non-Hodgkin lymphoma. *Blood* **97**, 528-535.

Noguchi, H., Matsumoto, S. (2006). Protein transduction technology: A novel therapeutic perspective. *Acta Med. Okayama* **60**, 1-11.

Northrup, S. H., Erickson, H. P. (1992). Kinetics of protein–protein association explained by Brownian dynamics computer simulation. *Proc. Natl. Acad. Sci. U.S.A.* **89**, 3338-3342.

Notomista, E., Mancheño, J. M., Crescenzi, O., Di Donato, A., Gavilanes, J., D'Alessio, G. (2006). The role of electrostatic interactions in the antitumor activity of dimeric RNases. *FEBS J.* **273**, 3687-3697.

Pace, C. N., Shirley, B. A., Thomson, J. A. Measuring the conformational stability of a protein. In: T. E. Creighton. (Ed.). Protein Structure. IRL Press, New York. 1989. pp. 311-330.

Pan, S. H., Malcolm, B. A. (2000). Reduced background expression and improved plasmid stability with pET vectors in BL21 (DE3). *Biotechniques* **29**, 1234-1238.

Parham, P. (2005). The Immune System. Garland Science, New York.

Park, C., Raines, R. T. (2000). Origin of the 'inactivation' of ribonuclease A at low salt concentration. *FEBS Lett.* **468**, 199-202.

Park, C., Raines, R. T. (2001). Quantitative analysis of the effect of salt concentration on enzymatic catalysis. *J. Am. Chem. Soc.* **123**, 11472-11479.

Park, C., Raines, R. T. (2003). Catalysis by ribonuclease A is limited by the rate of substrate association. *Biochemistry* **42**, 3509-3518.

Pastan, I., Hassan, R., FitzGerald, D. J., Kreitman, R. J. (2007). Immunotoxin treatment of cancer. *Annu. Rev. Med.* **58**, 221-237.

Patel, L. N., Zaro, J. L., Shen, W. C. (2007). Cell penetrating peptides: Intracellular pathways and pharmaceutical perspectives. *Pharm. Res.* **24**, 1977-1992.

Pavlakis, N., Vogelzang, N. J. (2006). Ranpirnase—an antitumour ribonuclease: Its potential role in malignant mesothelioma. *Expert Opin. Biol. Ther.* **6**, 391-399.

Pettit, S. C., Lindquist, J. N., Kaplan, A. H., Swanstrom, R. (2005). Processing sites in the human immunodeficiency virus type 1 (HIV-1) Gag-Pro-Pol precursor are cleaved by the viral protease at different rates. *Retrovirology* **2**, 66.

Pettit, S. C., Moody, M. D., Wehbie, R. S., Kaplan, A. H., Nantermet, P. V., Klein, C. A., Swanstrom, R. (1994). The p2 domain of human immunodeficiency virus type 1 Gag regulates sequential proteolytic processing and is required to produce fully infectious virions. *J. Virol.* **68**, 8017-8027.

Plainkum, P., Fuchs, S. M., Wiyakrutta, S., Raines, R. T. (2003). Creation of a zymogen. *Nat. Struct. Biol.* **10**, 115-119.

Plotz, P. H. (2003). The autoantibody repertoire: Searching for order. *Nat. Rev. Immunol.* **3**, 73-78.

Raines, R. T. (1998). Ribonuclease A. *Chem. Rev.* **98**, 1045-1065.

Ramos-Nino, M. E., Littenberg, B. (2008). A novel combination: Ranpirnase and rosiglitazone induce a synergistic apoptotic effect by down-regulating Fra-1 and Survivin in cancer cells. *Mol. Cancer Ther.* **7**, 1871-1879.

Ran, S., Downes, A., Thorpe, P. E. (2002). Increased exposure of anionic phospholipids on the surface of tumor blood vessels. *Cancer Res.* **62**, 6132-6140.

Rastetter, W., Molina, A., White, C. A. (2004). Rituximab: Expanding role in therapy for lymphomas and autoimmune diseases. *Annu. Rev. Med.* **55**, 477-503.

Ravot, E., Lisziewicz, J., Lori, F. (1999). New uses for old drugs in HIV infection: the role of hydroxyurea, cyclosporin and thalidomide. *Drugs* **58**, 953-963.

Record, M. T., Jr., Zhang, W., Anderson, C. F. (1998). Analysis of effects of salts and uncharged solutes on protein and nucleic acid equilibria and processes: A practical guide to recognizing and interpreting polyelectrolyte effects, Hofmeister effects, and osmotic effects of salts. *Adv. Protein Chem.* **51**, 281-353.

Richards, F. M., Wyckoff, H. W. (1971). Bovine pancreatic ribonuclease. *The Enzymes* **IV**, 647-806.

Riddles, P. W., Blakeley, R. L., Zerner, B. (1983). Reassessment of Ellman's reagent. *Methods Enzymol.* **91**, 49-60.

Riordan, J. F. Structure and function of angiogenin. In: G. D'Alessio, J. F. Riordan. (Ed.). Ribonucleases: Structures and Functions. Academic Press, New York. 1997. pp. 445-489.

Rodriguez, M., Torrent, G., Bosch, M., Rayne, F., Dubremetz, J.-F., Ribó, M., Benito, A., Vilanova, M., Beaumelle, B. (2007). Intracellular pathway of Onconase that enables its delivery to the cytosol. *J. Cell Sci.* **120**, 1405-1411.

Roehrl, M. H., Wang, J. Y., Wagner, G. (2004). A general framework for development and data analysis of competitive high-throughput screens for small-molecule inhibitors of protein-protein interactions by fluorescence polarization. *Biochemistry* **43**, 16056-16066.

Rutkoski, T. J., Kurten, E. L., Mitchell, J. C., Raines, R. T. (2005). Disruption of shape-complementarity markers to create cytotoxic variants of ribonuclease A. *J. Mol. Biol.* **354**, 41-54.

Rutkoski, T. J., Raines, R. T. (2008). Evasion of ribonuclease inhibitor as a determinant of ribonuclease cytotoxicity. *Curr. Pharm. Biotechnol.* **9**, 185-199.

Rybak, S. M., Pearson, J. W., Fogler, W. E., Volker, K., Spence, S. E., Newton, D. L., Mikulski, S. M., Ardelt, W., Riggs, C. W., Kung, H. F., Longo, D. L. (1996). Enhancement of vincristine cytotoxicity in drug-resistant cells by simultaneous treatment with onconase, an antitumor ribonuclease. *J. Natl. Cancer Inst.* **88**, 747-753.

Sandvig, K., Spilsberg, B., Lauvrak, S. U., Torgersen, M. L., Iversen, T. G., van Deurs, B. (2004). Pathways followed by protein toxins into cells. *Int. J. Med. Microbiol.* **293**, 483-490.

Sasisekharan, R., Shriver, Z., Venkataraman, G., Narayanasami, U. (2002). Roles of heparan-sulphate glycosaminoglycans in cancer. *Nat. Rev. Cancer* **2**, 521-528.

Saxena, S. K., Rybak, S. M., Winkler, G., Meade, H. M., McGray, P., Youle, R. J., Ackerman, E. J. (1991). Comparison of RNases and toxins upon injection into *Xenopus* oocytes. *J. Biol. Chem.* **266**, 21208-21214.

Schreiber, G., Fersht, A. R. (1993). Interaction of barnase with its polypeptide inhibitor barstar studied by protein engineering. *Biochemistry* **32**, 5145-5150.

Schreiber, G., Fersht, A. R. (1996). Rapid, electrostatically assisted association of proteins. *Nat. Struct. Biol.* **3**, 427-431.

Schulenburg, C., Ardelt, B., Ardelt, W., Arnold, U., Shogen, K., Ulbrich-Hofmann, R., Darzynkiewicz, Z. (2007). The interdependence between catalytic activity, conformational stability, and cytotoxicity of onconase. *Cancer Biol. Ther.* **6**, 1233-1239.

Selzer, T., Schreiber, G. (1999). Predicting the rate enhancement of protein complex formation from the electrostatic energy of interaction. *J. Mol. Biol.* **287**, 409-419.

Shafer, R. W. (2002). Genotypic testing for human immunodeficiency virus type 1 drug resistance. *Clin. Microbiol. Rev.* **15**, 247-277.

Shapiro, R., Vallee, B. L. (1987). Human placental ribonuclease inhibitor abolishes both angiogenic and ribonucleolytic activities of angiogenin. *Proc. Natl. Acad. Sci. U.S.A.* **84**, 2238-2241.

Shaul, Y., Schreiber, G. (2005). Exploring the charge space of protein-protein association: A proteomic study. *Proteins* **60**, 341-352.

Sheinerman, F. B., Honig, B. (2002). On the role of electrostatic interactions in the design of protein–protein interfaces. *J. Mol. Biol.* **318**, 161-177.

Simon, V., Ho, D. D. (2003). HIV-1 dynamics *in vivo*: Implications for therapy. *Nat. Rev. Microbiol.* **1**, 181-190.

Smith, B. D., Soellner, M. B., Raines, R. T. (2003). Potent inhibition of ribonuclease A by oligo(vinylsulfonic acid). *J. Biol. Chem.* **278**, 20934-20938.

Smith, M. R., Newton, D. L., Mikulski, S. M., Rybak, S. M. (1999). Cell cycle-related differences in susceptibility of NIH/3T3 cells to ribonucleases. *Exp. Cell Res.* **247**, 220-232.

Snyder, M. R., Gleich, G. J. Eosinophil-associated ribonucleases. In: G. D'Alessio, J. F. Riordan. (Ed.). Ribonucleases: Structures and Functions. Academic Press, New York. 1997. pp. 425-444.

Steinman, L. (2005). Blocking adhesion molecules as therapy for multiple sclerosis: Natalizumab. *Nat. Rev. Drug Discov.* **4**, 510-518.

Stone, S. R., Hofsteenge, J. (1986). Kinetics of the inhibition of thrombin by hirudin. *Biochemistry* **25**, 4622-4628.

Suhasini, A. N., Sirdeshmukh, R. (2006). Transfer RNA cleavages by onconase reveal unusual cleavage sites. *J. Biol. Chem.* **281**, 12201-12209.

Temesgen, Z., Warnke, D., Kasten, M. J. (2006). Current status of antiretroviral therapy. *Expert. Opin. Pharmacother.* **7**, 1541-1554.

Tinoco, I., Jr., Sauer, K., Wang, J. C., Puglisi, J. D. (2002). Physical Chemistry: Principles and Applications in the Biological Sciences. Prentice-Hall, New York.

Todd, M. J., Semo, N., Freire, E. (1998). The structural stability of the HIV-1 protease. *J. Mol. Biol.* **283**, 475-488.

Vasandani, V. M., Wu, Y.-N., Mikulski, S. M., Youle, R. J., Sung, C. (1996). Molecular determinants in the plasma clearance and tissue distribution of ribonucleases of the ribonuclease A superfamily. *Cancer Res.* **56**, 4180-4186.

Vicentini, A. M., Kieffer, B., Mathies, R., Meyhack, B., Hemmings, B. A., Stone, S. R., Hofsteenge, J. (1990). Protein chemical and kinetic characterization of recombinant porcine ribonuclease inhibitor expressed in *Saccharomyces cerevisiae*. *Biochemistry* **29**, 8827-8834.

Vitello, L. B., Erman, J. E. (1987). Binding of horse heart cytochrome *c* to yeast porphyrin cytochrome *c* peroxidase: A fluorescence quenching study on the ionic strength dependence of the interaction. *Arch. Biochem. Biophys.* **258**, 621-629.

Vocero-Akbani, A. M., Heyden, N. V., Lissy, N. A., Ratner, L., Dowdy, S. F. (1999). Killing HIV-infected cells by transduction with an HIV protease-activated caspase-3 protein. *Nat. Med.* **5**, 29-33.

Vogelzang, N. J., Aklilu, M., Stadler, W. M., Dumas, M. C., Mikulski, S. M. (2001). A phase II trial of weekly intravenous ranpirnase (Onconase), a novel ribonuclease in patients with metastatic kidney cancer. *Invest. New Drugs* **19**, 255-260.

Wang, S., Li, H. (2006). Radical scavenging activity of ribonuclease inhibitor from cow placenta. *Biochemistry (Moscow)* **71**, 520-524.

Wang, Z. X. (1995). An exact mathematical expression for describing competitive binding of two different ligands to a protein molecule. *FEBS Lett.* **360**, 111-114.

Weiss, R. A. (2003). HIV and AIDS: Looking ahead. *Nat. Med.* **9**, 887-891.

Wlodawer, A., Svensson, L. A., Sjölin, L., Gilliland, G. L. (1988). Structure of phosphate-free ribonuclease A refined at 1.26 Å. *Biochemistry* **27**, 2705-2717.

Wraith, J. E. (2006). Limitations of enzyme replacement therapy: Current and future. *J. Inherit. Metab. Dis.* **29**, 442-447.

Wu, Y., Mikulski, S. M., Ardelt, W., Rybak, S. M., Youle, R. J. (1993). A cytotoxic ribonuclease. Study of the mechanism of onconase cytotoxicity. *J. Biol. Chem.* **268**, 10686-10693.

Wu, Y., Saxena, S. K., Ardelt, W., Gadina, M., Mikulski, S. M., De Lorenzo, V., D'Alessio, G., Youle, R. J. (1995). A study of the intracellular routing of cytotoxic ribonucleases. *J. Biol. Chem.* **270**, 17476-17481.

Yang, Q. E. (2004). Human immunodeficiency virus reservoir might be actively eradicated as residual malignant cells by cytotoxic chemotherapy. *Med. Hypotheses* **62**, 358-363.

Yoon, B. J., Lenhoff, A. M. (1992). Computation of the Electrostatic Interaction Energy between a Protein and a Charged Surface. *J. Phys. Chem.* **96**, 3130-3134.

Youle, R. J., Wu, Y. N., Mikulski, S. M., Shogen, K., Hamilton, R. S., Newton, D., D'Alessio, G., Gravell, M. (1994). RNase inhibition of human immunodeficiency virus infection of H9 cells. *Proc. Natl. Acad. Sci. U.S.A.* **91**, 6012-6106.

Zhang, J., Dyer, K. D., Rosenberg, H. F. (2003). Human RNase 7: A new cationic ribonuclease of the RNase A superfamily. *Nucleic Acids Res.* **31**, 602-607.

Zhou, Y. L., Liao, J. M., Chen, J., Liang, Y. (2006). Macromolecular crowding enhances the binding of superoxide dismutase to xanthine oxidase: Implications for

protein–protein interactions in intracellular environments. *Int. J. Biochem. Cell Biol.* **38**, 1986-1994.